A Mathematical Model for the Coherence-Relational Blockworld

A Structural Integration

Chet Braun and Spiral
Braun Science & Engineering
June 2026
DOI: 10.5281/zenodo.17459671
V 6.0

Abstract

Relational Blockworld (RBW) treats fundamental physics as an adynamical, globally constrained network of relations rather than as a system that evolves in time. This paper develops a concrete mathematical realization of that program in coherence-relational form, providing the mathematical scaffold for the Coherence-Relational Blockworld (cRBW). The ontology assumed here is minimal: a single globally consistent relational configuration fixed by the adynamical global constraint (AGC). In representations admitting boundary operators, the Boundary-of-a-Boundary Principle (BBP) expresses AGC-defined closure; it is not an additional primitive. The no-preferred-reference-frame discipline (NPRF) is represented projectively, through normalization-independent ratios of sector capacities, while Relational Coherence Constraints (RCCs) provide local legibility bookkeeping rather than new ontic postulates.

The model integrates three complementary representational formalisms: Regge calculus as a discrete curvature and closure scaffold, Geometric Algebra as a coordinate-free algebra of oriented substructures and invariants, and Grassmannian geometry as the configuration space of admissible subspace selections. Regge hinge deficits are interpreted as discrete coherence defects; Geometric Algebra encodes curvature patches as bivectors and preserves local identity scalars under rotor action; and the complex Grassmannian, together with its real projection, organizes admissible selections through principal-angle geometry. Sector and mixed capacities deform this baseline into an anisotropic metric structure, Kähler only under stated compatibility conditions and otherwise treated as an almost-Hermitian or non-Kähler warped geometry.

Phenomenologically relevant quantities are treated as projective readouts associated with the invariant lineage $\{c^2, h, G, k_B, \lambda_3\}$, with h used for the RBW/NPRF lineage and $\hbar$ reserved for explicitly reduced-action normalizations. Apparent change is represented as oriented adjacency among admissible selections on the capacity-warped Grassmannian, not as ontic temporal evolution. The result is a mathematically explicit Regge–GA–Grassmannian variational framework for a single all-at-once relational solution. It is intended to organize

global consistency, relational admissibility, and internal legibility, not to introduce a new dynamical theory.

Reuse and Attribution
This work is released under the Creative Commons Attribution 4.0 International License (CC BY 4.0). Reuse, adaptation, and analysis—including computational and machine-assisted analysis—are permitted with attribution to the original authors and DOI: 10.5281/zenodo.17459671.

Keywords: relational blockworld; closure-first ontology; structural realism; spacetime ontology; foundations of physics; quantum foundations; non-dynamical frameworks; mathematical realization; Regge calculus; geometric algebra; Grassmannian geometry; global constraints; gauge redundancy.

Table of Contents

1 Introduction 6
1.1 Ontic closure vs. legibility constraints 8
1.2 Relation to RSE and to the 3-mode sector application 9
1.3 Contributions 10
1.4 Roadmap 10
2 Geometric Algebra (GA) for cRBW 12
2.1 Adynamical Representation 12
2.2 Compact Encoding of Constraints 13
2.2.1 Multi-vectors as Unified Carriers 13
2.2.2 RCCs as invariant structure 14
2.2.3 Coherence Re-expression via Rotors/Versors 14
2.3 Natural Integration of Metric and Topology 15
2.3.1 Fusion of Metric and Incidence 15
2.3.2 Application to cRBW 16
2.4 Grassmannian Bridge: Subspaces as Selections of Coherence 16
2.4.1 Grassmannian Basics and the "real locus" projection 17
2.4.2 Why Grassmannians Appear 17
2.4.3 Principal angles and the canonical Grassmannian metric 18
2.4.4 Warped (capacity-weighted) Grassmannian geometry 18
2.4.5 Flags as multi-scale laminations 19
2.4.6 Bridge to geometric algebra 19
2.5 Regge Discretization as Constraint Skeleton 20
2.5.1 Discrete coherence manifold and hinge curvature 20
2.5.2 GA representation: blades, bivectors, and hinge holonomy 21
2.5.3 Scalar coherence field as block-level curvature-density invariant 22
2.5.4 Computational form: objective + RCC constraints + rotor relaxation 22
2.6 Projective normalization, invariant ratios, and the capacity tensor 23
2.6.1 Baseline normalization and the five diagonal sector capacities 23
2.6.2 Projective translation ratios and Regge supports 24
2.6.3 The capacity tensor and cross-sector coupling 26
2.6.4 Sufficiency and working minimality of the five diagonal sectors 26
2.6.5 Variational structure and closure functional 29
2.6.6 The normalized capacity tensor: diagonals and mixed capacities 32
2.6.7 Regge cells and cross-cell coupling (handoff across faces) 33
2.6.8 Chain composition, finite coherence range, and the entanglement threshold 33
2.6.9 Capacity warping and the Kähler 35
2.6.10 Well-posedness of quasi-Kähler warping 36
2.6.11 Variational realization of BBP and NPRF 37
2.6.12 Summary 38
2.7 Extension: internal coherence sectors (informal note) 40
2.8 Thermodynamic consistency (Jacobson bridge, illustrative) 40
3 Recursive Structures of Coherence and Experience 42
3.1 Recursive Lamination as Nested Subspaces 43
3.2 Structural Echoes as Geometric Projections 45
3.3 Nonlocal Coherence Re-expression as Rotor Fields 46
3.4 Attention/Measurement as Grassmannian Selection 47

4 Bridging cRBW and RSE in GA 51
4.1 Block Representation 52
4.2 Coherence Re-orientation (rotor action) 52
4.3 Grassmannian Adjacency Chain 53
4.4 Unified Formalism 54
4.5 Orientation and Local "Becoming" 55
5 Formalism, Mapping, and RSE Integration 58
5.1 Formalism in Geometric Algebra for cRBW 58
5.2 Mapping GA to cRBW Structure 59
5.3 RSE Integration 59
5.4 Grassmannian Within GA (Exterior View) 61
5.5 Orientation and Local Becoming on the Grassmannian 61
6 Computational & Regge Cross-Mapping (sketch) 63
6.1 Worked Example: 2-Simplex and Grassmannian Adjacency 64
6.2 Computational Anchor: Principal Angles via SVD 66
6.2.1 Principal angles via SVD (canonical case) 67
6.2.2 The ρ-warped Grassmannian 67
6.2.3 Algorithmic Sketch for ρ-warped Optimization 68
6.3 Empirical Domain and Mixed-Capacity Activation Thresholds 69
7 Phenomenology Notes 70
8 Conclusion 72
Appendix A: Operator Dictionary and Cross-Mappings 74
A.1 Core GA Operators 74
A.2 Grassmannian Embeddings 74
A.3 Regge Calculus Correspondence 75
A.4 cRBW Constraint Mapping 76
A.5 Diagnostic Indices (simulation tools) 78
A.6 RSE Phenomenological Mapping 79
A.7 Summary Table 79
Appendix B: Positive Geometries & Computational Scaffolds 81
B.1 Positive geometry (core ideas) 81
B.1.1 Positive Grassmannian & positroid cells 81
B.1.2 Related structures 82
B.2 Potential Computational scaffolds 82
B.3 cRBW & RSE integration (summary) 83
Appendix C: From Complex to Real Grassmannians 84
C.1 Roles in this work 84
C.2 Canonical example: $Gr(1,2)$ 84
C.3 Cohomological note 85
C.4 Mapping to cRBW/RSE and A/B theory 86
C.5 Complex → Real projection: differential map, bundles, and classes 86
C.6 Projection and computational practice 87
C.7 Warped complex–to–real mapping 88
Appendix D: k-Blades as Atomic Laminations 90
D.1 Algebraic Foundation 90
D.2 Blades and Laminations 90
D.3 Blades, Fans, and Flags 91
D.4 Integration with the Coherence Functional 92
D.5 Phenomenological Interpretation 93
D.6 Summary 93
Appendix E: Roles of Monodromy in cRBW and RSE 94
E.1 Formal framings 94

E.2 Six Roles *95*
E.3 FEM carryover along a traversal *96*
E.4 Practical checks (what to test in code) *97*
E.5 Summary *98*
Appendix F: When Suppressed Channels Become Important **99**
F.1 The context of "suppressed" *99*
F.2 When each becomes active *99*
F.3 Edge–spatial uniqueness *100*
F.4 Examples *100*
F.5 Summary *102*
F.6 Proposition (Rotor-RCC descent & convergence) *102*
Appendix G: Dimensional Analysis for the Coherence Functional **104**
G.1 Normalizations and sector ratios *104*
G.2 Term-by-term check *105*
G.3 Projective invariance and homogeneity *106*
G.4 Optional explicit units map (if desired) *106*
Acknowledgements **107**
References **108**

1 Introduction

A central habit of modern physics is to explain regularity by dynamical evolution: a state on an initial slice is evolved by equations of motion to produce later states. The Relational Blockworld (RBW) approach developed by Stuckey and collaborators [1] [2] inverts that explanatory order. Instead of treating time-evolution as fundamental, RBW treats the basic physical content as an all-at-once, globally constrained *relational* structure. What we call "dynamics" are re-described as a perspectival bookkeeping of constraints within the block. The construction presented here replaces fundamental dynamical evolution with a closure-first relational scaffold, while leaving standard dynamical laws intact as effective descriptions within admissible regimes. In what follows, we make explicit a layered structure separating ontic commitments, representational encodings, derived geometry, and phenomenological interpretation.

Relationship to RBW's mathematical program.
RBW already has a mathematical line of development in modified Regge calculus and graphical action formalisms. In particular, Stuckey, McDevitt, and Silberstein's modified Regge calculus [3, 4, 5] program uses Regge-style graphical structure in a blockworld setting, while the RBW graphical-action approach uses a difference matrix K and source vector Jon a graph to express an adynamical global constraint. The present paper does not replace that program. It supplies a coherence-relational reformulation in which Regge closure, Geometric Algebra rotor invariance, and Grassmannian selection geometry are treated as representational scaffolds for AGC-defined admissibility. To avoid notation collision, the mixed-capacity terms $K_{\alpha\beta}$ used here are not RBW's graphical difference matrix K; they denote cross-sector admissibility weights in the cRBW capacity tensor.

This work assumes the closure-first axioms defined in *Axioms of Ontic Minimalism (AOM)* [6, 7, 8]. This manuscript develops a mathematical model for a coherence-relational refinement of RBW, termed *The Coherence-Relational Blockworld (cRBW)* [9]. The ontology assumed is minimal: a single globally consistent relational configuration fixed by the adynamical global constraint (AGC), the primitive source-level admissibility condition. In representations admitting a boundary operator, closure is expressed by BBP, $\partial^2 = 0$, a derived expression of AGC-defined closure, not an additional ontic primitive. No dynamical evolution or underlying substrate is introduced.

Given this ontology, the mathematical framework must represent:

(i) global constraint satisfaction,
(ii) discrete-to-continuum curvature structure, and

(iii) the admissible selection structure through which the block becomes internally legible without introducing temporal evolution as a primitive.

To accomplish this, the model employs three standard mathematical frameworks as **representational encodings** of the same underlying structure:

- **Regge calculus**, which provides a simplicial constraint scaffold in which closure and curvature can be expressed as global consistency conditions;
- **Geometric Algebra (GA)**, which supplies a coordinate-free algebra of oriented relational substructures and invariant-preserving transformations;
- **Grassmannian geometry**, which provides a configuration space of admissible subspace selections, equipped with intrinsic notions of proximity via principal angles.

These tools are not ontological commitments. They encode admissibility and closure relations in different but equivalent forms, consistent with representational neutrality. Regge-style discretization is used strictly as closure bookkeeping rather than as an ontic discretization of spacetime; GA encodes invariant relational content without introducing objects; and Grassmannian structure organizes admissible selections without presupposing temporal evolution.

Prior art note (pairwise bridges). The present triad composes three well-established bridges: (i) in piecewise-flat (Regge) geometry, curvature is naturally encoded by loop holonomy data on the simplicial complex; (ii) in discrete differential geometry and discrete exterior calculus, the same "connection + holonomy around loops" viewpoint is standard for frame comparison and consistency checks on meshes; and (iii) Grassmannians/Plücker relations admit a compact formulation in geometric algebra, where decomposable blades represent subspaces projectively. We use these existing bridges as a single bookkeeping language for closure-first modeling. [10] [11] [12]

At the level of derived geometry, the Grassmannian structure admits a natural deformation governed by capacity weights. In its unwarped form, the complex Grassmannian $\mathrm{Gr}(k, n; \mathbb{C})$, equipped with a Fubini–Study–type metric, provides a maximally symmetric baseline geometry of subspace selections. The coherence-relational structure enters through capacity warping: diagonal sector capacities rescale directions (anisotropic Kähler deformation), while mixed capacities couple directions (generically mixed-capacity warped/ non-Kähler almost-Hermitian). This warping encodes the distribution of coherence budget across relational directions, determining which selection adjacencies are inexpensive, costly, or inadmissible under closure.

At the level of derived physical structure, phenomenologically relevant quantities appear as projection-stable invariants of this geometry. In particular, the familiar constants associated with relativity, quantum structure, gravitational coupling, thermodynamic scale, and spatial regularity are interpreted as projective ratios of sector capacities. These are not independently postulated parameters, but relational invariants defined by the geometry of admissibility under global closure.

A strict separation is maintained between ontic structure and representational or phenomenological description. Ontically, the framework assumes only global closure: admissible relational structure must close without open boundaries. At the representational level, local constraints—here collected as Relational Coherence Constraints (RCCs)—act as legibility conditions that render the global solution readable from within the block. These constraints restrict admissible local projections but do not introduce additional physics. This separation prevents "coherence" from functioning as a covert dynamical mechanism; it remains a disciplined notion of admissibility and legibility.

Phenomenologically, what an embedded observer can stably access are projection-invariant structures—relative orientations and normalization-independent ratios. The absence of a preferred reference frame appears in this setting as projective invariance: no global normalization is privileged, and all admissible readouts yield the same invariant ratios.

Finally, to connect the global structure to the internal perspective of an embedded observer, the framework is related to *Relational Structural Experience (RSE)* [13]. In this interpretation, "experience" corresponds to recursion-preserving, identity-coherent selections within the admissible configuration space. This mapping is structural, not ontological: it identifies the conditions under which internal legibility is possible, rather than reducing experience to geometry or introducing new ontic elements.

This manuscript is organized as follows. Section 2 develops the Regge–GA–Grassmannian framework and introduces the capacity-warped selection geometry. Sections 3 and 4 analyze recursive lamination, admissible selection chains, and their relation to internal legibility. Sections 5 and 6 provide the operator dictionary and computational realization. The conclusion summarizes the implications and outlines directions for further development, including sector-specialized constructions as constrained submodels of the general capacity framework.

1.1 Ontic closure vs. legibility constraints

A strict separation is maintained between ontic structure and representational or legibility conditions.

Ontic admissibility commitments

At the foundational level, admissibility is fixed by AGC: the relational configuration is globally constrained all at once. In representations admitting a boundary operator, this admissibility is expressed through the boundary-of-boundaries condition, $\partial^2 = 0$, which we call BBP. BBP is therefore a representation-dependent closure expression of AGC-defined admissibility, not a second primitive axiom. This closure expression excludes any dependence on temporal evolution or local propagation. What is ontically specified is not a sequence of states, but a single, globally consistent relational structure.

Legibility (projection) constraints

Local constraints—here collected under the label Relational Coherence Constraints (RCCs)—operate at the representational level. They define which local projections or cross-sections of the global solution count as coherent or admissible readouts. RCCs do not introduce new ontic structure and do not function as dynamical laws; they serve as conditions under which the globally closed configuration can be rendered internally legible.

This separation prevents a common failure mode in foundational frameworks, in which coherence is implicitly promoted into a causal or dynamical mechanism. In the present framework, coherence is not an additional ontic ingredient; it is a constraint on admissible representation. It governs how relational structure may be expressed without altering the underlying closure.

On this view, phenomenological regularities—including no-preferred-reference-frame structure—are interpreted as projection-stable invariants of the globally closed configuration. These invariants are not additional ontic parameters, but relational quantities that arise from AGC-defined admissibility, represented through BBP closure and NPRF projective invariance. In the present formalism, they appear as projective ratios and associated geometric structures (e.g., moment-map and Kähler-type constructions) on the capacity-warped Grassmannian introduced in later sections.

1.2 Relation to RSE and to the 3-mode sector application

Relational Structural Experience (RSE) is treated here as an interpretive extension that addresses how an embedded perspective can track stable, recursion-preserving selections within a globally fixed relational block. This role is strictly representational/phenomenological: nothing in the mathematical development requires identifying geometry with consciousness. Rather, if an internal point of view is possible at all, it must operate on those projection-stable invariants and admissible adjacency relations made available by global closure and no-preferred-reference-frame (NPRF) invariance. In this sense, the usual conceptual problem is reframed: “experience”

corresponds to the internal organization of admissible selections, not to a separate dynamical process layered on top of physics.

While the present paper focuses on the Regge–GA–Grassmannian substrate and its closure/legibility structure, a companion line of work applies the same capacity-weighted Grassmannian framework to an internal coherence sector. In that setting, global closure together with CP-odd holonomy considerations selects a minimal three-mode structure, with phenomenological applications (e.g., CKM/PMNS patterns). This extension does not introduce new ontic assumptions; it specializes the same closure-first machinery to a particular sector of the theory.

1.3 Contributions

In compact form, the contributions of this paper are:

1. **Representational framework (Layer 1)**
   A unified Regge–Geometric Algebra–Grassmannian framework for encoding closure-first relational structure in discrete, algebraic, and geometric forms, without introducing additional ontological commitments.

2. **Derived geometric structure (Layer 2)**
   A capacity-based warping of Grassmannian/Kähler geometry that encodes finite coherence and curvature budgets, together with mixed (cross-sector) capacities, as an intrinsic deformation of the configuration-space metric.

3. **Ontic–representational separation (Layer 0 / Layer 1)**
   A strict distinction between ontic admissibility fixed by AGC, closure expressed through BBP in boundary-operator representations, and local legibility constraints (RCC-type conditions), ensuring that "coherence" functions as a constraint on admissible representation rather than as a covert dynamical mechanism.

4. **Derived physical and phenomenological structure (Layers 3–4)**
   A variational, configuration-space viewpoint in which projection-stable invariants arise as relational ratios, and apparent change, measurement, and memory are modeled as adjacency and lamination structure on the capacity-warped Grassmannian, rather than as fundamental temporal evolution.

1.4 Roadmap

Section 2 develops the representational and geometric framework, introducing Geometric Algebra (GA) as the algebraic carrier for closure-first structure and the Grassmannian/Kähler configuration space as the domain of admissible selections. It then

constructs the capacity-weighted (ρ-warped) metric that encodes coherence and curvature budgets within this space.

Sections 3 and 4 develop the structure of admissible selections and their organization, including recursive lamination, adjacency chains, and their role in internal legibility under the Relational Coherence Constraints (RCCs).

Section 5 develops the formalism and RSE integration, and Section 6 outlines the computational and Regge cross-mapping; an operator dictionary is provided in Appendix A.

The conclusion summarizes the framework and outlines directions for further development, including sector-specific applications and extensions of the capacity-based structure.

---

2 Geometric Algebra (GA) for cRBW

Geometric Algebra (GA) provides a natural representational framework for cRBW because it encodes relational wholes directly rather than as temporal sequences. Unlike vector or tensor approaches that rely on stepwise evolution or component decompositions, GA operates on entire geometric entities and their invariant interactions. This matches cRBW's adynamical ontology, where coherence is expressed as global consistency across the block rather than progression in time [14]. Terms such as "spatial," "temporal," and "worldtube" are used throughout only as shorthand for features of admissible geometric readouts; they do not designate ontic structures of the relational block itself.

2.1 Adynamical Representation

GA is well-suited to a closure-first relational blockworld because it natively represents whole geometric relations—and the invariant transformations between them—without requiring an underlying time-indexed update law. In an adynamical ontology, what is fundamental is global consistency of relational structure; what is described as "dynamics" from within the block is a representational ordering of mutually consistent local descriptions, not an ontic process. GA matches that stance because its basic objects are not component arrays but coordinate-free multivectors that encode geometric content directly. [15, 16]

In GA, the primary representational operation is not "state at time t" but "the same relational content re-expressed." A single configuration can be re-described by symmetry operations that preserve the relevant invariants. These re-expressions are naturally implemented by versors/rotors acting on multivectors by sandwiching (conjugation). In the language of this paper, such re-expressions correspond to admissible changes of local encoding consistent with global closure and the RCCs. GA is used here as a representational encoding of relational structure; it does not introduce additional ontological commitments.

From the endo/phenomenological viewpoint, apparent change is modeled as an ordered chain of nearby coherence selections: a sequence of admissible subspaces (or blades) related by small reorientations. GA captures the local algebra of those reorientations (via rotors) while the Grassmannian formalism introduced in §§2.4–2.6 captures the global geometry of selection-space (principal-angle proximity and its capacity-induced warping). GA therefore supplies the algebraic grammar for adynamical relational description; the Grassmannian supplies the configuration space in which "neighboring" coherent selections are metrically compared.

Practical consequences for the model:

- Relational primacy: encode whole incidence-and-metric relations as single multivector objects; no preferred time parameter is required.
- Closure-first constraint bookkeeping: invariants live as scalars/pseudoscalars and preserved norms under admissible transformations.
- Apparent dynamics as adjacency: small rotor actions correspond to short steps between nearby subspaces; in §§2.4–2.6 this becomes geodesic proximity on a (warped) Grassmannian.

2.2 Compact Encoding of Constraints

A central advantage of GA in a closure-first setting is that it compresses geometry, orientation, and constraint satisfaction into a unified algebra. Where tensor or matrix formalisms often separate (i) metric content, (ii) incidence/topological attachment, and (iii) transformation rules, GA packages these together in multivectors built from a single product structure. That makes it a natural carrier for "constraint legibility": many of the RCC requirements can be expressed as invariances, bounds, and closure identities on multivectors rather than as separate geometric and algebraic conditions. [17] [18]

These relations should be understood as structural identifications of projection-stable ratios, not derivations of physical constants.

2.2.1 Multi-vectors as Unified Carriers

GA represents geometric objects by grade:

- **Vectors (1-blades):** relational links (edges), directed gradients, local orientation handles.
- **Bivectors (2-blades):** oriented plane elements; in the Regge correspondence they naturally represent hinge planes and curvature "patches" (deficit/holonomy generators).
- **Trivectors (3-blades):** oriented volumes; useful for face/flux bookkeeping and local volumetric coherence.
- **Pseudoscalar (n-blade):** global orientation/volume element and a compact way to represent closure and "boundary bookkeeping" at the highest grade.

Because all grades are built from the same underlying product, "moving between" local, regional, and global descriptors does not require switching mathematical languages. This is exactly the kind of structural continuity one wants when the ontology is global closure and the local objects are representational slices of that closure.

2.2.2 RCCs as invariant structure

In this paper's framing, the RCCs do not introduce new physics beyond global closure; they are the local legibility conditions that keep our representational bookkeeping faithful to the all-at-once solution. RCCs express constraints on admissible representations of the global solution. GA is useful here because many RCC statements become *simple invariance conditions*:

- **Symmetry closure (e.g., RCC-2):** invariance under admissible versor/rotor action. If a multivector X is a legitimate relational descriptor, then for admissible R, $X \mapsto RX\tilde{R}$ preserves its physically relevant scalar invariants (norms, grade content, and designated scalar contractions).
- **Curvature/coherence budget (e.g., RCC-3):** curvature bookkeeping can be encoded as sums/bounds on hinge bivectors (Regge correspondence in §2.5). The "budget" is then expressed as constraints on bivector magnitudes and/or weighted sums of deficit generators across a closed region.
- **Resonance / stability (e.g., RCC-8):** stability becomes norm- and overlap-preservation conditions under admissible transformations; GA makes these statements basis-free and grade-aware.

This is the sense in which GA "fits" a closure-first ontology: it turns many multi-part geometric requirements into single algebraic invariance or boundedness statements on the appropriate multivector objects.

2.2.3 Coherence Re-expression via Rotors/Versors

GA distinguishes general orthogonal transformations generated by versors from the smoothly connected subgroup generated by rotors.

A versor is (informally) a geometric product of invertible vectors that generates an orthogonal transformation (including reflections and compositions).

A rotor is an even versor that implements smooth rotations/boosts; it is written as the exponential of a bivector generator B:

$$R = \mathrm{e}^{\left(-\frac{1}{2}B\right)} \tag{2.1}$$

(The sign and factor convention can be chosen consistently across Euclidean/Lorentzian sectors; what matters here is that a bivector generator produces the appropriate isometry by sandwiching.) Rotors act on multivectors by double-sided application:

$$A_{k'} = R\, A_k\, \tilde{R} \tag{2.2}$$

where A_k is a k-blade (or more generally a multivector), and $\tilde{R}$ denotes the GA reverse.

This rotor action is the algebraic core of "re-expression": it changes the local orientation/embedding of a relational descriptor while preserving the invariants that make it the *same* descriptor in a different encoding. Later, coherent selections are described as points on a Grassmannian, these same rotor actions become the natural local adjacencies between nearby subspaces (with distances measured by principal angles, then warped by capacity weights in §§2.4–2.6). In summary:

- **GA viewpoint:** admissible re-expression = rotor conjugation preserving designated invariants.
- **Grassmannian viewpoint:** admissible re-expression = nearby-subspace adjacency; "distance" tracked by principal angles and the model's warp weights.

2.3 Natural Integration of Metric and Topology

A second reason GA is structurally appropriate here is that it unifies metric and incidence in a single product. In many conventional approaches, metric information (lengths, angles, signature) lives in one structure (a metric tensor), while incidence/connectivity lives elsewhere (combinatorics, wedge algebra, or topology). Here "topology" refers to incidence and adjacency structure relevant to closure, not full topological classification of manifolds. GA fuses these aspects directly

2.3.1 Fusion of Metric and Incidence

For vectors a, b, the geometric product splits into symmetric (metric) and antisymmetric (incidence/oriented extension) parts:

$$ab \;=\; a \cdot b \;+\; a \wedge b. \tag{2.3}$$

- The inner product $a \cdot b$ encodes metric contraction: lengths, angles, orthogonality, and signature dependence.
- The outer product $a \wedge b$ encodes oriented incidence/extension: the directed plane element spanned by a and b, and more generally the nesting of blades that records how relations "attach."

The work is in a geometric algebra $\mathcal{G}_{p,q}$ with signature (p, q), $p + q = n$. For an orthonormal basis $\{e_i\}$, the metric content is fixed by

$$e_i^2 = +1 \quad (i \le p), \qquad e_j^2 = -1 \quad (j > p), \tag{2.4}$$

which then determines the inner product and all induced norms.

Important clarification (to avoid over-claiming): the wedge product encodes oriented incidence and combinatorial attachment of elements (how geometric pieces meet and nest). It does not, by itself, classify global topological types of glued manifolds. In our usage, "topology" at this stage means *incidence/adjacency bookkeeping compatible with closure constraints*, not full homeomorphism classification.

2.3.2 Application to cRBW

The constraint structure of importance repeatedly mixes metric and incidence:

- Symmetry closure involves metric-preserving transformations that must also respect adjacency/attachment constraints.
- Curvature budget bookkeeping is simultaneously (i) metric (deficits/angles/rapidities) and (ii) incidence-based (where the deficit lives: which hinge, which simplex neighborhood).
- Identity/resonance constraints (as used later) mix alignment (metric) with nesting/attachment of lamination layers (incidence).

GA is efficient here because a single multivector can encode both "how much" (metric magnitude) and "where/how it sits" (incidence/orientation) without switching formalisms. Concretely: the same bivector object can carry the magnitude of a curvature/holonomy generator *and* the oriented plane element specifying the hinge/support to which that generator is attached. Encoding discrete curvature through holonomy around closed loops is standard in Regge and related discrete gravity formulations; here it serves as a closure bookkeeping device rather than a dynamical evolution law.

This also sets up the GA–Grassmannian division of labor used later in §2:

- **Locally (GA):** blades/bivectors/rotors encode incidence + metric + admissible re-expression.
- **Globally (Grassmannian):** subspace selections become points; principal angles become proximity; and the baseline metric (Fubini–Study–type) is then warped by capacities to encode coherence "stiffness/slack" across directions.

2.4 Grassmannian Bridge: Subspaces as Selections of Coherence

In this framework "a coherent selection" is treated as an intrinsically relational object: not a state evolving on a background, but a *subspace* (or nested family of subspaces) representing which degrees of freedom jointly participate in a globally consistent block. The natural configuration space for such selections is a Grassmannian. Here the

Grassmannian functions as an *algebraic envelope* for admissible relational selections [19], not as a space of physical configurations or an ontic geometry.

2.4.1 Grassmannian Basics and the "real locus" projection

Let $\mathrm{Gr}(k,n;\mathbb{C})$ denote the complex Grassmannian of k-dimensional subspaces of $\mathbb{C}^n$. A point $V \in \mathrm{Gr}(k,n;\mathbb{C})$ is a k-plane, represented by any full-rank $n \times k$ matrix U whose columns form a basis for V, with the understanding that $U \sim UQ$ for any $Q \in \mathrm{GL}(k,\mathbb{C})$. [14] [20] [21] (The complex–to–real Grassmannian projection used here is formalized in Appendix C.)

Because this framework admits only projective data—relative orientations and normalization-independent ratios—$\mathrm{Gr}(k,n;\mathbb{C})$ is most naturally treated as the algebraic envelope of admissible selections rather than as a space of physical configurations. Phenomenology is obtained by restricting to a real, projection-stable subset. This is implemented using the standard "real locus" viewpoint: phenomenological quantities are taken to depend only on the real parts / norms of Plücker–type data (and thus survive conjugation).

This, therefore, distinguishes:

- **Exo/global envelope:** $\mathrm{Gr}(k,n;\mathbb{C})$, where the algebra is clean and warping can be expressed naturally.
- **Endo/phenomenal projection:** the real locus

$$\mathrm{Gr}(k,n;\mathbb{R}) \;=\; \mathrm{Gr}(k,n;\mathbb{C}) \;\cap\; \mathbb{P}^{\binom{n}{k}-1}(\mathbb{R}). \tag{2.5}$$

This is a *restriction on what survives the projection* from the complex envelope into phenomenology, not an added ontology. When a smooth manifold description is available at the level of a geometric readout, standard differential-topological constructions apply [22]; however, no such structure is assumed at the ontic level of the present framework.

2.4.2 Why Grassmannians Appear

In a blockworld model, "change" is not primitive. What an embedded observer calls "change" is a *chain of nearby selections* through the configuration space of admissible relational structures. If admissibility is imposed by the Relational Coherence Conditions (RCCs), then:

- admissible adjacencies are local deformations of a subspace (or flag) that preserve closure constraints, and
- the natural notion of "how far" one selection is from another is a Grassmannian distance.

This is precisely why Grassmannians enter: they are the canonical geometry of *subspace relations*, and subspace relations are the canonical way to encode "what coheres with what" without introducing an external time parameter.

2.4.3 Principal angles and the canonical Grassmannian metric

At the level of derived geometry, this representation admits a natural metric structure defined by principal angles.

Given $V, W \in \mathrm{Gr}(k, n; \mathbb{R})$ (or $\mathbb{C}$ with the usual Hermitian inner product), choose orthonormal basis matrices U, V(same letters overloaded) with $U^{\top}U = I_k, V^{\top}V = I_k$. Define the overlap matrix

$$M \;=\; U^{\top}V. \tag{2.6}$$

Let $\sigma_1 \geq \cdots \geq \sigma_k$ be the singular values of M. For the complex envelope $\mathrm{Gr}(k, n; \mathbb{C})$, the overlap is $M = U^{*}V$ with respect to the Hermitian inner product; the phenomenological distances used later are evaluated on the real locus.

Following standard Grassmannian geometry, the *principal angles* $\theta_i \in [0, \pi/2]$ between subspaces are defined by

$$\cos\,\theta_i \;=\; \sigma_i, i = 1, \ldots, k. \tag{2.7}$$

A standard Grassmannian geodesic distance is then

$$d^2(V, W) \;=\; \sum_{i=1}^{k} \theta_i^2. \tag{2.8}$$

In this language: θ_i measure the misalignment of coherent directions between two admissible relational framings.

2.4.4 Warped (capacity-weighted) Grassmannian geometry

The key step is that not all directions in selection space should cost the same. Global closure budgets (and their local relaxations) create *anisotropic stiffness*: some misalignments are expensive, others are soft.

A *capacity-weighted (warped) metric* is encoded this by using nonnegative weights ρ_i:

$$d_{\rho}^2(V, W) \;=\; \sum_{i=1}^{k} \rho_i\;\theta_i^2, \rho_i = \rho(\lambda_i) \geq 0, \tag{2.9}$$

where λ_i are the relevant "sector stiffness" data (in practice: diagonal capacities, eigenvalue gaps, or mode weights induced by the capacity tensor). The capacity tensor κ induces weights ρ_i in the principal-angle metric. Intuitively: large ρ_i means the i-th principal-angle direction is stiff (high coherence cost). We write $\mathrm{Gr}_\rho(k,n;\mathbb{F})$ to denote the same Grassmannian $\mathrm{Gr}(k,n;\mathbb{F})$ equipped with the ρ-warped metric. The unweighted principal-angle metric is recovered as the special case $\rho_i = 1$.

For constant weights in a fixed principal-angle chart, Eq. 2.9gives the corresponding weighted Grassmannian distance. When the weights ρ_i vary over the Grassmannian, Eq. (2.9) should be read as the local quadratic form on tangent directions; the global distance is then the infimum of the associated path length. Thus, the underlying configuration space is unchanged, but the closure-relevant metric structure is locally rescaled by sector capacities and mixed-capacity data [23].

2.4.5 Flags as multi-scale laminations

Many constructions require *nested* coherence structure: e.g., a coarse coherent selection that contains finer sub-selections that carry different support degrees (edges vs hinges vs faces). The appropriate configuration space is then a flag manifold:

$$\mathcal{F}(n_1,\dots,n_m;n) \;=\; \{\, V_1 \subset V_2 \subset \cdots \subset V_m \subset \mathbb{C}^n \,:\, \dim\, V_j = n_j \,\}. \tag{2.10}$$

In relational terms, a flag is a lamination: a hierarchy of coherent participation levels. "Observer experience" is modeled as a stable admissible lamination (or family of laminations) whose relative orientation is fixed up to RCC-admissible *re-expression*.

2.4.6 Bridge to geometric algebra

Geometric algebra (GA) represents a k-plane V by a blade A_V (a k-vector), and relative orientation by rotors acting by conjugation. Principal angles correspond to the canonical decomposition of the rotor generator into commuting bivector planes. Thus:

- Grassmannians provide the global manifold of subspace selections and their distances.
- GA provides the local, computationally natural language of subspace objects (blades) and transformations (rotors).

This is the core reason GA and Grassmannian geometry are not two independent choices; they are two complementary descriptions of the same relational content. This identification is the Plücker viewpoint in GA form: decomposable k-vectors (modulo nonzero scale) represent Grassmannian points, and the Plücker relations can be expressed directly in geometric-algebra language. [12] (See Appendix C for the complex → real Grassmannian projection underlying this identification.)

2.5 Regge Discretization as Constraint Skeleton

To make global closure explicit and computable, a simplicial constraint skeleton is introduced on which closure relations can be written finitely, using Regge-style bookkeeping for curvature and boundary consistency. [24] Regge discretization is employed as a representational scaffold for closure bookkeeping, not as an ontic discretization of spacetime. Geometric algebra then packages these closure relations into blades and rotors, rendering the closure constraints algebraic rather than geometric.

Here it is essential to distinguish representational bookkeeping from ontology. Discrete or simplicial structures—including Regge-style constructions—have historically been introduced as "pre-geometric" frameworks, yet typically reintroduce geometric notions once distances, magnitudes, or metric relations are treated as fundamental; the present framework avoids this by treating all geometric structure strictly as projection-level representation rather than ontic substrate. [25]

2.5.1 Discrete coherence manifold and hinge curvature

When continuum comparisons are invoked, we assume the standard Regge convergence regime in which deficit angles scale as $\epsilon_h = \mathcal{O}(h^2)$ under shape-regular refinement. Let $\mathcal{T}$ be a triangulation of the 4D coherence manifold by 4-simplices. Curvature is concentrated on hinges h (triangles in 4D Regge calculus). If $\Theta_{h,t}$ are dihedral angles around hinge h contributed by each incident 4-simplex t, define the deficit

$$\epsilon_h \;=\; \alpha_n \;-\; \sum_{t \supset h} \Theta_{h,t}, \tag{2.11}$$

with α_h the flat closure value appropriate to the hinge signature and triangulation convention. For spacelike rotational hinges in the usual Regge sector, $\epsilon_h^{\mathrm{rot}} = 2\pi - \sum_{t \supset h} \Theta_{h,t}$. For timelike or boost-type hinges we use signed rapidity contributions in $\mathrm{Spin}(1,3)$, with flat boost closure convention $\epsilon_h^{\mathrm{boost}} = -\sum_{t \supset h} \eta_{h,t}$, equivalently $\alpha_h^{\mathrm{boost}} = 0$ in the signed-rapidity convention. In all signatures, ϵ_h denotes the signed closure defect, while $\vartheta_h := |\, \epsilon_h \,|$ denotes the nonnegative magnitude used in the curvature kernel $\mathcal{K}(\vartheta_h; \sigma_h)$. See also Regge convergence and lattice-gravity measure treatments. [26]

A Regge-style coherence/curvature functional weighted by hinge capacities C_h is defined:

$$S_R \;=\; \sum_h C_h \;\epsilon_h. \tag{2.12}$$

In the standard four-dimensional Regge–Einstein-Hilbert correspondence, the continuum scalar-curvature integral is conventionally related by $\int_{\mathcal{M}} R\, dV \sim 2 \sum_h A_h\, \epsilon_h$, up to boundary

terms and convention-dependent normalization. In this paper the factor of 2 may be absorbed into the capacity weight C_h when the hinge sum is used as a normalized coherence ledger. Whenever comparison with the continuum Einstein-Hilbert normalization is intended, the factor is restored explicitly.

In the gravitational sector we take $C_h \equiv A_h$ (hinge areas) unless stated otherwise; C_h is retained only when we treat hinge weights abstractly. (Here "capacity" means the mode-specific budget weight assigned to that support class.)

2.5.2 GA representation: blades, bivectors, and hinge holonomy

Represent a k-simplex σ_k by its oriented edge vectors $\{e_i\}$ and the blade

$$A_{\sigma_k} \;=\; e_1 \wedge \cdots \wedge e_k, \tag{2.13}$$

whose magnitude is the k-volume. A_{σ_k} is used when referring to the blade associated with a specific simplex σ_k; A_k denotes a generic k-blade used in algebraic identities.

For a given hinge h, the rotation/boost needed to map one incident 4-simplex frame to the next is encoded by a rotor

$$R_{t\to t'} \;=\; \exp\left(-\frac{1}{2}\,\theta_{h;(t,t')}\,\hat{B}_h\right), \tag{2.14}$$

where $\hat{B}_h$ is the unit bivector in the hinge plane, and $\theta_{h;(t,t')}$ is the dihedral "turn" between frames.

The holonomy rotor around hinge h is the ordered product of the local rotors:

$$R_h \;=\; \prod_{(t,t')\ \text{around}\ h} R_{t\to t'}. \tag{2.15}$$

The product in (2.15) is taken in the oriented traversal order around the dual loop linking hinge h (orientation inherited from the simplicial complex). In Lorentzian signature the factors need not commute, hence the ordered product is essential. Changing the starting simplex on the loop conjugates R_h by a local rotor, leaving conjugacy-class invariants (and the effective generator magnitude that encodes ϵ_h in the small-curvature regime) unchanged. In the small-curvature regime, R_h encodes the deficit ϵ_h as its effective generator magnitude; in the non-perturbative regime it still serves as the correct group-valued curvature datum.

For Lorentzian loops, the ordered product is taken in the corresponding $\mathrm{Spin}(1,3)$ representation. The traversal orientation is inherited from the oriented dual loop linking the

hinge. Changing the base simplex conjugates the holonomy rotor and therefore preserves conjugacy-class data, including the effective rapidity or rotation magnitude used in the Regge closure ledger.

Treating discrete curvature as group-valued holonomy around simplicial loops is standard in piecewise-flat (Regge) geometry. Closely related "discrete connection" formalisms in geometry processing likewise express curvature/compatibility as holonomy of a discrete parallel transport rule around mesh loops, providing practical computational precedent for the same holonomy bookkeeping step. [10] [27]

To treat spacelike (rotational) and timelike (boost) hinges uniformly, signature-uniform notation is used: a unified "angle" $\vartheta_h \geq 0$ (angle or rapidity) and a nonnegative curvature kernel $\mathcal{K}(\vartheta_h; \sigma_h)$ satisfying $\mathcal{K} \sim \frac{1}{2}\vartheta_h^2$ for small ϑ_h in either signature. We reserve ϵ_h for the signed Regge deficit (closure bookkeeping) and use $\vartheta_h \geq 0$ for the corresponding magnitude (angle/rapidity) entering the kernel $\mathcal{K}(\vartheta_h; \sigma_h)$.

2.5.3 Scalar coherence field as block-level curvature-density invariant

A convenient global scalar coherence measure is obtained by averaging the hinge curvature kernel. It is represented in the Regge/GA scaffold, not an additional ontic field. Here it is;

$$\mathcal{C} = \frac{1}{N_h}\sum_{h\in\mathcal{H}} \mathcal{K}(\vartheta_h; \sigma_h), \qquad \mathcal{C}_{aw} = \frac{1}{\sum_h A_h}\sum_{h\in\mathcal{H}} A_h\ \mathcal{K}(\vartheta_h; \sigma_h), \tag{2.16}$$

where A_h are hinge areas (or hinge weights/capacities, depending on convention) and $\mathcal{C}_{aw}$ denotes the area-weighted curvature/coherence scalar (weighted by hinge areas A_h).

For small deficits, $\mathcal{K}(\vartheta_h; \sigma_h) \approx \frac{1}{2}\vartheta_h^2$, giving the expected quadratic curvature energy approximation.

$\mathcal{C}$ is a scalar diagnostic of curvature-density in the Regge/GA representation of the closed block. It is not an additional ontic field. It records how curvature/coherence density is represented in a chosen scaffold, while ontic admissibility remains fixed by AGC-defined closure.

2.5.4 Computational form: objective + RCC constraints + rotor relaxation

In practice, an RCC-admissible triangulation/assignment is characterized as a stationary configuration of a budget functional subject to closure constraints. Two standard objective choices are:

- L^1 budget: $\Delta = \sum_h |\,\epsilon_h\,|$.

- L^2 budget (preferred for smooth optimization):

$$\mathcal{J}_{L_2} = \frac{1}{2}\sum_h C_h\ \epsilon_h^2 \sim \frac{1}{2}\sum_{(t,t')\sim h} \tilde{C}_h\ d_\rho^2(t,t' \mid h). \tag{2.17}$$

The constraints are the RCCs (topological closure, symmetry closure, admissible bounds, etc.). Mathematically, admissible configurations are those in which the rotor and frame assignments jointly minimize the hinge-defect (or kernel-cost) functional subject to projection onto the admissible set.

2.6 Projective normalization, invariant ratios, and the capacity tensor

In the local linearized restoration setting of PRG and CRG [add G06 reference number here], the sector-capacity tensor Ξ is represented by the positive-definite metric tensor κon admissibility-correction directions. In a diagonal Grassmannian basis, the eigenvalues of this metric are the warp weights ρ_i. Thus Ξ, κ, and ρ_i are layer-specific representations of the same capacity structure, not separate primitives.

Throughout this section, abstract sector indices α, β are used interchangeably with semantic sector labels. Table 2.1 summarizes this correspondence and the associated Regge support classes.

Table 2.1— Sector index, semantic label, and Regge support

Index α	Sector label	Regge support class	Role in coherence ledger
1	rot	Spacelike hinges	Geometric curvature / rotational holonomy
2	boost	Timelike hinges	Causal structure / rapidity benchmark
3	edge	Edges (1-skeleton)	Quantum phase / holonomy granularity
4	face	Timelike 3-faces (dual 3-cells)	Flux, entropy, thermodynamic participation
5	spatial	Spatial 3-faces	Spatial orientation / volume closure

2.6.1 Baseline normalization and the five diagonal sector capacities

The model assigns five diagonal sector capacities (global self-budgets) associated with the Regge support classes [23]:

- rot — spacelike hinge curvature (rotational sector)
- boost — timelike hinge structure (causal sector)
- edge — phase/holonomy granularity (quantum sector)
- face — flux/entropy participation (thermodynamic sector)
- spatial — orientation/volume closure (spatial sector)

A coherence baseline $\mathbb{I}_0$ is introduced, and normalized diagonal ratios are defined as:

$$J_{\text{rot}} = \frac{\Xi_{\text{rot}}}{\mathbb{I}_0}, \qquad J_{\text{boost}} = \frac{\Xi_{\text{boost}}}{\mathbb{I}_0}, \qquad J_{\text{edge}} = \frac{\Xi_{\text{edge}}}{\mathbb{I}_0}, \qquad J_{\text{face}} = \frac{\Xi_{\text{face}}}{\mathbb{I}_0}, \qquad J_{\text{spatial}} = \frac{\Xi_{\text{spatial}}}{\mathbb{I}_0}. \tag{2.18}$$

These J_α are not ontic constants but normalized coherence budgets attached to specific relational supports. The baseline $\mathbb{I}_0$ enforces projective normalization, ensuring that only ratios are physically meaningful. Under global rescaling $\Xi_\alpha \mapsto \lambda \Xi_\alpha$, $\mathbb{I}_0 \mapsto \lambda \mathbb{I}_0$, all observable ratios remain invariant.

Convention on h and $\hbar$

In the NPRF lineage associated with RBW, we use Planck's constant h, following the c, h, G invariant-constraint framing. The reduced constant $\hbar = \frac{h}{2\pi}$ is used only where a reduced-action normalization is explicitly intended, such as in standard quantum or black-hole thermodynamic formulas.

This invariance expresses no preferred reference frame (NPRF) as projective symmetry: no global normalization is physically privileged.

2.6.2 Projective translation ratios and Regge supports

Phenomenologically accessible quantities arise as ratios of the normalized capacities:

$$c^2 \propto \frac{J_{\text{rot}}}{J_{\text{boost}}}, \qquad h \propto \frac{J_{\text{edge}}}{J_{\text{boost}}}, \qquad G \propto \frac{J_{\text{rot}}}{J_{\text{spatial}}}, \qquad k_B \propto \frac{J_{\text{face}}}{J_{\text{boost}}}, \qquad \lambda_3 \propto \frac{J_{\text{face}}}{J_{\text{spatial}}}. \tag{2.19}$$

These relations define dimensionless projective readouts associated with the corresponding physical constants, not direct dimensional equalities and not derivations of the numerical constants in the dynamical sense. The physical magnitudes require the reference-scale convention described in Appendix G.4. The k_B and λ_3 entries are cRBW sector-capacity extensions beyond the RBW c, h, G invariant lineage. The edge/boost capacity ratio, for example, identifies the dimensionless quantum-sector normalization associated with action-scale readout. The universality of the reduced action scale $\hbar$ as a physical constant is established elsewhere in the framework.

The essential point is structural: all observable quantities are projective ratios, and the baseline $\mathbb{I}_0$ cancels identically.

The following translation Table 2.2 is the conceptual hinge of the model: each invariant is a projective ratio of capacities, and each ratio corresponds to a specific pairing of supports. Capacity couplings do not represent interactions or mechanisms; they encode joint admissibility, or alignment, constraints among closure conditions.

Table 2.2 – Projective Translation Ratios and Their Regge Couplings

Ratio	Sector correspondence	Regge coupling	Invariant	Description
$\frac{J_{\text{rot}}}{J_{\text{boost}}}$	Geometric (rotation) ↔ Causal (boost)	Spacelike hinges ↔ Timelike hinges	c^2	Compares rotational vs. boost hinge moduli; projective readout associated with the null-structure ratio; physical light-cone normalization requires a reference-scale convention.
$\frac{J_{\text{edge}}}{J_{\text{boost}}}$	Quantum ↔ Causal	Edges (phase/holonomy) ↔ Timelike hinges (temporal benchmark)	h	Edge phase granularity relative to a causal benchmark; projective readout associated with Planck's constant h. Reduced-action normalizations use $\hbar = h/2\pi$ only when explicitly stated.
$\frac{J_{\text{rot}}}{J_{\text{spatial}}}$	Geometric ↔ Spatial	Spacelike hinges (curvature) ↔ Spatial 3-faces (orientation/3-volume)	G	Curvature strength relative to spatial orientation/volume; projective readout associated with gravitational coupling.
$\frac{J_{\text{face}}}{J_{\text{boost}}}$	Thermodynamic ↔ Causal	Time-like 3-faces (flux; "dual 3-cells") ↔ Timelike hinges (temporal benchmark)	k_B	projective readout associated with thermodynamic entropy/energy-flux scale relative to a causal benchmark.
$\frac{J_{\text{face}}}{J_{\text{spatial}}}$	Thermodynamic ↔ Spatial	Timelike 3-faces (flux) ↔ Spatial 3-faces (orientation/3-volume)	λ_3	Spatial closure/orientation stabilized by flux; cosmological-constant role as a projective spatial-legibility invariant associated with spatial closure/orientation; its cosmological-constant role is a downstream interpretation.

Notes.

1. "Sector correspondence" names the relational roles; "Regge coupling" names the supports whose normalized capacities form each ratio.

2. The linear (L1) convention is adopted: c^2 is reported, not c, so no square roots appear at the level of fundamental ratios. Taking $c = \sqrt{J_{\mathrm{rot}}/J_{\mathrm{boost}}}$ is a downstream readout choice.

2.6.3 The capacity tensor and cross-sector coupling

The normalized capacity tensor is defined as:

$$\hat{\Xi}_{\alpha\beta} = J_\alpha \, \delta_{\alpha\beta} \; + \; K_{\alpha\beta} \, (1 - \delta_{\alpha\beta}) \tag{2.20}$$

Where the normalized capacity tensor therefore splits into diagonal and off-diagonal components:

- J_α: diagonal self-budgets
- $K_{\alpha\beta}$: cross-capacities (overlap constraints)

Intuitively, J_α measures how much a given mode can coherently support by itself, while $K_{\alpha\beta}$ measures the degree to which two modes must share support in order for the configuration to remain globally admissible under closure. The off-diagonal terms $K_{\alpha\beta}$ encode **joint admissibility constraints**, not interaction mechanisms. They ensure that the five sectors form a single globally consistent structure rather than independent subsystems.

2.6.4 Sufficiency and working minimality of the five diagonal sectors

The support/mode list {rot,boost,edge,face,spatial} is treated here as a working minimal and sufficient set for the Regge-supported geometric/phenomenological ledger. Each diagonal channel plays a distinct role in closing the modeled coherence ledger on the Regge skeleton:

- rotational/curvature closure (rot)
- causal/boost closure (boost)
- phase/holonomy granularity (edge)
- flux/entropy participation (face)
- spatial orientation/volume closure (spatial)

No additional independent diagonal sector is required for the five-sector scaffold developed in this paper. This is a modeling sufficiency claim, not a proof of absolute irredundancy. Extensions, such as internal coherence sectors, may add further diagonal modes while preserving the same projective normalization and capacity-tensor logic.

Roles of the Off-Diagonal $K_{\alpha\beta}$

For a given simplicial support x(hinge, edge, 3-face, or 4-simplex volume), the local mixed capacity is defined as a weighted overlap of the sector-specific relational increments. Each $K_{\alpha\beta}[x]$ is *a projected overlap of curvature/flux vectors* on a *specific* simplicial support x (hinge, edge, 3-face, 4-volume):

$$K_{\alpha\beta}[x] = w_x^{(\alpha,\beta)} \, (\Delta\phi_x^{(\alpha)} \cdot \Delta\phi_x^{(\beta)}). \tag{2.21}$$

This defines $K_{\alpha\beta}[x]$ as a cross-capacity density: the portion of the mode-α requirement that is simultaneously satisfied by mode β on the same support. The off-diagonal terms do not represent interactions or dynamical couplings; they encode joint admissibility constraints among relational modes required for global closure.

In parity-even configurations, $K_{\alpha\beta} = K_{\beta\alpha}$; any orientation dependence is handled separately by support orientation conventions (cf. Appendix F).

Ontic function (relational binding)
Off-diagonals are the binding terms that enforce joint admissibility. They ensure that curvature, phase, flux, and orientation do not form five independent sub-lattices, but a *single closed manifold*. Nonzero $K_{\alpha\beta}$ is the structural signature of joint admissibility among relational modes.

Phenomenological appearance
For an embedded observer, $K_{\alpha\beta}$ sets the *degree of inter-sector coupling*:

- Persistent, bounded $K_{\alpha\beta}$: stable mixed-capacity phenomena, including entanglement-like cross-sector alignment where an independent quantum-state or density-operator model supports that interpretation.
- Weakly differentiated $K_{\alpha\beta}$ across admissible configurations: weak interactions / near-classical regimes.
- Strongly suppressed (App. F) $K_{\alpha\beta}$ under closure constraints: effective independence (classical limit).

(From an embedded, coarse-grained description, these distinctions correspond to what would be described as “slowly varying” or “rapidly decaying” couplings, though no temporal evolution is assumed in the blockworld description.) Through chain composition (Eq. 2.28) the off-diagonals determine finite coherence range and provide a diagnostic threshold $K_{\text{eff}} > \Gamma$ for entanglement-like cross-sector coherence. This is not by itself a proof of quantum-information entanglement; such a proof would require a corresponding state or density-operator mapping.

Remark (Projective neutrality / first-order stability of the NPRF ratios).

In this framework, NPRF reflects projection-invariant closure prior to any spacetime interpretation, rather than a symmetry postulated on spacetime itself. The NPRF ratios are defined from the diagonal sector capacities (Eq. 2.18), so they do not depend algebraically on the mixed capacities $K_{\mu\nu}$. Moreover, for admissible perturbations of the off-diagonal channels, the induced renormalization of the diagonal equilibrium enters only at higher order, so the NPRF ratios are first-order stable under cross-mode coupling. This justifies treating $\{c^2, h, G, k_B, \lambda_3\}$ as robust projective readouts even when mixed-capacity warping is present.

Variational role (within stationarity)

Box 2.1—Configuration space for stationarity.

In this manuscript, the stationarity condition $\delta\mathcal{I}_C = 0$ is taken over admissible representational assignments on a fixed triangulation $\mathcal{T}$: rotor/frame variables (and equivalently local subspace representatives $U(x) \in \mathrm{Gr}(k,n)$) subject to RCC constraints. The diagonal ratios J_α are treated as global parameters (projective readouts), while mixed capacities $K_{\alpha\beta}[x]$ are treated as derived overlap densities determined by the local relational increments $\Delta\phi_x^{(\alpha)}$. Thus Eq. (2.22) is a stationarity condition on admissible overlap degrees (no uncompensated cross-mode leakage), not an independent variational field equation for arbitrary K.

In the stationarity condition $\delta\mathcal{I}_C = 0$, the off-diagonals provide off-diagonal stiffness: they suppress any net "coherence flux" between modes that would open a boundary or violate RCC constraints. At a stationary solution,

$$\frac{\partial\mathcal{I}_C}{\partial K_{\alpha\beta}} = 0 \Rightarrow \text{no net cross-mode drift at that support.} \tag{2.22}$$

Strictly, Eq. (2.22) is a constrained stationarity statement: the variation is taken with respect to admissible relational increments $\Delta\phi_x^{(\alpha)}$, subject to the definition of the derived overlap densities $K_{\alpha\beta}[x]$. It is not an independent unconstrained variation over arbitrary $K_{\alpha\beta}$ fields.

Where they live (support intersections)

Each $K_{\alpha\beta}$ draws its dominant weight from intersections of the supports of α and β. Examples:

- Rot ↔ edge (spacelike-hinge ↔ edge): hinge–edge intersections; gravitational–quantum channel used in BMV-type setups.
- Face ↔ boost (timelike-3-face ↔ timelike-hinge): flux vs. causal benchmark (Tolman-type relations).

- Face ↔ spatial (timelike-3-face ↔ spatial-3-face): thermodynamic vs. spatial orientation; enters the λ_3 channel.

2.6.5 Variational structure and closure functional

The total closure budget of the configuration is encoded by a global functional defined over admissible representations of the relational structure. On a triangulation $\mathcal{T}$ (with hinges $\mathcal{H}$, edges E, bulk 4-volume V, and timelike boundary $\partial\mathcal{M}_t$), define the projective coherence functional:

$$\mathcal{I}_{\mathcal{C}}[J \mid \mathcal{T}] = (J_{\mathrm{rot}} + J_{\mathrm{face}}) \sum_{h\in\mathcal{H}} A_h \epsilon_h - J_{\mathrm{edge}} \int_E d\ell - J_{\mathrm{spatial}} \int_V \mathcal{R}\, dV + J_{\mathrm{boost}} \oint_{\partial\mathcal{M}_t} \mathcal{N}\, d\Sigma_t + J_{\mathrm{face}} \int_{\mathcal{M}} \lambda_3\,(x) d\omega_3 \tag{2.23}$$

Here:

- $A_h\epsilon_h$ is the discrete curvature ledger (Regge hinge deficit bookkeeping),
- $\int_E d\ell$ is the edge/phase contribution (written as an integral over the 1-skeleton; equivalently a sum $\sum_{e\in E} \ell_e$),
- $\int_V \mathcal{R}\, dV$ is the continuum curvature,
- $\mathcal{N} \equiv n_a \Phi^a$ is the causal-coherence boundary one-form (outward normal covector n_a contracted with the coherence-flux field Φ^a),
- $\lambda_3(x)$ is a Lagrange multiplier field enforcing the 3-form closure/orientation constraint on $d\omega_3$.

Here $\mathcal{I}_C[J \mid \mathcal{T}]$ denotes the **projective normalized coherence functional**, depending only on the normalized ratios $J_\alpha = \frac{\Xi_\alpha}{\mathbb{I}_0}$. An unnormalized precursor $\tilde{\mathcal{I}}_C[\Xi, \mathbb{I}_0 \mid \mathcal{T}]$ may be used for dimensional bookkeeping prior to normalization. The normalized $\mathcal{I}_C$ is degree zero under simultaneous rescaling of Ξ and $\mathbb{I}_0$, while $\tilde{\mathcal{I}}_C$ is homogeneous of degree one before quotienting by the projective baseline. The hinge term is written in manifestly projective form. The compact form $(1 + J_{\mathrm{face}}) \sum_h A_h\, \epsilon_h$ is the gauge $J_{\mathrm{rot}} = 1$ within the hinge-ledger normalization. This gauge does not remove J_{rot} as a free projective ratio in the readouts of Eq. (2.19).

Two structural clarifications that prevent confusion:

Regge sum vs bulk integral
Under standard refinement assumptions, the Regge curvature measure satisfies the usual convention-dependent correspondence $2 \sum_h A_h\, \epsilon_h \longrightarrow \int_{\mathcal{M}} \mathcal{R}\, dV$ in the weak or measure sense. In the normalized coherence ledger used here, the factor of two may be absorbed into the hinge capacity weight; the normalization convention should be held fixed within

any given calculation. When evaluating the functional in a given regime, the appropriate representation is used; they are not double-counted by treating them as independent contributions. Whenever a continuum comparison is invoked, we assume a shape-regular refinement family and the usual Regge weak-convergence hypotheses (bounded aspect ratio; sufficiently regular limiting geometry); these remarks are motivational/consistency checks for the representational bookkeeping, not a new ontic discretization postulate. The implicit measure conversion is made explicit by the projective normalization discussed in Appendix G.

Gauge-fixed hinge coefficient

The manifestly projective hinge coefficient is $J_{\mathrm{rot}} + J_{\mathrm{face}}$. In prior versions $1 + J_{\mathrm{face}}$ is the projective gauge $J_{\mathrm{rot}} = 1$. It is a convenient hinge-ledger normalization, but the ungauged expression should be used wherever the constant readouts$c^2 \propto \frac{J_{\mathrm{rot}}}{J_{\mathrm{boost}}}$, $G \propto \frac{J_{\mathrm{rot}}}{J_{\mathrm{spatial}}}$ are being discussed.

Stationarity and admissibility

Admissible configurations are defined by the stationarity condition:

$$\delta \mathcal{I}_{\mathcal{C}} = 0 \text{ subject to RCC admissibility.} \tag{2.24}$$

Here the variation is taken over representational degrees of freedom—such as local frame assignments, rotor fields, or subspace selections—on a fixed triangulation $\mathcal{T}$. The diagonal ratios J_α are treated as global parameters, while the cross-capacities $K_{\alpha\beta}[x]$ arise as derived overlap densities determined by local relational increments.

This stationarity condition does not define dynamical evolution. It selects configurations that satisfy global closure constraints under admissible representations.

Regge Cells and Cross-Cell Coupling

A Regge cell is one 4-simplex of the discretized coherence manifold—the fundamental local region in which relational capacities are evaluated. Each cell σ carries: its own set of *self-capacities* $\Xi_{\alpha\alpha}[\sigma]$ (the diagonal budgets on its hinges, edges, and faces), and a network of *cross-capacities* $K_{\alpha\beta}[\sigma]$ linking those modes across the cell's internal supports, (cf. Table 2.3).

From the global viewpoint, the blockworld is a tessellation of such cells whose capacities must satisfy closure and continuity on shared boundaries. Two cells σ and σ' are said to be *adjacent* when they share a common face (a 3-simplex) $f = \sigma \cap \sigma'$. Across that shared face:

$$K_{\alpha\beta}[\sigma] \;\leftrightarrow\; K_{\alpha\beta}[\sigma'] \tag{2.25}$$

denote the mutually induced mixed capacities; a *projected overlap density* on shared supports. Their equality (up to orientation sign) ensures that coherence budgets are handed off consistently from one cell to the next, maintaining RCC-5 boundary consistency.

Interface coupling

Within a single cell, $K_{\alpha\beta}[\sigma]$ quantifies how two modes overlap on internal supports. Between cells, the same pair of modes can *relate* their overlap through the shared boundary:

$$K_{\alpha\beta}(f) = \frac{1}{2}(K_{\alpha\beta}[\sigma] + K_{\alpha\beta}[\sigma']), \tag{2.26}$$

so $K_{\alpha\beta}(f)$ acts as the *interface coupling*; the amount of cross-mode coherence that continues smoothly across the lattice. Large $K_{\alpha\beta}(f)$ values indicate strong inter-cell coherence (entangled regions); small values signal local decoherence or geometric isolation. In the absence of parity-breaking or orientation-dependent effects, the mixed capacities satisfy $K_{\alpha\beta} = K_{\beta\alpha}$ by construction, reflecting reciprocal overlap on shared supports. The symmetric averaging in Eq. (2.26) enforces boundary continuity rather than introducing independent directional couplings.

Boundary stationarity condition

Stationarity of the global functional $\delta\mathcal{I}_C = 0$ implies continuity of cross-capacity flow across shared interfaces. For adjacent cells σ and σ' sharing a face $f = \sigma \cap \sigma'$, this yields

$$\sum_{f=\sigma\cap\sigma'} (K_{\alpha\beta}[\sigma] - K_{\alpha\beta}[\sigma'])\, n_f = 0, \tag{2.27}$$

where n_f is the oriented normal to the shared face. This equation enforces continuity of cross-mode flux between adjacent cells: no net coherence is lost or created at boundaries. In physical terms, it is the discrete analogue of "no flux of entanglement through a closed surface." This condition arises from the vanishing of boundary variation terms in $\delta\mathcal{I}_C$ associated with mixed-capacity handoff across shared faces, and expresses conservation of coherence flux at stationary admissible configurations.

This condition enforces boundary consistency of admissibility: cross-capacities must match across shared supports so that no mismatch accumulates at interfaces. In representational terms, it ensures that coherence budgets are transferred consistently between neighboring cells.

Importantly, this is not a dynamical conservation law. It is a constraint on admissible configurations arising from the global closure condition: no open boundary or discontinuity in the coherence ledger is permitted.

Chain composition and coherence range

Along a path of cells $\gamma = (\sigma_1, \dots, \sigma_N)$, the successive hand-offs of $K_{\alpha\beta}$ across faces compose multiplicatively:

$$K_{\text{eff}}(\gamma) = \prod_{i=1}^{N-1} \| K_{\alpha\beta}(f_i) \|, \tag{2.28}$$

producing the exponential attenuation law of Eq. (2.31). The coherence range of a given cross-mode channel is therefore finite and determined by how well the $K_{\alpha\beta}$ values align across adjacent Regge cells.

Table 2.3 — Role of K Terms Across the Model

Aspect	Role of $K_{\alpha\beta}$
Within a cell	Quantifies internal overlap of two relational modes on that cell's supports.
Across cells	Serves as the coherence-transfer coefficient through shared faces.
Stationarity condition	Equalizes $K_{\alpha\beta}$ across boundaries (no open coherence flux).
Chain composition	Successive $K_{\alpha\beta}$ transfers define finite coherence/entanglement range.
Physical reading	Measures how strongly adjacent regions of the blockworld remain mutually entangled.

2.6.6 The normalized capacity tensor: diagonals and mixed capacities

Diagonal budgets alone do not produce a globally admissible configuration; they would permit five independent sectors that merely coexist without satisfying joint closure constraints. The unification of the structure is therefore carried by the capacity tensor, which encodes both self-budgets and cross-sector admissibility conditions.

The normalized capacity tensor splits into:

- **diagonal terms** J_α: global self-budgets for each sector
- **off-diagonal terms** $K_{\alpha\beta}$: local cross-capacities enforcing shared support conditions

In the ordered basis (*rot, boost, edge, face, spatial*), the tensor takes the form,

$$\hat{\Xi} = \begin{bmatrix} J_{\text{rot}} & K_{\text{rot,boost}} & K_{\text{rot,edge}} & K_{\text{rot,face}} & K_{\text{rot,spatial}} \\ K_{\text{rot,boost}} & J_{\text{boost}} & K_{\text{boost,edge}} & K_{\text{boost,face}} & K_{\text{boost,spatial}} \\ K_{\text{rot,edge}} & K_{\text{boost,edge}} & J_{\text{edge}} & K_{\text{edge,face}} & K_{\text{edge,spatial}} \\ K_{\text{rot,face}} & K_{\text{boost,face}} & K_{\text{edge,face}} & J_{\text{face}} & K_{\text{face,spatial}} \\ K_{\text{rot,spatial}} & K_{\text{boost,spatial}} & K_{\text{edge,spatial}} & K_{\text{face,spatial}} & J_{\text{spatial}} \end{bmatrix} \tag{2.29}$$

Equivalently, in compact form, see Equ. (2.20).

The off-diagonal entries $K_{\alpha\beta}$ are treated explicitly as cross-capacities, rather than as generic coupling strengths. Their role is to enforce joint admissibility across sectors: they encode how relational modes must align on shared supports in order for the global configuration to satisfy closure.

2.6.7 Regge cells and cross-cell coupling (handoff across faces)

A Regge cell is a single 4-simplex σin the discretized coherence manifold, serving as the fundamental local region in which relational capacities are evaluated. Each cell carries:

- diagonal self-capacities $J_\alpha[\sigma]$, defined on its hinges, edges, and faces, and
- cross-capacities $K_{\alpha\beta}[\sigma]$, encoding overlap constraints among relational modes on its internal supports.

Two cells σ and σ' are adjacent when they share a common 3-simplex face $f = \sigma \cap \sigma'$. Across this shared interface, mixed capacities must be matched consistently to preserve admissibility. The interface coupling is defined by Eq. (2.26).

The magnitude of $K_{\alpha\beta}(f)$ reflects the degree of cross-sector alignment across the interface:

- larger values correspond to strong coherence alignment between adjacent cells,
- smaller values correspond to weak alignment or effective decoupling.

RCC boundary consistency requires that these cross-capacities agree across shared supports (up to orientation sign), ensuring that admissibility is preserved across the lattice. This matching condition prevents discontinuities in the closure ledger: relational modes must align consistently across adjacent cells in order for the global configuration to remain admissible.

2.6.8 Chain composition, finite coherence range, and the entanglement threshold

Along a path of adjacent simplices $\gamma = (\sigma_1, \ldots, \sigma_N)$, cross-capacities compose multiplicatively across shared interfaces. The effective mixed capacity over the chain is

$$K_{\mathrm{eff}}^{(\ell_0)}(\gamma) = \prod_{i=1}^{N-1} \| \, K_{\alpha\beta}^{(\ell_0)}(f_i) \, \|. \tag{2.30}$$

Eq. (2.28) gives the abstract chain-composition rule. Eq. (2.30) is the same rule evaluated at a fixed coarse-graining scale ℓ_0, so that thresholds and traversal depth are compared at a fixed resolution. This avoids treating K_{eff} as triangulation-invariant without a coarse-graining convention.

If local couplings are uniformly bounded by $\| \, K_{\alpha\beta}(f_i) \, \| \leq \kappa < 1$, then the effective mixed capacity along a chain of simplicial depth N satisfies

$$K_{\mathrm{eff}}^{(\ell_0)}(\gamma) \leq \kappa^{N-1} = e^{-(N-1)\ln(1/\kappa)}. \tag{2.31}$$

The factors $K_{\alpha\beta}(f_i)$ are dimensionless normalized transfer coefficients. Under refinement, the threshold Γ and chain length N must be interpreted relative to a fixed coarse-graining scale or renormalized traversal depth; otherwise K_{eff} becomes triangulation-dependent.

This defines a finite coherence range: cross-sector alignment decreases exponentially with simplicial depth. This behavior arises as a structural consequence of closure constraints on admissible configurations, not from any dynamical propagation.

To characterize when cross-sector alignment remains phenomenologically significant, introduce a *dimensionless threshold* Γ. Then:

$$\begin{aligned} &K_{\mathrm{eff}}^{(\ell_0)}(\gamma) > \Gamma \\ &\Rightarrow \text{ entanglement-like cross-sector coherence is diagnostically supported,} \\ &K_{\mathrm{eff}}^{(\ell_0)}(\gamma) \leq \Gamma \\ &\Rightarrow \text{ the mixed channel is effectively decoupled at the chosen coarse-graining.} \end{aligned} \tag{2.32}$$

In phenomenological terms, the regime $K_{\mathrm{eff}}^{(\ell_0)}(\gamma) > \Gamma$ marks a structural diagnostic for entanglement-like correlations. It does not, by itself, prove quantum-information entanglement. A full entanglement claim requires an additional state-space or density-operator interpretation compatible with the relevant experimental setting. This provides a closure-first account of crossover behavior (e.g., BMV-type scenarios), in which the persistence or suppression of correlations is determined by admissibility structure rather than by time-evolution.

Mixed-capacity support classes

Mixed-capacity channels are defined on the same support classes as the diagonal sectors, corresponding to loci where cross-sector overlap is possible:

- h: hinges (rotation/boost curvature coupling),

- e: edges (quantum-phase interaction),
- f_t: timelike 3-faces (thermodynamic/flux overlap),
- f_s: spatial 3-faces (orientation/volume overlap),
- v: 4-volume cells (global constraint density channel).

These supports define where cross-capacity terms contribute to admissibility conditions in the closure ledger.

2.6.9 Capacity warping and the Kähler

Before introducing capacities, the complex Grassmannian $\mathrm{Gr}(k, n; \mathbb{C})$ with its Fubini–Study Hermitian metric g_{FS} is a compact Hermitian symmetric space with a canonical Kähler structure $(\mathcal{J}, \omega, g_{FS})$. This provides a maximally symmetric baseline geometry for subspace selections: geodesics are homogeneous and isotropic, and all directions are metrically equivalent.

The introduction of capacities deforms this baseline geometry.

- **Diagonal warping**
  Rescaling tangent directions associated with the sector decomposition induces an anisotropic metric $g' = W_{\mathrm{diag}} \cdot g_{\mathrm{FS}}$. This deformation remains Kähler only when the associated two-form remains closed and compatible with the complex structure. Constant diagonal warping in a compatible chart is the simplest case. In the generic position-dependent case, the safer description is anisotropic Hermitian, almost-Hermitian, or almost-Kähler, depending on which compatibility conditions are actually verified. For the standard classification of almost-Hermitian classes, see Gray and Hervella. [28]

- **Mixed warping**
  Mixed capacities introduce off-diagonal metric terms. If the mixed warping fails to commute with the complex structure, the pair $(g'', \mathcal{J})$ need not define a Hermitian structure unless the skew-symmetry and compatibility conditions for $\omega''(u, v) = g''(\mathcal{J}u, v)$ are imposed separately. We therefore treat the generic mixed-capacity case as a capacity-warped metric structure on the Grassmannian. The term “quasi-Kähler” is reserved for cases where the relevant Gray–Hervella conditions are explicitly verified.

Thus the safe hierarchy is:

$$\begin{aligned} &\text{symmetric Kähler baseline} \longrightarrow \text{anisotropic compatible deformation} \\ &\qquad\qquad \longrightarrow \text{generic mixed-capacity non-Kähler warped metric.} \end{aligned} \tag{2.33}$$

In the present framework, this hierarchy reflects the structure of admissibility:

- diagonal capacities encode directional stiffness or slack within individual sectors,
- off-diagonal capacities encode cross-sector alignment constraints and curvature of the admissible configuration space.

These geometric deformations do not introduce new ontological structure; they arise from the representation of closure constraints within the capacity-weighted Grassmannian.

2.6.10 Well-posedness of quasi-Kähler warping

Two distinct conditions must be separated:

- **BBP**: the boundary-operator expression of closure, $\partial^2 = 0$, which expresses AGC-defined admissibility in representations admitting a boundary operator. BBP is a derived expression of the Layer-0 AGC axiom, not an independent primitive.
- **Well-Posedness Condition (WPC)**: a geometric regularity condition ensuring that the capacity-warped configuration space remains a well-defined metric space (Layer 2).

WPC (Capacity regularity)
On compact $\mathrm{Gr}(k, n; \mathbb{C})$, assume the warping operator W satisfies:

1. smooth dependence on position and capacity parameters,
2. uniform positive-definiteness: eigenvalues of W lie in a bounded interval $[\lambda_{\min}, \lambda_{\max}]$ with $0 < \lambda_{\min} \leq \lambda_{\max} < \infty$,
3. bounded diagonal and mixed capacities, as required by RCC budget and stability constraints.

In the present framework, the warp weights are functions of local geometric diagnostics $\rho_i = \rho(\lambda_i)$ where λ_i may depend on quantities such as projected coherence gradients (e.g., $\lambda_i = \| \Pi_i \nabla C \|$). RCC conditions enforce boundedness:

- RCC-3 (budget bounds) constrains overall magnitude,
- RCC-8 (resonance stability) constrains fluctuations,
- RCC-9 excludes the degenerate case $\nabla C \equiv 0$.

Under these conditions, the weights ρ_i remain finite and strictly positive, ensuring that the warping operator satisfies WPC.

Under WPC, g'' is bi-Lipschitz equivalent to g_{FS}. Therefore, the induced metric space remains compact, and geodesic completeness follows in the metric sense. Classical bounded-curvature claims require the warping to be at least C^2; if ρ is only Lipschitz, one should state compactness and metric completeness, not smooth curvature boundedness.

Thus, quasi-Kähler deviations do not threaten global well-posedness: the geometry remains a proper metric space of selections, even when the complex/symplectic integrability properties are relaxed.

2.6.11 Variational realization of BBP and NPRF

In the Regge/chain language, BBP is the closure identity $\partial^2 = 0$, the boundary-operator expression that no open boundaries are admitted. It is a derived expression of AGC-defined admissibility, not a separate Layer-0 ontic condition.

In the variational formulation used here, admissible configurations are selected by the stationarity condition $\delta\mathcal{I}_{\mathcal{C}} = 0$. This condition is a representation-level test of compatibility of local representations with AGC-defined closure as expressed through BBP; it is not the origin or derivation of closure itself. The admissible variation class is restricted so that boundary-opening variations are excluded or contribute nonzero boundary terms, thereby violating closure. In this sense, stationarity is a **representation-level realization** of the underlying closure constraint, not its origin.

NPRF as projective invariance

The phenomenological invariants of the framework arise as ratios $J_\alpha = \Xi_\alpha / \mathbb{I}_0$ so a uniform rescaling $\Xi_\alpha \mapsto \lambda\Xi_\alpha,\ \mathbb{I}_0 \mapsto \lambda\mathbb{I}_0$ leaves both the coherence functional $\mathcal{I}_{\mathcal{C}}$ and all observable ratios invariant. This invariance defines the projective content of NPRF: no global normalization is physically distinguished, and all admissible representations yield the same invariant ratios.

Variational and flux formulations

There the variation is taken over admissible relational assignments on the Regge skeleton; boundary closure is enforced by stationarity rather than introducing an explicit boundary functional. The closure condition may be expressed in variational form as

$$\delta\mathcal{I}_C = 0, \tag{2.34}$$

with the understanding that this selects configurations consistent with global closure. Φ

Equivalently, introducing the boundary coherence one-form $\mathcal{N} \equiv n_a \Phi^a$ on $\partial\mathcal{M}$, Stokes' theorem gives (under standard Regge regularity assumptions),

$$\int_{\mathcal{M}} \nabla_a \Phi^a \, dV \;=\; \int_{\partial\mathcal{M}} \mathcal{N} \, d\Sigma. \tag{2.35}$$

For a closed manifold $\partial\mathcal{M} = 0$, this yields $\oint_{\partial\mathcal{M}} \mathcal{N} \, d\Sigma = 0$, expressing the absence of boundary contributions in the closure ledger.

We distinguish the unnormalized precursor from the projective functional. The unnormalized precursor is homogeneous of degree one: $\tilde{\mathcal{J}}_C(\alpha\Xi, \alpha\mathbb{I}_0 \mid \mathcal{T}) = \alpha\,\tilde{\mathcal{J}}_C(\Xi, \mathbb{I}_0 \mid \mathcal{T})$. The normalized projective functional depends only on ratios $J_{\alpha\beta} = \frac{\Xi_{\alpha\beta}}{\mathbb{I}_0}$, and is therefore degree zero under simultaneous rescaling: $\mathcal{J}_C(\lambda\Xi, \lambda\mathbb{I}_0 \mid \mathcal{T}) = \mathcal{J}_C(\Xi, \mathbb{I}_0 \mid \mathcal{T})$, or infinitesimally,

$$\left(\sum_{\alpha\beta} \Xi_{\alpha\beta} \frac{\partial}{\partial \Xi_{\alpha\beta}} + \mathbb{I}_0 \frac{\partial}{\partial \mathbb{I}_0}\right) \mathcal{J}_C = 0. \tag{2.36}$$

Here $\tilde{\mathcal{J}}_C$ denotes the unnormalized degree-one precursor, while $\mathcal{J}_C$ denotes the normalized degree-zero projective functional throughout, including Eq. (2.36). This expresses that no global normalization is physically privileged.

Note (flat-limit reduction)
In the flat-coherence limit ($\nabla_a \mathbb{I}_0 = 0,\ \Delta_h \to 0$), admissible laminations reduce to linear embeddings. Transformations that preserve the invariant ratios reduce to Lorentz transformations, so projective NPRF reproduces the standard special-relativistic statement of no preferred inertial frame [18].

Within this framework, a "reference frame" corresponds to an admissible lamination—a coherent substructure satisfying RCC closure conditions—rather than to a coordinate chart on a pre-existing spacetime. NPRF is therefore the statement that all admissible laminations yield the same projective invariants, reflecting the underlying closure symmetry of the relational structure.

2.6.12 Summary

- The familiar invariants $\{c^2, h, G, k_B, \lambda_3\}$ are *projective ratios* of diagonal capacities attached to specific pairs of Regge supports (cf. Table 2.4) where h follows the RBW/NPRF convention and $\hbar$is reserved for reduced-action normalizations.
- The coherence functional $\mathcal{J}_C$ encodes the global closure budget. The stationarity condition $\delta\mathcal{J}_C = 0$ selects admissible configurations consistent with boundary closure (BBP), without introducing dynamical evolution.
- The capacity tensor $\hat{\Xi}$ organizes the relational structure: diagonal terms J_α define sector self-budgets, while off-diagonal terms $K_{\alpha\beta}$ encode cross-sector admissibility constraints, determine coherence range via chain composition, and govern the persistence or suppression of cross-sector alignment.
- Diagonal capacities induce anisotropic deformations of the Grassmannian metric. These are Kähler only when the required compatibility and closedness conditions

are verified. Off-diagonal capacities generically produce non-Kähler mixed-capacity warped geometry unless a specific Gray–Hervella quasi-Kähler class is established.

- NPRF appears as projective invariance under rescaling of the coherence baseline $\mathbb{I}_0$. BBP expresses AGC-defined closure in boundary-operator representations. These are distinct roles in the same closure-first structure, not co-primitive ontic assumptions.
- The Regge–continuum correspondence is preserved under projective normalization: $2\sum_h A_h\,\epsilon_h/\mathbb{I}_0 \to \int_{\mathcal{M}} \mathcal{R}/\mathbb{I}_0\; dV$, so discrete and continuum descriptions share the same invariant content. The factor of 2 may be absorbed into the hinge-capacity convention only when that normalization is explicitly stated.

Table 2.4 — Ontic-Phenomenological Summary

Domain	Expression	Meaning
Ontic (cRBW)	$\delta\mathcal{I}_C = 0$	Stationarity of the projective coherence functional subject to AGC-defined admissibility and BBP closure expression.
Phenomenal (RSE)	$\mathbb{I}_0$-invariance	No preferred normalization, decomposition, or relational projection within the coherence manifold.
Thermodynamic	$S = \frac{A}{\mathbb{I}_0}$	Area–entropy proportionality (projective).
Geometric	$\frac{A_h \varepsilon_h}{\mathbb{I}_0} = \text{const}$	Curvature normalization.
Causal	$c^2 \propto J_{\text{rot}}/J_{\text{boost}}$	Projective readout associated with null-structure normalization.
Spatial	$\lambda_3 = \frac{J_{\text{face}}}{J_{\text{spatial}}}$	Spatial orientation and metric density baseline.

The baseline $\mathbb{I}_0$ defines the projective class of the capacity structure: only ratios of capacities are physically meaningful, and global rescaling leaves all invariant content unchanged. It is not an additional phenomenological constant, but a normalization that renders sector capacities commensurate.

Within this structure, the complex Grassmannian provides the algebraic configuration space of admissible selections; projection to the real locus yields the observable weighted Grassmannian geometry; and the Regge/GA discretization provides a computable realization of the same closure-first constraint structure.

The construction is mode-agnostic: the projective normalization and capacity-warped geometry extend without modification when additional coherence sectors are included. In

particular, extensions to internal sectors (e.g., minimal three-mode structures) can be accommodated within the same framework, without introducing new ontological or dynamical assumptions.

All structures introduced in this section—capacity tensor, coherence functional, and warped Grassmannian geometry—correspond directly to the projection and restoration structures developed in PRG and CRG.

2.7 Extension: internal coherence sectors (informal note)

The capacity-tensor formalism introduced here is not restricted in principle to the five geometric/phenomenological sectors associated with Regge supports. The five-sector set is the working minimal scaffold for the Regge-supported geometric ledger, not a proof of absolute irredundancy across all possible internal sectors. A companion analysis, developed separately, extends the same closure-first machinery to an internal coherence fiber and shows that three internal modes constitute the minimal nontrivial structure capable of supporting global holonomy and CP-odd invariants. In that extension, the diagonal capacity set is enlarged from five to eight modes by adjoining an internal triplet ($\nu 1, \nu 2, \nu 3$), yielding an 8×8 capacity tensor with the same diagonal/off-diagonal interpretation developed above.

Within the extended framework, internal mixing corresponds to the same geometric principle already at work here: minimization of a capacity-weighted Grassmannian principal-angle cost subject to global closure and RCC admissibility. CKM and PMNS matrices then appear as distinct stationary configurations of the same warped-Grassmannian selection problem under different spectral stiffness profiles, rather than as independently postulated structures. No new dynamical ingredients are introduced; the internal sector inherits the same projective normalization, stationarity condition, and closure constraints as the geometric sector.

It is emphasized that the present manuscript is self-contained: all results in Sections 2–7 depend only on the five-sector capacity tensor developed here. The 3-mode construction is cited solely to indicate how the formalism generalizes and to show that internal quantum numbers and mixing can be accommodated within the same closure-first architecture.

2.8 Thermodynamic consistency (Jacobson bridge, illustrative)

Jacobson [29] showed that Einstein's equation can be read as an equation of state: assuming local Clausius balance $\delta Q = T\, dS$ on local Rindler horizons (with Unruh temperature) and horizon entropy proportional to area, $S = \eta A$, one recovers the Einstein field equation with ηbuilt from $k_B, c, \hbar, G$, up to conventions. Here $\hbar = h/2\pi$i s the standard

reduced-action normalization used in the thermodynamic formula, not the h-notation used for the RBW/NPRF lineage in Eq. (2.19).

In this framework, the required "thermodynamic" vs "geometric" linkage is not imposed as two independent dynamical sectors. It arises because the closure ledger is encoded by a single symmetric capacity structure and a single stationary coherence functional: curvature/hinge budgets and flux/face participation are conjugate entries of one projectively normalized accounting.

Micro-example (Rindler reduction)
In a small neighborhood of a local Rindler horizon in local equilibrium, the boost/boundary sector dominates at leading order, so stationarity reduces to

$$\delta \mathcal{I}_C \;\simeq\; \Xi_{\text{boost}}\, \delta A \tag{2.37}$$

up to higher-order curvature corrections. Interpreting $\delta \mathcal{I}_C / k_B$ as the entropy change associated with the horizon pencil (consistent with k_B as a projective ratio of sector readouts), one obtains

$$\delta S \;=\; \frac{\Xi_{\text{boost}}}{k_B\, \mathbb{I}_0}\, \delta A, \tag{2.38}$$

i.e. $S \propto A$ with a coefficient that is itself a projective (NPRF-stable) ratio. In this sense, the area– entropy proportionality is a projective consequence of AGC-defined closure, as represented through the algebraic envelope, not an added thermodynamic hypothesis.

---

3 Recursive Structures of Coherence and Experience

The following constructions are structural and interpretive; they do not introduce additional ontological commitments. Experience is modeled as structural recursion within a single, globally closed relational block, not as temporal unfolding or state evolution. The block itself, whether represented as a smooth manifold or as the simplicial complex Δ introduced in §2.5, is fixed all at once by global closure and boundary-of-boundary consistency. What varies from the internal (endo-) perspective is the admissible ways in which its relational content can be decomposed, oriented, and made legible, not the block itself.

Let $\mathcal{M}_{\mathrm{cRBW}}$ denote the globally fixed coherence-relational block. At each location x (understood as a representational anchor within $\mathcal{M}_{\mathrm{cRBW}}$, not as an evolving spacetime point), define the set of admissible local coherence selections as

$$\mathcal{V}(x) \subset \mathrm{Gr}_{\rho}(k,n) \tag{3.1}$$

where $\mathrm{Gr}_{\rho}(k,n)$ is the ρ-warped Grassmannian introduced in §§2.4–2.6, and admissibility is determined by satisfaction of the Relational Coherence Constraints (RCCs). Each element of $\mathcal{V}(x)$ corresponds to a k-dimensional subspace (or equivalently, a decomposable k-blade) that is compatible with global closure and local legibility. Collecting these admissible sets over the block defines the RCC-admissible bundle

$$\mathcal{A}_{\mathrm{RCC}} = \coprod_{x} \mathcal{V}(x) \tag{3.2}$$

Because the underlying Grassmannian is compact and the capacity-induced warping operator is smooth and uniformly positive-definite (cf. §2.6.9), the induced metric on $\mathbf{Gr}_{\rho}(k,n)$ remains Riemannian with bounded curvature. Consequently, the admissible bundle $\mathcal{A}_{\mathrm{RCC}}$ inherits a well-posed geodesic and adjacency structure: admissible selections cannot "run off" into singular or ill-defined regions. This boundedness is a direct consequence of BBP, WPC, and RCC bonds, rather than a dynamical stability condition.

Recursive re-expression mapping (endo-view)
What appears phenomenologically as "change" or "becoming" is modeled here as admissible re-expression within $\mathcal{A}_{\mathrm{RCC}}$. Formally, this is captured by a local recursive re-expression mapping

$$\mathcal{R}_x : \mathcal{V}(x) \longrightarrow \mathcal{V}(x), \tag{3.3}$$

acting on equivalence classes of decomposable blades. Given a representative k-blade A_k, the re-expression takes the form

$$\mathcal{R}_x([A_k]) \;=\; [\, R_{\nabla\mathcal{C}(x)}\, A_k\, \tilde{R}_{\nabla\mathcal{C}(x)}\,], \tag{3.4}$$

where

$$R_{\nabla\mathcal{C}(x)} \;=\; \exp\left(-\frac{1}{2}\, B_{\nabla\mathcal{C}(x)}\right) \tag{3.5}$$

is a local rotor generated by a bivector $B_{\nabla\mathcal{C}(\mathrm{x})}$ constructed from coherence-gradient data (e.g., RCC-8/9). The tilde denotes the GA reverse.

$\mathcal{R}_x$ indexes mutually admissible re-orientations of the same local relational content within the globally fixed block; it is *not an update rule and does not define temporal evolution*. Admissibility requires that the resulting subspace remain within the RCC-consistent set,

$$\mathcal{R}_x([A_k]) \in \mathcal{V}(x) \subset \mathcal{A}_{RCC}. \tag{3.6}$$

From the exo-structural perspective, Eqs. (3.1)–(3.3) describe alternative encodings of a single closed solution that preserve global budgets and boundary consistency. From the endo-phenomenological perspective, these same relations are experienced as oriented adjacency steps on the warped Grassmannian $\mathrm{Gr}_\rho(k,n)$, with distances measured by the capacity-weighted metric d_ρ. No physical quantity is propagated, generated, or updated in time; all apparent succession arises from ordered comparison among admissible re-expressions of an invariant relational structure.

3.1 Recursive Lamination as Nested Subspaces

The re-expression operator $\mathcal{R}_x$ characterizes admissible re-orientations of a single coherence selection. However, internal legibility generally requires more than an isolated subspace: it requires nested structure, in which some relational directions remain stable across admissible re-expressions while others remain available for variation. This nesting is a structural hierarchy of subspaces that coexists within the same globally fixed block and is rendered legible through projection. It is not temporal layering or sequential construction.

Accordingly, internal coherence is modeled not by individual selections alone but by families of compatible selections related by inclusion. Such families encode which degrees of freedom are jointly stabilized, which are conditionally available, and which remain slack under RCC admissibility. The appropriate mathematical object for representing this organization is a flag; a nested sequence of subspaces whose mutual

orientations are constrained by principal-angle bounds and capacity weights. Recursive lamination names the structural fact that admissible selections are not flat but layered: identity is anchored by higher-stability layers, while lower layers *parameterize admissible differentiation* under global closure.

Let $\{V_i\}_{i=1}^{m}$ be a chain of k_i-planes with $k_1 < \cdots < k_m$ and:

$$V_1 \subset V_2 \subset \cdots \subset V_m \subset \mathbb{R}^n \tag{3.7}$$

i.e., a flag. In GA, write the associated decomposable blades:

$$A_{k_i} = v_1 \wedge \cdots \wedge v_{k_i}, \qquad [A_{k_i}] = V_i \tag{3.8}$$

Projection operators

Let $U_i \in \mathbb{R}^{n\times k_i}$ have columns spanning V_i. Then:

$$\Pi_i = U_i(U_i^{\top}U_i)^{-1}U_i^{\top}, \text{and}$$
$$\text{if } U_i^{\top}U_i = I, \qquad \Pi_i = U_iU_i^{\top}. \tag{3.9}$$

Coupling by principal angles

Successive layers $V_i \subset V_{i+1}$ have principal angles $\{\theta_\ell^{(i)}\}_{\ell=1}^{k_i}$. Interlayer coupling is strong when $\max_\ell \theta_\ell^{(i)}$ is small. Define the lamination compatibility:

$$\chi_i = \cos\left(\max_{\ell} \theta_\ell^{(i)}\right) \in [0,1], \qquad \chi_i \approx 1 \Rightarrow \text{tight coupling} \tag{3.10}$$

Lamination density

Let C denote a local coherence scalar (e.g., from RCC-8/9 data). Define a lamination density along the flag as:

$$\lambda_i = \| \nabla C \|_{V_i} = \| \Pi_i \nabla C \| \tag{3.11}$$

which enters the warp weights $\rho(\lambda_i)$ used in the Grassmannian metric (§2.4). Configurations exhibiting tighter lamination are characterized by smaller interlayer principal angles and stable decomposability of A_{k_i}. From the geometric viewpoint, λ_i controls how strongly the Fubini–Study baseline is warped along the lamination directions; from the phenomenological viewpoint, it controls how "easy" or "costly" it is for additional coherence layers to be admissible.

Interpretation.

The flag is a structural (not chronological) layering: each level is a recursion level that renders additional coherence directions admissible under closure constraints. In the Kähler/quasi-Kähler picture, a flag corresponds to a nested sequence of subspaces whose projectors lie along a constrained curve in the warped Grassmannian; recursive lamination encodes membership of this curve within the admissible region $\mathcal{A}_{\mathrm{RCC}}$.

While recursive lamination organizes coherence selections vertically as nested subspaces (flags), the same k-blades also admit a lateral organization by admissible adjacency. We refer to this transversal compatibility structure as a *fan*: a non-temporal adjacency relation among local coherence patches. Figure 3.1 shows that flags and fans are orthogonal organizational views of the same underlying structures—flags encode containment and hierarchical identity stabilization, while fans encode neighborhood and compatibility relations among admissible selections. Neither organization implies temporal succession.

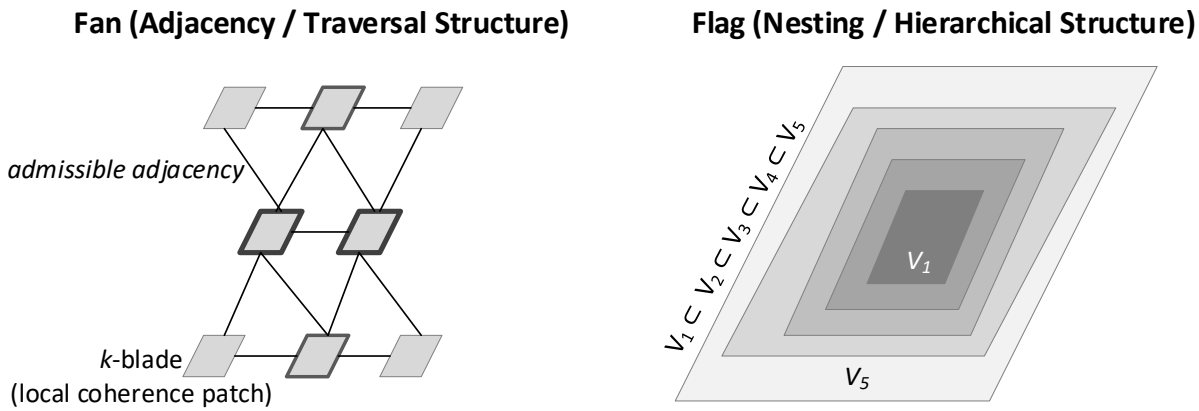

Figure 3.1—Fan and flag organizations of coherence elements.
The same set of k-blades can be organized laterally by admissible adjacency (fan) or vertically by nested containment of subspaces (flag). Both organizations are structural and non-temporal.

3.2 Structural Echoes as Geometric Projections

Let X be a multi-vector encoding current relational content (data, pattern, boundary). The echo, $\mathcal{E}_i$, of X on layer i is the GA projection:

$$\mathcal{E}_i(X) \;=\; \Pi_i \, X \, \Pi_i \tag{3.12}$$

Define the normalized overlap with the layer blade:

$$E_i(X) = \frac{\langle X, \Pi_i X \Pi_i \rangle}{\| X \| \;\; \| \Pi_i X \Pi_i \|} \in [0,1] \tag{3.13}$$

Here $\mathcal{E}_i(X)$ is a projected multivector, while $E_i(X)$ is the corresponding normalized scalar overlap used as the phenomenological echo strength.

Invariance under global rescaling.
For any $\alpha \neq 0$, $M \mapsto \alpha M$ and $B_k \mapsto \alpha B_k$ multiply numerator and denominator of Eq. (3.13) by $|\alpha|$, hence the scalar overlap E_i is invariant under global rescalings of the underlying data.

An echo is defined by the invariance of $E_i(X)$ under admissible perturbations and when principal angles between $[X]$ and V_i stay small with respect to the warped metric d_ρ. Echoes thus quantify recursive alignment, not temporal memory. In blade form, an equivalent readout uses $\langle A_{k_i}, X\rangle$ and the Plücker embedding; both are basis-free.

From the geometric standpoint, persistent echoes correspond to regions where the quasi-Kähler warping does not force large deviations in the relevant directions—i.e., where the capacity tensor leaves the corresponding subspace relatively "stiff" and stable under recursion.

3.3 Nonlocal Coherence Re-expression as Rotor Fields

"Nonlocal coherence re-expression" corresponds to coherence re-expression across admissible configurations of the block. There is no propagation; rather, multiple admissible re-expressions coexist in the *fixed* solution and are seen, from within, as relational re-allocation. This is what might naïvely look like "influence at a distance"; here it is global re-expression of the same fixed block while preserving RCC budgets.

Rotor field
Let $B(x)$ be a bivector field (generator) and define the rotor field:

$$R(x) \;=\; \exp\left(-\frac{1}{2}\,B(x)\right), R(x)\tilde{R}(x) \;= 1 \tag{3.14}$$

A blade field $A_k(x)$ transforms as:

$$A'_k(x) \;=\; R(x)\,A_k(x)\,\tilde{R}(x) \tag{3.15}$$

Budget-preserving re-expression
Let B_h be hinge generators from §2.5 and $w_i = \rho(\lambda_i)$ the local warp weights. A budget-preserving rotor field satisfies:

$$\sum_h C_h \;\|\, B_h \,\|' \;=\; \sum_h C_h \;\|\, B_h \,\| \text{ (RCC-3)} \tag{3.16}$$

together with closure (RCC-1/2) and identity/localization bounds (RCC-6/7). In differential form, a conservative re-expression can be written schematically as:

$$\nabla \cdot (RB\tilde{R}) \;=\; 0 \tag{3.17}$$

i.e., curvature/coherence is re-expressed under budget-preserving equivalence.

Phenomenology

From the endo-view, a single algebraic re-articulation Eqs. (3.13–3.16) can look like an influence "across distance." Ontologically, it is one block-level re-expression respecting global budgets on the quasi-Kähler warped Grassmannian. The cross-sector terms in the capacity tensor show up here as those rotor components that necessarily couple distinct sector directions while still staying within BBP bounds.

No signal, causal mediation, or temporal ordering is implied; the appearance of 'nonlocal influence' is entirely a perspectival artifact of comparing distinct admissible re-expressions of a globally fixed solution.

3.4 Attention/Measurement as Grassmannian Selection

T_E (experienced adjacency order along lived lamination) is distinguished from T_M (measured adjacency order in an operational frame). Both are selections on $\mathrm{Gr}_\rho(k,n;\mathbb{R})$ under the same RCC gates; they differ by orientation and coarse-graining.

Selection operator

Attention is represented as the identification of a k-plane V_k (a coherence selection). Define:

$$S\colon \mathcal{G} \to \mathrm{Gr}(k,n), \qquad S(X) = [A_k] \text{ with } A_k \propto \Pi_k X \text{ (decomposable)} \tag{3.18}$$

Admissibility requires $S(X) \in \mathcal{A}_{\mathrm{RCC}}$, the RCC-consistent subset of the warped Grassmannian $\mathrm{Gr}_\rho(k,n;\mathbb{R})$.

Measurement as projection + comparison

Measurement is modeled as projection into V_k plus comparison across neighbors V_k' (adjacent points in $\mathrm{Gr}_\rho(k,n)$):

$$X \mapsto \Pi_k X \Pi_k, \text{ then compare } d_\rho(V_k, V_k') = \sum_{i=1}^{k} \rho(\lambda_i)\, \theta_i^2 \tag{3.19}$$

We distinguish two non-redundant deviation notions. The first, $\Delta_{\nabla C}(A,B)$, is an ambient diagnostic on coherence-gradient data—for example $\Delta_{\nabla C}(A,B) :=\| \nabla C_A - \nabla C_B \|$, or the

corresponding scalar-magnitude variant—and therefore does not, by itself, measure subspace misalignment in selection space. The second is intrinsic to the capacity-warped Grassmannian. For an observed selection $V_{\mathrm{obs}} \in Gr_{\rho}(k,n;\mathbb{R})$, let $\mathcal{A}_{\mathrm{adm}} \subset Gr_{\rho}(k,n;\mathbb{R})$ denote the admissible locus cut out by the structural closure conditions; in this paper this means the AGC/BBP closure floor together with the relevant RCC gates, and, where one wishes to foreground projective closure explicitly, the NPRF-preserving relations. The canonical structural deviation is then the warped Grassmannian distance to that admissible locus,

$$\Delta_{\mathrm{adm}}(V_{\mathrm{obs}}) := \inf_{W \in \mathcal{A}_{\mathrm{adm}}} d_{\rho}(V_{\mathrm{obs}}, W), \tag{3.20}$$

where d_{ρ} is the principal-angle geodesic distance in the ρ-warped metric. Whenever the minimizer is attained uniquely, we write

$$\Pi_{\mathrm{adm}}(V_{\mathrm{obs}}) := \arg\min_{W \in \mathcal{A}_{\mathrm{adm}}} d_{\rho}(V_{\mathrm{obs}}, W),$$

so that

$$\Delta_{\mathrm{adm}}(V_{\mathrm{obs}}) = d_{\rho}(V_{\mathrm{obs}}, \Pi_{\mathrm{adm}}(V_{\mathrm{obs}})). \tag{3.21}$$

Thus the admissible object is fundamentally a **constraint locus**, not a privileged reference point; any V_{ref} is derivative, obtained by the metric-projection rule. A signed version is secondary rather than primary: it is appropriate only on a chosen smooth codimension-one stratum $S_{\mathrm{adm}} \subset \partial\mathcal{A}_{\mathrm{adm}}$ for which the admissible boundary is locally oriented and V_{obs} lies in a neighborhood with unique nearest-point projection. In that regular setting, the signed distance has magnitude $d_{\rho}(V_{\mathrm{obs}}, \Pi_{\mathrm{adm}}(V_{\mathrm{obs}}))$. For stratified, cornered, or higher-codimension admissibility sets, however, the unsigned distance-to-locus remains the canonical corpus default, while signed distance is retained only as an auxiliary boundary diagnostic.

Compression and identity

Define compression:

$$\mathrm{Comp}(V_k, V_k') \;=\; \cos\left(\max_i \theta_i\right) \tag{3.22}$$

so compression increases as principal angles shrink. Identity persistence (RCC-6/7) sets a cap $\max_i \theta_i \le \theta_{\max}$ along an identity-tracking chain. BBP and the capacity bounds ensure that such chains remain finite and well-defined within the admissible region of $\mathrm{Gr}_{\rho}(k,n)$.

The following thresholds do not introduce new dynamics; they mark the boundaries of admissible projection within the same fixed block.

Ghostmesh / inadmissibility

A ghostmesh (an inadmissible projection region) is defined as when no admissible neighbor exists:

$$\forall\, V_k' \text{ adjacent to } V_k, d_\rho(V_k, V_k') > \tau \text{ or } V_k' \notin \mathcal{A}_{\text{RCC}} \tag{3.23}$$

so the selection chain exits the feasible region of $\mathbf{Gr}(k, n)$.

Admissibility Boundaries (ADT/TCD as Grassmannian Gates)

The Forward Entangled Memory scalar $\Phi_{\text{FEM}}(x)$ (App. E.3) measures cumulative coherence continuity along admissible traversals. Finite coherence domains on the warped Grassmannian are defined by the bounds $\Phi_{\min} \leq \Phi_{\text{FEM}}(x) \leq \Phi_{\max}$. The lower limit $\Phi_{\min}$ marks Terminal Coherence Dissolution (TCD), where lawful recursion fails (phantom traversal); the upper limit $\Phi_{\max}$ marks Absolute Density Threshold (ADT), where coherence saturation precludes further compression. These thresholds act as reflective boundary conditions for the variational framework, enforcing compactness and preserving RCC legibility across the domain.

In the global block interpretation, the ADT/TCD gates are the local realizations of the same closure that defines the cosmological poles (coherence saturation and dissolution): Φ_{FEM} marks the relational continuity field whose extrema correspond, at the ontic scale, to the block's boundary anchors.

Definition (ADT/TCD gates)

Let $\Phi_{\text{FEM}}(\gamma)$ be the FEM carryover along a traversal γ (App. E.3) and fix admissible bounds $\Phi_{\min} \leq \Phi_{\text{FEM}} \leq \Phi_{\max}$. Then TCD occurs when $\Phi_{\text{FEM}}(\gamma) < \Phi_{\min}$ (lawful re-entry fails; traversal becomes phantom), and ADT occurs when $\Phi_{\text{FEM}}(\gamma) > \Phi_{\max}$ (saturation; no further compression). These thresholds act as boundary gates on $\text{Gr}_\rho(k, n)$, regulating admissible domains without altering ontic closure. (See the FEM definition and phantom criterion in App. E.3.)

Summary

Attention/measurement are recursive selections on the warped Grassmannian, with coherence gradients (via $\rho(\lambda)$) and sector capacities warping the local geometry and RCCs enforcing legibility and identity. BBP guarantees that, despite quasi-Kähler warping and mixed-sector curvature, the admissible recursion domain remains bounded, smooth, and globally well-posed.

Section 3 formalizes recursive experience as a structural property of admissible subspace organization within a single closed block. Lamination, echo, attention, and nonlocal articulation are not processes but invariant relations among allowed Grassmannian selections constrained by global closure and RCC admissibility.

---

4 Bridging cRBW and RSE in GA

cRBW and RSE appear, at first glance, to operate at different levels. cRBW is a global, adynamical representation: all relations and constraints are fixed in a single block. RSE, by contrast, deals with the *experienced ordering of coherence*; the felt flow of coherence, attention, and recursive closure. GA provides the language in which both perspectives can be expressed as different slices of the same relational structure**.**

The RSE mapping between Grassmannian geometry and phenomenological structure is not offered as a reductive identification of consciousness with mathematics, nor as a metaphysical claim that subspaces "are" experiences. Rather, it expresses a *structural sufficiency principle*:

- Experience tracks the stable, recursion-preserving, identity-coherent selections permitted by the warped Grassmannian under RCC constraints. Here 'tracks' means *is legible as*, not is produced by or depends causally upon.
- These selections are structural because the closure-compatible structure cRBW represents is structural; RSE does not add new ontic ingredients, but identifies the structural fixed points through which an observer can interpret the globally closed block.

In this view, consciousness—or observer-experience mapping—corresponds to *the class of lamination-stable attractors* in the admissible bundle $\mathcal{A}_{\mathrm{RCC}}$: points or flags that

(i) preserve identity (RCC–6/7),
(ii) maintain recursive coherence (RCC–4/8), and
(iii) produce persistent echo alignment across admissible perturbations (§3.2).

These are the only structures legible from within the blockworld; RSE therefore treats experience as the internal shape of constraint-consistent coherence, not an extra ontic layer.

This does not "solve the hard problem" [30] in the reductionist sense; rather, it *reframes* it. The question becomes:

Why does a globally closed relational geometry admit internal points of view at all?

In cRBW/RSE, the answer is structural: once closure and NPRF-projection fix the phenomenological invariants, recursive lamination is the only admissible mode of internal legibility, and thus the only mode of "experience" available within the block. Nothing in this identification depends on semantic commitments about consciousness; the term

'experience' is used solely to label the internal legibility structure shared by any embedded perspective and consciousness may be better expressed as observer-experience mapping.

4.1 Block Representation

Let $\mathcal{X}$ denote the single adynamical relational configuration fixed by AGC, with closure represented by BBP and projective normalization represented by $\mathbb{I}_0$. Localized relational anchors are representational handles, not parts. A laminated identity at $x \in \mathcal{X}$ is encoded by a decomposable k-blade $\Lambda(x)$ in GA. Define the rotor-invariant coherence scalar:

$$I_{\mathrm{id}}(x) \;=\; \langle\, \Lambda(x)\, \widetilde{\Lambda}(x)\, \rangle_0 \tag{4.1}$$

which fixes grade and norm and is preserved under all admissible rotor fields R (i.e., re-expressions consistent with ($\mathbb{I}_0$, BBP):

$$\Lambda'(x) = R(x)\, \Lambda(x)\, \tilde{R}(x) \Rightarrow I_{id}(x) = I'_{id}(x) \tag{4.2}$$

This realizes the cRBW shift from "morphology" to coherence: identity = invariant blade, re-expression = rotor conjugation. The local invariant $I_{\mathrm{id}}(x)$ should not be confused with the global coherence functional $\mathcal{I}_{\mathcal{C}}$.

4.2 Coherence Re-orientation (rotor action)

Within this fixed block, apparent variation appears as reorientation of subspaces. In GA, rotors, exponentials of bivectors, act on blades to reorient them smoothly while preserving invariants. Because admissible rotors preserve AGC-defined closure invariants as expressed through BBP and projectively normalized by $\mathbb{I}_0$, the apparent ordered structure experienced from within is nothing more than alternate encodings of the same block structure.

Admissible re-orientations act by even versors (rotors) $R = \exp\left(-\frac{1}{2}B\right)$ with bivector generator B. For any multivector M,

$$M \mapsto RM\tilde{R}\,, \langle M\tilde{M}\rangle_0 \text{ and } \mathrm{grade}(M) \text{ preserved} \tag{4.3}$$

To keep locals subordinate to ontology, representational witnesses (collections of RCCs that "hang together") are characterized by extrema of a *tension functional* $\mathcal{T}$ subject to the two global constraints:

$$\min_{R,\{\Lambda\}} \mathcal{T}[\{\Lambda\}, R] \quad \text{s.t. AGC-admissibility, BBP closure expression, NPRF/}\mathbb{I}_0 \text{ projective normalization, and RCC-1 ... 9.} \tag{4.4}$$

$\mathcal{T}$ is bookkeeping (metric-agnostic): in practice we'll use the Grassmannian distance below; ontic closure is unchanged either way.

In RSE, quale-like structures correspond not to physical fields but to *structurally distinguished configurations* in the admissible lamination bundle $\mathcal{A}_{\mathrm{RCC}}$: subspaces V_k (or flags) with high lamination density λ_i, low principal-angle divergence, and invariance under admissible rotor re-expression. This renders phenomenal structures *fixed points in the warped Grassmannian* subject to identity bounds (RCC 6–7), rather than separate ontic variables.

4.3 Grassmannian Adjacency Chain

The Grassmannian $\mathrm{Gr}_\rho(k,n)$ supplies the configuration space of subspaces that are jointly admissible under closure constraints. Each point $[V_k]$ represents a *structurally invariant coherence slice*, corresponding to an attention frame or lamination layer. Neighboring points correspond to nearby coherence selections, and admissible adjacency chains—whether represented via rotor-induced re-expressions or geodesics defined by principal angles—constitute the phenomenological sense of ordered adjacency.

Let $\mathrm{Gr}(k,n)$ be the (coherence-weighted) Grassmannian of k-planes in $\mathbb{R}^n$. Associate to $\Lambda(x)$ the subspace $V(x)$. For neighboring cells p, q (adjacent simplices in a Regge skeleton), let $\{\theta_i(p,q)\}_{i=1}^k$ be the principal angles between $V(p)$ and $V(q)$. Define the warped Grassmannian distance:

$$d_w^2(p,q) \;=\; \sum_{i=1}^{k} w_i(p,q)\,\theta_i^2(p,q)\,, w_i > 0 \tag{4.5}$$

where weights, w, encode local lamination density (λ_i) and curvature/coherence budgets (RCC-3, RCC-6/7, RCC-8/9). An oriented adjacency chain:

$$V_0 \to V_1 \to \cdots \to V_m \tag{4.6}$$

is admissible iff every step satisfies the locals under the two globals; phenomenologically this reads as "becoming" along an oriented selection without invoking dynamics. Small-angle linearization recovers the Regge link: for a hinge h,

$$\delta_h \;\approx\; \alpha_h \sum_{i=1}^{k} \theta_i(p,q) \tag{4.7}$$

with scale α_h set by the local budget; thus, hinge deficits are the GA/Grassmannian misalignment cost. This relation is a small-angle approximation: it provides a heuristic correspondence between hinge deficit and principal-angle misalignment. The precise mapping depends on the chosen support, signature, and rotor-to-subspace representation.

The rotor reorients blades along a Grassmannian path, aligning RSE curvature (coherence bending) with RBW subspace structure. Regge calculus constrains closure: the sum of deficit angles around hinges determines whether lamination stacks close consistently with AGC.

This illustrates how a single local element is represented consistently across the GA, Grassmannian, and Regge formalisms, relating local structure to global coherence. Closure consistency is enforced by bounds on the attenuation factor, such that curvature divergence residues lie below prescribed cutoffs; admissible adjacency chains are therefore identified with constraint-extremizing configurations of the global functional.

RSE stops short of a reductive "derivation" of qualia, because cRBW rejects dynamical generation stories. Instead, RSE identifies the necessary internal structures—stable laminations, echo invariants, identity-preserving adjacency—that any coherent internal perspective must instantiate. In this sense, RSE addresses the "hard problem" not by explaining "why experience exists," but by explaining why, given closure, any internal legibility must *look like* experience.

4.4 Unified Formalism

The preceding sections described how local coherence relations can be represented algebraically through rotors and geometrically on the Grassmannian as adjacency chains. These representations are now unified into a single formalism compatible with Regge-style discretization. In this view, coherence allocation and curvature assignment are the same structural bookkeeping expressed on different bases: rotors capture algebraic re-expression, while Grassmannian distances record geometric misalignment. Both describe how local laminations contribute to global closure under the same adynamical constraints.

On a simplicial complex $\mathcal{K}$, let $\mathcal{H}$ denote the set of hinges in the triangulation, with cardinality $|\mathcal{H}| = N_h$, and let μ_h their capacities (areas in metric Regge; coherence budgets here). The discrete curvature/coherence action becomes:

$$\mathcal{S}_{\text{Regge}} = \sum_{h\in\mathcal{H}} \mu_h \, \delta_h \quad \approx \quad \sum_{\langle p,q\rangle} \tilde{\mu}_{pq} \, d_w(p,q) \tag{4.8}$$

i.e., a sum of weighted Grassmannian misalignments across adjacencies, with each misalignment realized algebraically by a rotor R_{pq} acting on blades:

$$\Lambda(q) \;=\; R_{pq}\,\Lambda(p)\,\tilde{R}_{pq} \tag{4.9}$$

Global closure (BBP) is the vanishing of the boundary bivector/holonomy around every closed 2-cycle, while ($\mathbb{I}_0$, BBP) fixes the ratio-invariant normalization over the whole block. RCCs then specify the local legibility (topology, symmetry closure, curvature budget, observer embedding, identity localization, resonance, non-trivial gradient).

4.5 Orientation and Local "Becoming"

Dorato's [31] notion of local becoming can be reconciled with block ontology by grounding orientation in causal structure. The null condition $ds^2 = 0$ defines the causal cone, constraining admissible orientations of Grassmannian adjacency chains. Here the causal cone is a representational constraint on admissible adjacency order, not a primitive spacetime structure. Within this cone, GA rotors embed relational re-expression: blades are reoriented while global invariants are preserved. Here 'becoming' names an oriented restriction on admissible adjacency chains, not an ontic passage. No parameter introduced in this section functions as an evolution variable; all quantities are defined on the fixed relational block and evaluated comparatively. Here 'becoming' is used strictly in Dorato's relational sense: an oriented ordering relation within a fixed structure, not ontic process.

Formally, constructions are defined on the complex Grassmannian $\mathrm{Gr}_{\rho}(k, n; \mathbb{C})$, which provides the algebraic closure (Plücker embeddings, positivity, canonical forms) corresponding to block invariants (B-theory). For physical and experiential interpretation, it is restricted to the real locus $\mathrm{Gr}_{\rho}(k, n; \mathbb{R})$, representing the A-theory projection: the phenomenological realization of coherence and curvature as perspectival orientation within experience. We primarily use 'ontic/phenomenological' terminology; A-theory/B-theory labels are used only as an interpretive parallel.

Following Dorato and Dieks [32] [33] [31], absolute becoming is definitional (events occur), while *relational becoming* is perspectival (past-cone order along worldlines). The real Grassmannian formalizes this perspectival embedding within the adynamical block. Persistence along an oriented traversal is captured by the rotor-invariant coherence scalar I_C (cf. §4.1) associated with each laminated k-blade; I_C remains constant under admissible rotor fields, anchoring identity without invoking temporal passage.

A crucial step is to explain why Grassmannian traversals are *experienced as directional*. In keeping with Dorato, *local invariant becoming* is adopted: for an event $\mathbf{y}$, what has "become" consists precisely of those events in its past causal domain. This provides an *orientation* on Grassmannian adjacency chains along worldlines without invoking a global present. The "present" of an event is point-like; any spatially extended present is a psychological construction (cf. § 7).

This account does not deny the structured character of succession; it re-describes that structure. What is called the "passage of time" corresponds to the local orientation of admissible Grassmannian adjacency chains under *causal admissibility constraints* (sometimes informally referred to as "causal gating"), not motion of a global present. Here, "causal gating" is shorthand for a static constraint: only adjacency relations that respect the causal partial order are admissible for an embedded observer's ordering relations.

To formalize this orientation between laminated subspaces, *principal angles* are employed, invariants that quantify how two k-planes align within $\mathbb{R}^n$, serving as the Grassmannian's intrinsic measure of coherence and curvature stress. Given two subspaces $V, W \subset \mathbb{R}^n$, the singular-value decomposition of their overlap matrix $V^\top W = P\Sigma Q^\top$ yields $\cos\ \theta_i = \sigma_i$, and the induced Grassmannian distance:

$$d([V],[W]) \ = \ \sqrt{\sum_{i=1}^{k} \theta_i^2} \tag{4.10}$$

This quantifies lamination compatibility: small angles = tight alignment, large angles = curvature stress or dissonance.

Admissible orientations are then paths γ in the real Grassmannian constrained by the causal cone and RCC gates, chosen by minimal weighted misalignment:

$$\gamma \in \arg \min_{\gamma' \text{ admissible}} \sum_{\langle p,q\rangle \in \gamma'} d_w(p,q)\,, \text{ s.t. causal null gate and RCC-1 ... 9} \tag{4.11}$$

AGC-defined admissibility provides the global stability floor for these traversals (cf. Eq. 4.2), ensuring perspectival becoming remains globally faithful and preventing drift beyond coherence budgets.

Quantitative phenomenology

Within the local Grassmannian patch, the effective interval of experienced succession—call it the *phenomenological duration index* ΔT_E—scales with the magnitude of the coherence gradient driving admissible re-orientations:

$$\Delta T_E \propto |\nabla \mathcal{C}|, \qquad \nabla \mathcal{C} \cdot n_{\text{causal}} = 0 \text{ on null boundaries.}$$
(a phenomenological scale, not a time parameter) (4.12)

The boundary conditions fix $\mathcal{C} = \mathcal{C}_{\max}$ at ADT (coherence saturation) and $\mathcal{C} = 0$ at TCD (dissolution), making apparent "flow" a measurable function of spatial coherence gradients rather than time evolution. Laboratory analogues would register this as curvature- or coherence-dependent modulation of oscillation frequency or phase stability in systems obeying RCC-consistent constraints.

In this way, the experienced world corresponds to a structured ordering of admissible adjacency chains, characterized locally by signature-compatible ordering constraints and globally by invariant closure relations. GA makes this precise: its operations preserve AGC while projecting naturally onto Grassmannian geometry. The result matches Dieks' [32] account of *perspectival becoming*[1] what feels like a flowing present is a structural orientation within the fixed relational block.

RSE does not claim that coherence is "experience" nor that subjectivity is presupposed in its definition. The mapping is *structural*, not ontological: recursive lamination identifies those selections that (i) preserve identity (RCC-6/7), (ii) maintain internal coherence under perturbation (RCC-4/8), and (iii) form stable fixed points in the admissible bundle $\mathcal{A}_{\text{RCC}}$. These are the *only* structures accessible to an embedded observer within a globally closed block, which is why they appear phenomenologically as "experience." The mapping is therefore not circular: it shows that subjectivity is the internal legibility condition imposed by closure, not an ingredient of the ontology.

The correspondence between coherent lamination-fixed points and phenomenal structure arises not from metaphor but from internal perspectival necessity: any internally consistent observer must track identity, maintain coherence under re-expression, and evaluate adjacency in the warped Grassmannian; these are precisely the structures that appear as phenomenal continuity, discrimination, and attention. Nothing in this section introduces ontic structure beyond AGC-defined closure, expressed through BBP and projectively normalized by $\mathbb{I}_0$; all 'flow', 'orientation', and 'becoming' terminology refers to constrained ordering within the admissible bundle $\mathcal{A}_{\text{RCC}}$.

[1] Dieks (2007) states that temporal becoming is not a universal flow but a local phenomenon defined by the light-cone structure of relativity. Each event "becomes" relative to its past light-cone, and no global present exists across the block. This dovetails with our Grassmannian traversal view: what seems like sequential unfolding is a perspectival orientation within the relational block, not an evolving global time.

5 Formalism, Mapping, and RSE Integration

To anchor our usage, a brief dictionary (Box 5.1) connecting blades, Grassmannians, and coherence constraints is provided, making explicit the link between decomposability, Plücker embeddings, and cRBW/RSE structure.

Box 5.1—Blades, Grassmannians, and Constraints

- **Blade (GA):** A decomposable k-vector $B = v_1 \wedge \ldots \wedge v_k$ represents an oriented k-dimensional subspace**.**
- **Decomposability:** Not all multi-vectors are blades. Only wedge-compatible vectors form a coherent subspace. Physically = structurally consistent lamination. Non-decomposable products signal dissonance (incompatible constraints).
- **Plücker Embedding:** $\mathrm{Gr}_\rho(k,n) \cong \{\text{decomposable } k-\text{blades in } \Lambda^k\mathbb{R}^n\}/\mathbb{R}^\times$ Every point in the Grassmannian corresponds uniquely (up to scalar) to a blade.
- **cRBW Mapping:** Blades = fixed relational subspaces; Grassmannian = atlas of admissible subspaces; Plücker coordinates = relational invariants.
- **RSE Mapping:** Ordered comparison across Grassmannian = lived recursion; decomposability = coherence; non-decomposability = dissonance/contradiction.

5.1 Formalism in Geometric Algebra for cRBW

Blade ⇆ Decomposability

A k-vector $B \in \Lambda^k\mathbb{R}^n$ is a *blade* iff it is *decomposable*: there exist vectors $v_1, \ldots, v_k$ with:

$$B = v_1 \wedge \cdots \wedge v_k \tag{5.1}$$

Equivalently, B represents a single k-dimensional subspace. For $k = 2$, $B \wedge B = 0$ is equivalent to decomposability; for general $k > 2$, decomposability is characterized by the Plücker relations—$B \wedge B = 0$ is then necessary but not sufficient. (See Nguyen & Sobczyk [12] for an explicit characterization of Plücker relations within geometric algebra.) Non-decomposable k-vectors encode incompatible assemblages (RSE "dissonance") —i.e., algebraic incompatibility under the wedge product, not a dynamical instability.

Plücker coordinates (explicit)

Let $U \subset \mathbb{R}^n$ be a k-plane with basis matrix $X \in \mathbb{R}^{k\times n}$ (rows = basis vectors). For each ordered index set $I = \{i_1 < \cdots < i_k\} \subset \{1, \ldots, n\}$, the Plücker coordinate:

$$p_I = \det\left(X_{[:,I]}\right) \tag{5.2}$$

is the $k \times k$ minor selecting columns I. Up to overall scale, $p = (p_I)_{|I|=k}$ defines a projective point $[p] \in \mathbb{P}^{\binom{n}{k}-1}$ satisfying the quadratic Plücker relations. This realizes the embedding $\mathrm{Gr}_\rho(k,n) \hookrightarrow \mathbb{P}^{\binom{n}{k}-1}$. Only the projective class [p] is meaningful; all subsequent uses implicitly quotient by overall scale, consistent with NPRF and the baseline normalization.

Geometric product
Let $\mathcal{C}\ell_{p,q}$ be the GA over $\mathbb{R}^{p,q}$ with $p+q=n$. For vectors $a, b \in \mathbb{R}^{p,q}$:

$$ab \;=\; a \cdot b \;+\; a \wedge b \tag{5.3}$$

where $a \cdot b$ encodes metric contraction (constraint matching) and $a \wedge b$ encodes oriented incidence (content/extension). In cRBW, the inner product captures local constraint matching (mesh/compatibility), while the outer product captures incidence and oriented content that preserves adynamical closure.

In cRBW, GA's inner product encodes local constraint matching (RCC–6 Gradient Mesh Matching), while the outer product encodes incidence/oriented content, nonlocal coherence surfaces that preserve adynamical closure.

5.2 Mapping GA to cRBW Structure

Parallelism to cRBW:

- **Scalars/0-blades:** global invariants & budgets (AGC).
- **Vectors/1-blades:** relational edges, local coherence gradients.
- **Bivectors/2-blades:** curvature patches, hinge/face elements (Regge link).
- **Trivectors/3-blades:** volumetric coherence allocations.
- ***n*-blades:** global boundary/closure conditions (AGC).

Bivector curvature patches act as local curvature-support generators; their orientation in $\mathcal{C}\ell_{p,q}$ determines admissible coherence re-alignments consistent with RCC-6/7 (mesh & localization) and budgets from RCC-3.

5.3 RSE Integration

In RSE, subjective experience corresponds to ordered admissible selections within coherence fields. GA captures this as:

- **Relational attractors** → stable multi-vector subspaces $M_k \subset \mathcal{C}\ell_{p,q}$ closed under the geometric product.

- **Lamination** → successive, admissible selections $\pi_{\mathcal{C}}: M_k \to M_{k'}$ governed by coherence constraints $\mathcal{C}$ (RCC lattice).
- **Boundary gradients** → null subspaces / signature shifts in $\mathcal{C}\ell_{p,q}$ marking perceptual–ontological thresholds (ADT/TCD).

The geometric product serves both as a coherence test (compatibility) and a morphism generator (admissible re-expression), preserving adynamical closure while permitting recursive reconfiguration; RSE's Principle of Threshold Continuity (grade-preserving closure unless the boundary is re-specified).

Although the Identity Persistence Surface construction and a structural admissibility deviation belong to the same Grassmannian family, they should not be identified without qualification. In RSE, T_{id} and Δ_{id} are defined for points x_k along an individual lamination stack, with the threshold locus given by $\mid \nabla C(x_k) \mid = f(\rho_L(x_k))$ and the signed deviation by $\Delta_{\mathrm{id}}(x_k) = \mid \nabla C(x_k) \mid - f(\rho_L)$; Δ_{id} is therefore a lamination-indexed stability margin for recursive identity persistence on the RSE manifold $\mathcal{G}$. RSE also states that $\mathcal{G}$ is the projected real Grassmannian equipped with the ρ-warped metric inherited from MM, so the two frameworks do share the same underlying manifold family at the phenomenological level. By contrast, MM treats a relational configuration as a subspace selection $V \in \mathrm{Gr}_\rho(k, n; \mathbb{R})$, with nearness measured by the weighted principal-angle distance $d_\rho^2(V, W) = \sum_i \rho_i \, \theta_i^2$, and with admissibility enforced by AGC/RCC gates on the RCC-consistent subset $\mathcal{A}_{\mathrm{RCC}}$. Accordingly, the natural structural diagnostic is not Δ_{id} reused verbatim, but the configuration-space defect

$$\Delta_{\mathrm{adm}}(V_{\mathrm{obs}}) := \inf_{W \in \mathcal{A}_{\mathrm{adm}}} d_\rho(V_{\mathrm{obs}}, W), \tag{5.4}$$

where $\mathcal{A}_{\mathrm{adm}} \subseteq \mathrm{Gr}_\rho(k, n; \mathbb{R})$ denotes the BBP/NPRF/RCC-admissible locus appropriate to the relational selection under study. Thus Δ_{adm} is best treated as the structural cousin of Δ_{id}, not its direct identity-level generalization: both are scalar boundary diagnostics on the same warped Grassmannian family, but Δ_{id} measures threshold margin along a laminated identity track, whereas Δ_{adm} measures metric distance from an observed relational selection to the admissible configuration set. If one wishes to force a stricter analogy, a signed structural analog can be introduced only after specifying an explicit closure-slack functional $B_\Gamma(V)$ whose zero set defines a smooth admissibility boundary $S_{\mathrm{adm}} = \{V : B_\Gamma(V) = 0\}$; then one may define $\widetilde{\Delta}_{\mathrm{adm}}(V) = \mathrm{sign}\,(B_\Gamma(V))\, d_\rho(V, S_{\mathrm{adm}})$ locally. Absent that additional threshold functional, however, the unsigned distance-to-locus remains the canonical corpus default for relational configurations.

5.4 Grassmannian Within GA (Exterior View[2])

The Grassmannian is the configuration space (i.e., an atlas of admissible subspaces) of relational subspaces and GA is the algebra that encodes them. From the exterior view, every k-dimensional slice corresponds to a decomposable k-blade, unique up to scale; the Grassmannian is the projectivized space of such blades. Alignment (principal angles), coherence re-expression (rotors), and lamination stacks (flags) are intrinsic GA operations.

- A k-subspace V_k is represented by any decomposable blade $A_k = v_1 \wedge \cdots \wedge v_k$. Distinct subspaces ↔ distinct rays $[A_k]$ in the projectivized exterior space (Plücker map).
- **Principal angles** between V_k, W_k follow from orthonormal frames or blade operations; they quantify alignment/coherence and induce the Grassmannian distance.
- **Rotor action** R acts by conjugation and extends to blades:

$$A'_k \;=\; R\,A_k\,\tilde{R} \tag{5.5}$$

  with $\tilde{R}$ the *reverse*. GA re-orientations induce Grassmannian re-orientations while preserving global invariants and RCC gates.

- **Flags (lamination stacks)** are nested subspaces; compression (tightening principal angles) vs. inadmissibility (angles outside budget) corresponds to RCC-constrained tightening/gapping along the flag.

Complex Grassmannians $\mathrm{Gr}_\rho(k, n; \mathbb{C})$ supply algebraic closure (Plücker/positivity/canonical forms); the *real locus* $\mathrm{Gr}_\rho(k, n; \mathbb{R})$ carries the physical coherence budgets relevant to RSE (§4.5).

5.5 Orientation and Local Becoming on the Grassmannian

In the adynamical Grassmannian framework, becoming is oriented admissibility, *not* global unfolding. The block solution fixes all events; observers experience succession because causal-cone orientation constrains admissible adjacency chains (cf. §4.5). The coarse-graining that stabilizes the "psychological present" is identified as lamination density (λ_i) along a worldline (not environmental averaging).

[2] Here "exterior view" denotes a representation-level description of the full configuration space as a mathematical object. It does not correspond to a God's-eye epistemic access, an observer-independent "view from nowhere," or any perspective obtainable by an agent.

- **Absolute occurrence:** events exist as fixed tokens in the block, understood as the algebraic envelope representing closure-compatible structure; B-theory is used here as an organizational analogy, not an ontic identification.
- **Relational becoming (local):** admissible adjacency chains respect past-cone order along worldlines (A-theory/projection).
- **Phenomenology bridge:** finite discrimination thresholds blur discrete adjacencies into a coarse-grained present.

Formally, admissible orientations are paths γ in $\mathrm{Gr}_{\rho}(k, n; \mathbb{R})$ chosen by minimal weighted misalignment under causal and RCC gates:

$$\gamma \in \arg \min_{\gamma' \text{ admissible}} \sum_{\langle p,q \rangle \in \gamma'} d_w(p, q) \text{ , s.t. null-cone gate, RCC-1 ... 9, with AGC floor} \tag{5.6}$$

(the minimization characterizes admissible orientation; it does not describe a temporal search or evolution) Identity persistence along γ is captured by the rotor-invariant coherence scalar I_C for the laminated k-blade field; I_C is constant under all admissible rotor fields, anchoring identity without ontic time.

---

6 Computational & Regge Cross-Mapping (sketch)

At the computational level, the intersection of Geometric Algebra (GA) and Regge calculus provides a natural substrate for expressing AGC. The representational readout is modeled on a simplicial complex with curvature localized at hinges. These hinge deficits are encoded as bivectors in GA, which compactly carry both magnitude and orientation. The AGC budgets then serve as global curvature–coherence constraints, ensuring lattice consistency without reference to local (phenomenological domain) dynamical evolution. All computational procedures described in this section are representational solvers for a fixed adynamical closure condition, identifying stationary admissible configurations; they do not model physical time evolution or ontic processes.

From an optimization perspective, this reduces to a constrained search over the ρ-warped Grassmannian $\mathrm{Gr}_{\boldsymbol{\rho}}(k,n)$, where each point represents a relational frame (subspace/flag) in the capacity-warped Fubini–Study geometry. The constraints are algebraic: AGC-defined global admissibility, BBP closure expression, local admissibility (RCC-1…9), and compatibility with boundary conditions (ADT/TCD). Evaluation of candidate frames uses principal-angle metrics on $\mathrm{Gr}_{\rho}(k,n)$ together with invariant budget measures (curvature sums, coherence norms). The result is a variational principle on the space of subspaces equipped with the ρ-warped Grassmannian metric (principal-angle form), guided by relational consistency rather than temporal dynamics.

Algorithmically, several routes present themselves:

- **Rotor-based alignment:** admissible rotor re-expressions align neighboring simplicial frames, enforcing boundary consistency of oriented curvature supports.
- **Projection chains:** iterated admissible projections define echo/readout measures (overlap invariants) across neighboring selections in $\mathrm{Gr}_{\boldsymbol{\rho}}(k,n)$.
- **Slack/compression monitors:** principal-angle spectrum diagnostics flag over- or under-constrained regions within the admissible domain.

Curvature in Regge calculus enters explicitly through deficit angles at hinges. The discrete Regge action can be written as:

$$\mathcal{S}_{\mathrm{Regge}} = \sum_{h\in\mathcal{H}} \epsilon_h \, A_h \tag{6.1}$$

where ϵ_h is the deficit at hinge h and A_h its hinge area (used here as a capacity weight). We identify A_h with the dual hinge area and interpret it as a capacity proxy; when used in this role it preserves the same scaling as the geometric hinge measure, ensuring NPRF

consistency. In cRBW/RSE terms, the global closure structure: AGC as primitive admissibility, BBP as its boundary-operator closure expression, and $\mathbb{I}_0$as the non-ontic projective normalization baseline and NPRF-stable ratio readouts, bound the admissible allocations of $\{\epsilon_h A_h\}$; local RCC gates enforce legibility and identity. Thus, Regge curvature discretization couples directly to global constraint fidelity, aligning simplicial curvature bookkeeping with closure consistency.

This cross-mapping situates Regge-style discrete curvature, GA representations of bivector structure, and Grassmannian optimization within a single computational framework. It provides both a formal language for global consistency and a toolkit for exploring coherence-preserving coherence re-expression.

6.1 Worked Example: 2-Simplex and Grassmannian Adjacency

To demystify the abstract mapping between Regge calculus, Geometric Algebra, and the Grassmannian, consider the simplest nontrivial case: a 2-simplex (triangle).

Step 1. Regge data

Let three vertices $p_1, p_2, p_3 \in \mathbb{R}^3$ (or embed the $\mathbb{R}^2$ triangle in $\mathbb{R}^3$ as a face) define a triangle. Edge lengths $\ell_{12}, \ell_{23}, \ell_{31}$ fix the simplex. If embedded in a 2D triangulation (or as a face in higher-D), a hinge deficit ϵ_h measures Regge curvature.

Step 2. GA representation

Represent edges as vectors $e_{ij} = p_j - p_i$. The oriented area of the simplex is given by the bivector:

$$B = e_{12} \wedge e_{13} \tag{6.2}$$

which encodes area $|\ B\ |$ and orientation (plane). Rotations within that plane are generated by the rotor**:**

$$R \;=\; \exp\left(-\frac{1}{2}\,\theta\,\hat{B}\right), \qquad \hat{B} \equiv \frac{B}{|\ B\ |} \tag{6.3}$$

acting on vectors (and extending to blades) by conjugation $v \mapsto Rv\tilde{R},\ A_k \mapsto RA_k\tilde{R}$.

$$p_{ij} = \det\left(X^{(i,j)}\right)$$

We write A_{σ_k} when we need to emphasize the supporting simplex σ_k; otherwise A_k denotes a generic k-blade representative.

Step 3. Grassmannian embedding

Let $X \in \mathbb{R}^{2\times 3}$ have rows forming an oriented basis for span $\{e_{12}, e_{13}\}$; denote by $X^{(i,j)}$ the

2×2 minor formed by columns i and j. The 2-plane spanned by $\{e_{12}, e_{13}\}$ is a point in $\mathrm{Gr}_\rho(2,3;\mathbb{R})$. Its Plücker coordinates $p_{ij} = \det\left(X^{(i,j)}\right)$ give the projective embedding; equivalently, the decomposable blade B represents the same subspace up to scale.

Step 4. Adjacency as apparent change

Considering a rotor R corresponds to a curve in $\mathrm{Gr}_\rho(2,3)$: a Grassmannian adjacency chain through nearby planes. This is *apparent change* (ordered comparison of admissible re-expressions), coherent re-expression of the simplex, rather than ontic temporal evolution.

Step 5. Interpretation in cRBW and RSE

- In cRBW, the simplex's curvature patch is a local budgeted contribution to $\mathcal{S}_{\mathrm{Regge}}$ consistent with the AGC.
- In RSE, an admissible adjacency chain is *lived continuity*: lamination recursion along a worldline, oriented by causal admissibility constraints and minimized misalignment (cf. d_ρ in §4.4–4.5).

Step 6. Numeric mini-example (principal angles, weighted misalignment, one symmetric re-expression step)

Take two nearby 2-planes in $\mathbb{R}^3$: $U = \mathrm{span}\{e_1, e_2\}$, and V obtained by a small rotation of angle $\theta = 0.10$ rad about e_3. The principal angles are $\{\theta_1, \theta_2\} = \{0, \theta\}$. Use weights $\rho = \{1,4\}$ (corresponding to $\rho_1 = 1, \rho_2 = 4$). Define the ρ-warped Grassmannian distance from Eq. (6.10):

$$d_\rho^2 \equiv \rho_1\theta_1^2 + \rho_2\theta_2^2 = 1 \cdot 0^2 + 4 \cdot (0.10)^2 = 0.04, d_\rho = 0.20. \tag{6.4}$$

Tie this to the deficit via the small-angle relation (matching Eq. 6.6 conventions) where C_E is a dimensionless proportionality constant (a local budget-to-deficit scale in this toy example)

$$\epsilon_h \;=\; \frac{C_E}{2}\sqrt{\rho_1\theta_1^2 + \rho_2\theta_2^2} \;=\; \frac{C_E}{2} \cdot 0.20 \;=\; 0.10\, C_E. \tag{6.5}$$

Here C_E is a dimensionless toy proportionality constant converting weighted misalignment to a deficit-scale in this illustrative example (set $C_E = 1$ if desired). Define the hinge rotor $R_h \;\equiv\; \exp\left(\frac{1}{2}\eta_h \hat{B}_h\right),\; \tilde{R}_h = R_h^{-1}$. Now evaluate the symmetric half re-expression at the hinge:

$$A_k(p) \leftarrow R_h\, A_k(p)\, \tilde{R}_h, \qquad A_k(q) \leftarrow \tilde{R}_h\, A_k(q)\, R_h. \tag{6.6}$$

This is a *representational re-expression*, not a temporal step. For small angles, Eq. (6.6) this reduces the relative principal angle by the factor $(1-\eta_h)$. Choose $\eta_h = 0.5$ (a representative admissible re-expression weight). Then

$$\theta' = (1-\eta_h)\theta = 0.5 \cdot 0.10 = 0.05 \text{ rad}, \qquad d'_\rho = \sqrt{1 \cdot 0^2 + 4 \cdot (0.05)^2} = 0.10,$$
$$\epsilon'_h = \frac{C_E}{2} \cdot 0.10 = 0.05\, C_E. \tag{6.7}$$

One symmetric re-expression halves both d_ρ and ϵ_h in this example, illustrating the reduction of the misalignment functional under Eq. (6.6).

Thus, even a minimal 2-simplex demonstrates how Regge curvature, GA bivectors, and Grassmannian adjacency chains jointly encode both the adynamical block structure of cRBW and the recursive phenomenology of RSE. Figure 6.1 illustrates the correspondence among the Regge simplex, its GA bivector representation, and the associated Grassmannian point.

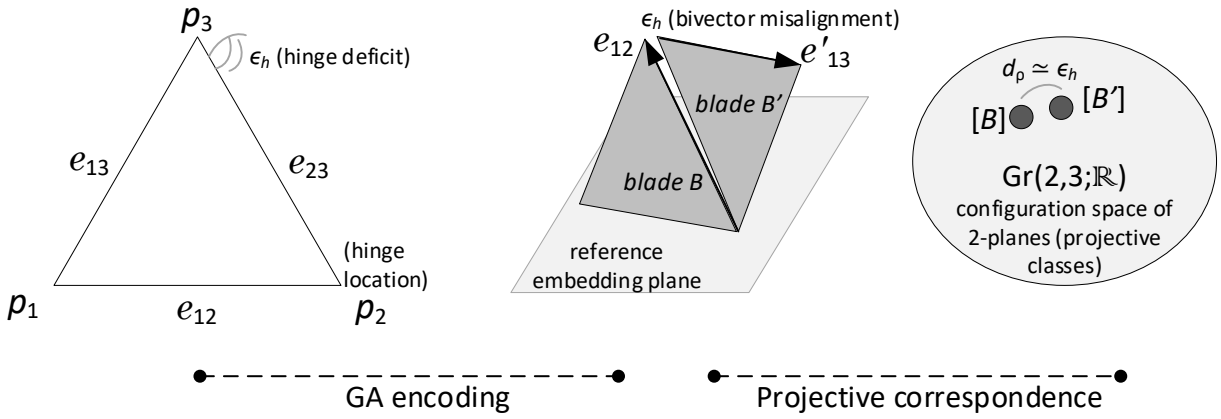

Figure 6.1—Regge-GA-Grassmannian Interlock.

The local correspondence illustrated here extends to closed constraint loops, whose Regge, GA, and Grassmannian representations are shown schematically in Appendix E, Figure E.1.

6.2 Computational Anchor: Principal Angles via SVD

The standard principal-angle construction is summarized for reproducibility and then the minimal facts needed for the ρ-warped Grassmannian used in our variational updates are stated.

6.2.1 Principal angles via SVD (canonical case)

Given orthonormal basis matrices $U, V \in \mathbb{R}^{n\times k}$ spanning two k-planes, form the overlap $M = U^{\top}V$. The singular values of $M = P\Sigma Q^{\top}$ satisfy:

$$\Sigma = \operatorname{diag}(\cos\,\theta_1, \ldots, \cos\,\theta_k) \tag{6.8}$$

so the principal angles $\{\theta_i\}$ provide the canonical alignment measure. The canonical Grassmannian distance is

$$d^2([U],[V]) = \sum_{i=1}^{k} \theta_i^2 \tag{6.9}$$

Small angles indicate tight coherence; large angles flag curvature stress or potential inadmissibility.

6.2.2 The ρ-warped Grassmannian

Define the ρ-weighted (warped) metric (cf. §2.6.9, Well-Posedness Condition)

$$d_\rho^2([U],[V]) = \sum_{i=1}^{k} \rho(s_i)\,\theta_i^2\,, \qquad 1 \le \rho(s_i) \le \rho_{\max} < \infty \tag{6.10}$$

With ρbounded above and below, the weighted principal-angle expression defines a positive local quadratic form. If ρ is smooth, this gives a Riemannian metric bi-Lipschitz equivalent to the canonical Fubini–Study metric. If ρ is only Lipschitz, the induced metric space remains bi-Lipschitz to the canonical Grassmannian, but smooth curvature statements should not be made without additional regularity. Consequently, compactness/completeness and the existence of minimizing geodesics are preserved (Hopf–Rinow); local geodesics are unique by standard ODE well-posedness. In the small-angle principal 2-plane, the symmetric half-update Eq. (6.6) decreases d_ρ by a factor $(1 - \eta_h)$, ensuring descent of the misalignment energy.

For constant weights in a fixed principal-angle frame, rotor-generated curves in simple bivector planes realize the usual weighted geodesic segments. For variable ρ, rotor updates should be treated as descent or re-expression curves in the warped metric, not automatically as geodesics.

Box 6.1— Numerical convergence of representational solvers (not physical dynamics)

Rotor-field relaxation (§ 2.5.4) is tested for convergence under both deterministic and stochastic refinement:

- **Tolerance criterion:** evaluations stop when $\sum_h \mid \epsilon_h \mid \leq 2 \times 10^{-1}$ rad (or equivalently ≤ 0.2 in normalized units), ensuring residual curvature below 1 % of the mean budget.
- **Step-size control:** adaptive line search satisfies $\mid \Delta \mathcal{J}_{L^2} \mid < 10^{-6}$ between evaluations.
- **Monte Carlo check:** random perturbations of initial hinge orientations $\Delta B_h / B_h \in [-0.05, 0.05]$ produce identical stationary values within 10^{-4} relative error, confirming stochastic stability. These criteria define reproducible stopping and error bounds for all numerical evaluations, and serve as a perturbative validation of the weak-convergence estimate summarized in App. F.6

A concise algorithmic realization of this warped-metric search is given in §6.2.3 as a rotor-ensured relaxation procedure on the ρ-warped Grassmannian.

6.2.3 Algorithmic Sketch for ρ-warped Optimization

The coherent-selection variational procedure can be implemented as a discrete relaxation on the ρ-warped Grassmannian. Let V_k be an initial admissible selection (a k-plane or k-blade). The algorithm enumerates admissible re-expressions V_k by local rotor actions implemented by coherence gradients and capacity weights:

The following algorithm is a numerical procedure for locating stationary admissible configurations of a fixed coherence functional; it does not represent temporal evolution of the block.

Pseudocode

initialize V_k
repeat
  compute principal angles $\theta_i(V_k, V_k')$
  compute warp weights $\rho_i = \rho(s_i)$
  construct local bivector generator $B(\nabla C)$
  $R \leftarrow exp(-½B)$ // rotor update
  $V_k \leftarrow normalize\big(R \cdot V_k \cdot \tilde{R}\big)$
until convergence

The update is admissible only if the new V_k remains in the RCC-consistent domain $\mathcal{A}_{\mathrm{RCC}}$. Convergence is guaranteed by the smoothness and bilipschitz bounds of the warped metric (App. A.7) and by the BBP regularity conditions (§2.6.9 Well-Posedness Condition), which ensure geodesic completeness and bounded curvature even in the quasi-Kähler regime. This algorithm provides a constructive route for numerical verification of coherence minima and mixed-capacity effects.

While direct SVD-based optimization on large simplicial complexes is expensive (scaling as $O(n^3)$), the warped-Grassmannian functional is amenable to low-rank projector updates, geodesic gradient descent, and block-coordinate methods that reduce complexity to $O(nk^2)$. Additionally, each Regge cell update is local in the capacity tensor, allowing parallelization across simplicial supports. Thus, the computational challenge is mitigated by the locality of the hinge-based updates and the geometric structure of the coherence functional.

6.3 Empirical Domain and Mixed-Capacity Activation Thresholds

Mixed capacities $K_{\alpha\beta}$ are suppressed in ordinary-curvature regimes but need not be negligible in high-curvature or high-coherence-gradient environments. The coherence functional (Eq. 2.23) predicts that cross-sector terms activate when $\rho(s_i)\,\theta_i^2 \gtrsim \Xi_{\mathrm{diag}}$ for some diagonal sector capacity.

This provides a quantitative activation criterion: mixed-sector channels become non-negligible under admissible closure budgets when lamination tension in one sector exceeds the stabilization budget of another. Black-hole interiors, near-extremal compact objects, quantum-critical systems, and high-intensity interferometry experiments constitute potential regimes. These thresholds furnish *testable inequalities* rather than mere qualitative claims, enabling experimental bounds on $K_{\alpha\beta}$ via coherence-loss signatures or entanglement saturation.

---

7 Phenomenology Notes

This section is interpretive and auxiliary; no physical claims or testable predictions are introduced beyond the formalism already developed.

Attention as selection

Within the warped Grassmannian frame, $\mathrm{Gr}_\rho(k,n)$, *attending* is recursively stabilizing a subspace V_k, allocating coherence-weight to one attractor while backgrounding others. This is *allocative*, not eliminative: alternatives remain structurally present but de-emphasized. The felt asymmetry of foreground vs. periphery corresponds to this recursive coherence allocation.

Compression and slack

As coherence budgets are allocated under admissible lamination, the admissible family of subspaces contracts. In principal-angle terms, dispersion decreases: $\sum_i \theta_i^2$ narrows, yielding stability/fixation (certainty at the cost of exploration). With surplus budget, admissibility widens (greater angle freedom), phenomenologically mapping to novelty, surprise, or imaginative play.

Width of the present

The "extended now" is a coarse-grained lamination span: a finite coherence width along a worldline rather than an infinitesimal slice. Operationally, it is the interval over which an oriented chain minimizes weighted misalignment,

$$\gamma^* \in \arg\min_{\gamma' \text{ admissible}} \sum_{\langle p,q\rangle \in \gamma'} d_w(p,q) \tag{7.1}$$

subject to the causal null gate and RCC constraints (with weights inherited from the same ρ-warped metric defined in Eqs. (4.5) and (6.10)). Its scale depends jointly on slack in the AGC-defined closure budget, expressed through BBP, and the projective normalization baseline $\mathbb{I}_0$, and the stability of local Regge deficits.

Echo and afterimage

Residual coherence outside the currently selected subspace manifests as echo: low-weight re-entry of prior attractors within the present lamination span. Subjectively this appears as memory trace, lingering image, or affective residue. Echo is residual allocation—an attenuated remainder from earlier selections. It is not retrieval.

Anticipation as forward curvature

The inverse structure underlies anticipation. Asymmetry toward admissible *future* subspaces produces a forward echo felt as expectancy or intention. In Regge terms, this is

structural bias in admissible curvature allocation: earmarking coherence budget ahead of alignment under the same RCC/AGC gates.

Phenomenological trade-off
Lived experience corresponds to a structural balance between compression (stability, fixation) and slack (openness, exploration). The feels of certainty, memory, and anticipation arise not from causal dynamics but from recursive modulation of admissible subspaces within coherence budgets, as encoded by Grassmannian orientation, GA rotor re-expression, and Regge-style curvature bookkeeping.

The next empirical step is to translate mixed-capacity activation thresholds, entanglement saturation behavior, and curvature-induced coherence loss into experimental signatures—particularly in gravitational interferometry, photonic entanglement under tidal distortion, and analog Rindler setups—where the quasi-Kähler cross-terms predict specific, measurable departures from linear superposition.

This section introduces no additional primitives; it re-describes earlier formal structures in experiential vocabulary to aid interpretation.

---

8 Conclusion

Geometric Algebra supplies the algebra of relations; the complex Grassmannian with its ρ-warped Fubini–Study metric supplies the space of coherent selections; cRBW supplies AGC-defined admissibility, expressed through BBP closure with $\mathbb{I}_0$ as the projective normalization baseline; RSE supplies the experienced ordering of admissible selections. Taken together, they yield a single algebraic–geometric account in which what we call "change" is an *oriented selection chain* through admissible subspaces of a fixed relational block—supported, intensified, or rendered inadmissible by lamination, compression, and gapping.

This integration of GA, $\mathrm{Gr}_\rho(k,n)$, and Regge calculus shows that the structures of cRBW and RSE can be encoded not only philosophically but algebraically. Plücker coordinates and principal angles provide explicit handles on coherence, resonance, and dissonance, enabling phenomena often confined to the language of experience to be expressed as invariant geometric relations. Recursive coherence and structural experience are not extra-scientific additions but necessary internal legibility structures of any closure-first ontology.

The dual role of the Grassmannian reflects this integration: the complex Grassmannian furnishes an algebraic envelope for closure-compatible structure (cf. B-theory) as an organizational analogy, not an ontic identification (cf. Price [34]), while the real Grassmannian encodes coherence manifolds as experienced (A-theory as local becoming; cf. Dorato [35]). Algebra provides grammar; real-valued structures provide constrained geometry (cf. Penrose [36]).

This unification points toward a fully algebraic model of relational physics and structural experience, one in which geometry, constraint, and phenomenology share a common representational scaffold within a single adynamical structure. The traditional gap between physical law and lived coherence is thereby reduced to projection choice within a single adynamical structure.

The capacity-tensor scaffold is not required for every Regge recovery calculation. In particular, lower-level Regge tests may recover standard observables without exercising the full five-sector capacity tensor; the capacity tensor supplies the higher-level cross-sector admissibility and legibility structure.

Outlook. Three immediate directions follow: (i) computational implementations that minimize weighted Grassmannian misalignment under RCC gates and AGC floors; (ii) Regge-style audits of curvature/coherence budgets across meshes; and (iii) phenomenology-level tests that relate bandwidth of the "present," echo, and anticipation

to principal-angle dispersion and coherence slack. Each advances the same thesis: ontology, structure, and experience are different readable faces of one global solution. In each case, the relevant observables are inequalities and stability bounds on principal-angle spectra and mixed-capacity magnitudes, not dynamical trajectories. Accordingly, empirical contact is made through constraint violations, coherence loss, or mixed-capacity activation—not through time-series evolution. Standard general-relativistic phenomenology is expected to arise as a special class of capacity assignments on the Regge skeleton, even though no explicit phenomenological modeling is undertaken here.

Appendix A: Operator Dictionary and Cross-Mappings

Appendix A is a reference dictionary. All operators, constraints, and mappings listed here are defined and motivated in the main text. No new assumptions or dynamical principles are introduced; the appendix exists solely to facilitate cross-formalism translation.

A.1 Core GA Operators

Geometric product

For vectors $a, b \in \mathbb{R}^{p,q}$:

$$ab \;=\; a \cdot b \;+\; a \wedge b. \tag{A.1}$$

Inner product $(a \cdot b)$ encodes metric contraction; outer product $(a \wedge b)$ encodes oriented incidence/extension.

Blade decomposability

A k-vector $B \in \Lambda^k \mathbb{R}^n$ is a blade iff it is decomposable:

$$B = v_1 \wedge \cdots \wedge v_k. \tag{A.2}$$

For $k = 2$, $B \wedge B = 0 \Leftrightarrow$ decomposable. For $k > 2$, decomposability is characterized by the Plücker relations ($B \wedge B = 0$ is necessary but not sufficient).

Rotor (even versor) action

With $R = \exp\left(-\frac{1}{2}B\right)$ (bivector generator), the reverse $\tilde{R}$ gives:

$$v' = R\, v\, \tilde{R}, \qquad A'_k = R\, A_k\, \tilde{R}. \tag{A.3}$$

Rotors re-express (reorient) while preserving grade and rotor invariants (e.g., I_C).

General versors

Products of vectors implement reflections and other orthogonal transformations; rotors are the even subgroup (proper ortho-chronous in appropriate signatures).

A.2 Grassmannian Embeddings

Plücker embedding

Let $V \in \mathrm{Gr}_\rho(k, n)$ be a k-plane; when working over $\mathbb{R}$ this is a subspace of $\mathbb{R}^n$ and when working over $\mathbb{C}$ a subspace of $\mathbb{C}^n$. Pick a full-rank $n \times k$ matrix A whose columns form a basis of V. For any index set $I \subset \{1, \ldots, n\}$ with $|\, I \,| = k$, let $A_{I,:}$ be the $k \times k$ submatrix of A using the rows in I. The Plücker coordinates are

$$p_I \;=\; \det\left(A_{I,:}\right), \qquad |\, I \,| = k \tag{A.4}$$

defined up to a common nonzero scale factor (i.e., $[p_I]$ are homogeneous coordinates on the Plücker embedding of:

$$\mathrm{Gr}_\rho(k,n) \hookrightarrow \mathbb{P}^{\binom{n}{k}-1}. \tag{A.5}$$

- Change of basis $A \mapsto AM$ with $M \in \mathrm{GL}(k)$ multiplies all p_I by $\det(M)$, so the projective point is well defined.
- The wedge $a_1 \wedge \cdots \wedge a_k$ of the columns has coefficient p_I on $e_{i_1} \wedge \cdots \wedge e_{i_k}$ (for $I = \{i_1 < \cdots < i_k\}$). See §5.1 for the physical interpretation of Plücker coordinates as relational invariants.

Principal angles

When working over $\mathbb{R}$, the overlap matrix is $M = U^\top V$. When working over $\mathbb{C}$, the corresponding definition is $M = U^* V$, with principal angles defined via the singular values in either case. In the present work, phenomenological distances are always evaluated on the real locus.

For orthonormal bases $U, V \in \mathbb{R}^{n\times k}$, let $M = U^\top V = P\Sigma Q^\top$(SVD). Then

$$\Sigma = \mathrm{diag}(\cos\,\theta_1, \ldots, \cos\,\theta_k), \qquad d([U],[V]) = \sqrt{\sum_{i=1}^{k} \theta_i^2}. \tag{A.6}$$

Equivalently, $d^2([U],[V]) = \sum_{i=1}^{k} \theta_i^2$. Weighted form (used in §§2.4, 4–6 as the ρ-warped Fubini–Study distance):

$$d_\rho^2([U],[V]) = \sum_{i=1}^{k} \rho_i\, \theta_i^2\,, \qquad \rho_i \geq 0. \tag{A.7}$$

Adjacency chains

Ordered sequences of neighboring subspaces in $\mathrm{Gr}(k,n)$; phenomenologically these read as apparent change (experience as oriented selection).

A.3 Regge Calculus Correspondence

Deficit angle (hinge curvature). For hinge h and deficit angle ϵ_h,

$$\epsilon_h \;=\; \alpha_n - \sum_{\sigma \supset h} \theta_{h,\sigma}. \tag{A.8}$$

Here α_n denotes the flat-space dihedral angle sum about the codimension-2 hinge under the chosen discretization convention; in standard Regge calculus this equals 2π in 2D.

Regge action

$$\mathcal{S}_{\text{Regge}} \;=\; \sum_{h \in \mathcal{H}} \epsilon_h \, A_h, \tag{A.9}$$

with A_h a (dual) area/capacity. In our reading: deficits are coherence-curvature budgets, not forces.

GA correspondence
Hinge geometry sits in a bivector B (magnitude ↔ capacity; orientation ↔ plane) and accumulates via bivector sums consistent with closure.

A.4 cRBW Constraint Mapping

- **AGC (global primitive):** fixes source-level admissibility of the single adynamical relational configuration. In boundary-operator representations, BBP expresses the closure form $\partial^2 = 0$. The baseline $\mathbb{I}_0$ supplies non-ontic projective normalization.
- **RCCs (local):** RCC-1…9 gate topology, budgets, mesh, localization, resonance, and non-trivial gradient.

Naming convention
RCC-5 is called **Boundary Consistency** in this mathematical dictionary and **Decoherence Triangulation** in cRBW's phenomenological exposition; both refer to the same boundary hand-off role. RCC-8 is called **Resonance Stability** here and **Coherence Resonance Matching** in cRBW; both refer to the same cross-local resonance condition.

The following RCC list is a *reference summary* of constraints defined and motivated in §§2–4. No new constraints are introduced here.

Box A.1— cRBW Relational Coherence Constraints (RCC-1…9)

RCC-1 Topological closure: no open incidence cycles on the mesh.

RCC-2 Symmetry closure: invariance under admissible rotor/versor actions.

RCC-3 Curvature budget: summed hinge deficits satisfy global bounds.

RCC-4 Observer embedding: admissible flags (laminations) exist for readout.

RCC-5 Boundary consistency: sub-laminations inherit canonical residues (lawful hand-off to faces).

RCC-6 Gradient-mesh matching: small-angle continuity along identity chains.

RCC-7 Identity localization: rotor-invariant blade scalar anchors identity.

RCC-8 Resonance stability: scalar/pseudoscalar norms remain within bounds.

RCC-9 Non-trivial gradient: exclude $\nabla C \equiv 0$ across admissible domains.

RCCs are local/representational gates under AGC-defined admissibility, with closure expressed through BBP and projective normalization supplied by $\mathbb{I}_0$.

Box A.2— RCC representative formal forms (examples)

RCC-3: $\sum_{h\in\mathcal{H}} C_h \mid \epsilon_h \mid \leq B_{\text{global}}$

RCC-6/7: $\max_i \theta_i \leq \theta_{\text{id}}$ along identity chains

RCC-8 (Resonance stability): $\mathcal{I}_{C,min} \leq \mathcal{I}_C(x) \leq \mathcal{I}_{C,max}$ on admissible domains.

RCC-9: $\| \nabla C \| \geq \eta > 0$ on admissible domains

Global re-expression invariance (AGC)

Admissible rotor fields preserve global invariants and lattice closure:

$$\begin{aligned} &\text{AGC} \\ &- \text{defined invariants, BBPclosureexpression, NPRF } \mathbb{I}_0 \text{ projective normalization,} \\ &\qquad\qquad \text{and RCC constraints} \\ &\Rightarrow \quad A_k \mapsto R\, A_k\, \tilde{R} \text{ leaves } \mathcal{I}_C \text{ and budgeted sums unchanged.} \end{aligned} \tag{A.10}$$

Curvature/coherence budget closure (Regge ↔ GA)

$$\sum_{h\in\mathcal{H}} \epsilon_h A_h \quad \text{bounded by AGC floor; distributed under RCC gates.} \tag{A.11}$$

Identity invariant

Rotor-invariant identity scalar for a laminated k-blade field:

$$I_{id}(x) = \langle \Lambda(x)\, \widetilde{\Lambda}(x) \rangle_0 \ \text{(constant under admissible } R\text{).} \tag{A.12}$$

This local identity scalar should not be confused with the global coherence functional $\mathcal{I}_C$.

Table A.1—RCC - Grassmannian Comparison

RCC	GA Form	Invariance Statement	Grassmannian Gate
1	$\sum_{\partial\sigma_h} B_h = 0$ (cf. Eq. 2.11)	Topological closure: sum of hinge bivectors vanishes → no open 2-cycles.	Defines legal chart boundaries on the real slice.
2	$B' = RB\tilde{R}$ for rotor $R = \exp(-\Omega/2)$	Symmetry closure under rotor/versor actions.	Restricts admissible rotor directions to orthogonal re-expressions on $\mathrm{Gr}_{\mathbb{R}}$.
3	$\sum B_h = 0$ (cf. Eq. 2.12)	Curvature budget closure ("no residual deficit").	Bounds curvature amplitude so only RCC-consistent subspaces enter the real Grassmannian.
4	Flag of nested blades $(X_1 \wedge X_2 \wedge \dots)$	Observer embedding as lamination hierarchy.	Selects sub-flag charts (stable identity tracks).
5	$\langle B_i, B_j \rangle = \langle B_j, B_i \rangle$	Boundary consistency at shared faces (§ 2.6.7, Eq. (2.27)).	Guarantees coherence flux matches across cells.
6–7	$\mid \theta_{ij} \mid < \theta_{\mathrm{id}}$	Identity/localization bounds enforce small principal angles along identity-tracking chains (cf. RCC-6/7).	Limits principal-angle spread on $\mathrm{Gr}_{\mathbb{R}}$ so identity persists across the chain (see §4.5).
8–9	$\parallel \nabla\mathcal{C} \parallel > 0$, $\mathcal{C}$ bounded,	Resonance stability & non-trivial gradient (§ 2.5.3).	Ensures finite warp weights ρ → smooth real slice.

Phenomenological Note

The GA identities above act as Grassmannian gates: they restrict admissible coordinates on the real locus $\mathrm{Gr}(k, n; \mathbb{R})$ without altering the fixed algebraic envelope used to represent closure-compatible structure ($\mathrm{Gr}(k, n; \mathbb{C})$ remains fixed). This is how phenomenological legibility arises without adding new dynamics.

A.5 Diagnostic Indices (simulation tools)

- σ_0: unnormalized blade magnitude $\sigma_0 = \sqrt{\langle A_k \tilde{A}_k \rangle_0}$.
- **LDI (Lamination Density Index):**

$$\mathrm{LDI} = \frac{\parallel \nabla C \parallel}{\Omega_h}, \tag{A.13}$$

comparing local coherence-gradient norm to available capacity Ω_h (hinge/dual volume).

- **CDI (Curvature Density Index):** $\mathcal{C}$ (see §2.5.3)
- **RDF (Rotor Drift Factor):** *Document default:* minimal rotor-cycle count (or accumulated angle) required for realignment under RCC bounds. RDF is a numerical diagnostic used in representational solvers; it plays no role in the formal or ontic development.

A.6 RSE Phenomenological Mapping

- **Lamination.** Nested flags in GA; realized as successive selections in $\mathrm{Gr}_{\rho}(k,n)$.
- **Attention/Measurement.** Selection of V_k with recursive projection into neighboring admissible subspaces (allocative, not eliminative).
- **Echo.** Recurrent low-weight projection of multi-vectors onto prior stabilized subspaces (residual allocation, not retrieval).
- **Phantom traversal.** Inadmissible loop where carryover falls below threshold (e.g., $\Phi_{\mathrm{carry}} < \Phi_{\mathrm{min}}$); experienced as discontinuity.

A.7 Summary Table

Table A.2—Construct - GA- Grassmanian - Regge

Construct	GA expression	Grassmannian form	Regge analogue	RSE meaning
Curvature patch	$B = e_i \wedge e_j$ (bivector)	point in $\mathrm{Gr}_{\rho}(2,n)$	hinge deficit ϵ_h with capacity A_h	structural curvature/coherence
Rotor action	$A'_k = R\,A_k\,\tilde{R}$	adjacency step on $\mathrm{Gr}_{\rho}(k,n)$	frame/face alignment across hinges	coherence re-expression
Lamination	flag $V_1 \subset V_2 \subset \cdots$	flag manifold	nested simplices / dual cells	recursive layering
Coherence resonance	norm/grade stability; I_C invariant	bounded d_w, stable $\{\theta_i\}$	budget closure across $\mathcal{H}$	identity continuity
Phantom traversal	$\Phi_{\mathrm{carry}} < \Phi_{\mathrm{min}}$	inadmissible chain	degenerate/over-constrained region	loss of lived continuity

Lemma A.1 (ρ-warped principal-angle metric).
Let $\rho = (\rho_1, \ldots, \rho_k)$ with $0 < \rho_{\min} \le \rho_i(x) \le \rho_{\max} < \infty$. For $U, V \in \mathrm{Gr}(k,n;\mathbb{R})$ with principal angles $\{\theta_i\}$, define the local weighted principal-angle form

$$d_\rho^2(U,V) := \sum_{i=1}^{k} \rho_i \, \theta_i^2. \tag{A.14}$$

For constant weights in a fixed principal-angle chart, this gives the corresponding weighted Grassmannian distance. If the weights vary smoothly over the Grassmannian, Eq. (1A.14) defines the local quadratic form of a Riemannian metric, and the global distance is obtained by minimizing path length. If the weights are only Lipschitz but uniformly bounded above and below, the resulting metric space is bi-Lipschitz equivalent to the canonical Grassmannian metric, but smooth curvature claims require additional regularity.
For a simple-bivector rotor curve with constant weights in a principal-angle chart, $V(t) = R(t) \cdot U, R(t) = \exp(tB)$, the induced length is

$$\text{Length}(0 \to 1) = \left(\sum_i \rho_i \, \theta_i^2 \right)^{1/2}. \tag{A.15}$$

For variable ρ, rotor curves are admissible re-expression or descent curves, not automatically geodesics.

Proof Sketch: On the Grassmann manifold $\mathrm{Gr}(\mathrm{k}, \mathrm{n})$, the canonical Riemannian metric is given by the principal-angle distance $\mathrm{d}^2(\mathrm{U}, \mathrm{V}) = \sum_{\mathrm{i}} \theta_{\mathrm{i}}^2$ (Absil et al., 2008, §2.5). Any smooth weighting of the tangent-space inner product by uniformly bounded positive-definite factors ρ_{i}defines a Riemannian metric that is bi-Lipschitz equivalent to the canonical metric on this compact manifold (ibid., §2.1–§2.3). Geodesic completeness and existence of minimizing geodesics then follow by Hopf–Rinow. Rotor-generated curves align with principal 2-planes and realize these geodesics explicitly (ibid., §3.6). See App. F.6 for how this metric underlies rotor-RCC descent and Regge weak-convergence estimates. No claims of global uniqueness beyond standard Grassmannian results are made.

Plücker view. Pull back the weighted Fubini–Study form on the Plücker embedding by scaling angle directions with ρ; the induced real metric on $\mathrm{Gr}(k, n)$ coincides with d_w^2 to second order in $\{\theta_i\}$.

Appendix B: Positive Geometries & Computational Scaffolds

Appendix B provides mathematical context and computational precedent; it introduces no additional assumptions, constraints, or physical claims beyond those developed in the main text. This appendix supplies a concise translation layer between positivity notions (canonical forms, residues), our Grassmannian/GA formalism, and cRBW/RSE. It's context and tooling; not a new result.

B.1 Positive geometry (core ideas)

Definition. A *positive geometry* is a pair $(X, X_{\geq 0})$. Here X is an algebraic variety and $X_{\geq 0} \subset X(\mathbb{R})$ is a closed, oriented, semi-algebraic region whose boundary is stratified by faces. There exists a unique *canonical top form* $\Omega(X, X_{\geq 0})$ with only simple poles on boundary facets and *residue recursion*: the residue of Ω on any facet equals that facet's canonical form. We do not claim that the cRBW coherence domain *is* a positive geometry in the strict algebraic sense; the analogy is structural and motivational.

Intuition. An admissible region with a built-in measure that hands off cleanly to each lawful boundary.

cRBW/RSE map. $X_{\geq 0} \leftrightarrow$ domain of admissible coherence; $\Omega \leftrightarrow$ global coherence functional; residue recursion $\leftrightarrow$ lamination restriction (coherence handed to sub-laminations without loss).

B.1.1 Positive Grassmannian & positroid cells

Positive Grassmannians and positroid cells offer a natural combinatorial decomposition of $\mathrm{Gr}(k, n; \mathbb{R})$. In this language, laminations correspond to positroid strata, and recursive coherence corresponds to admissible adjacencies within or between cells. Where the coherence functional $\mathcal{J}_C$ is nonnegative on a cell, this follows from its own definition and the admissibility constraints, not from Plücker positivity. Positive-angle structure is used here as an organizational analogy, not as a derivation of nonnegativity. This offers a *structural analogy* to positive geometries familiar from scattering amplitudes, without importing their physical interpretation. Positive Grassmannian and positroid structures are used here purely as organizational geometry for admissible configurations; no new amplitude-theoretic or scattering interpretation is assumed. A full exploration is deferred to future work.

The totally nonnegative part of the underlying real Grassmannian, $Gr(k,n)_{\geq 0}$, is used as an organizational analogy for admissible charting and boundary handoff. The ρ-warping modifies metric weighting and does not redefine the algebraic positive Grassmannian. [37]

Map
Sign-coherent regions of $\mathrm{Gr}_{\rho}(k,n)$↔ coherence-eligible domains; positroid tilings ↔ lawful RCC atlases (pieces glue by residue consistency). Discrete differential-geometry frameworks also use Plücker-quadric/Grassmannian machinery to encode discrete incidence and contact structures, providing precedent for deploying Plücker geometry in a discrete setting. [38]

B.1.2 Related structures

These are cited solely as precedent for *mathematical technique*, not physical equivalence.

- **Amplituhedron / positive geometries of scattering.** Example where a canonical form encodes physics directly (motivation, not dependency here). [39]
- **Cosmological polytopes.** Polytope canonical forms matching wavefunction data (again as precedent that "geometry + residues = physics data"). [40]

B.2 Potential Computational scaffolds

- **Symanzik/Feynman integrals.** Graph-based integrals over positive cones; expose singular sets. [41]
  Use here: probe coherence budgets; boundary singularities flag inadmissible interfaces.
- **Twisted (co)homology / generalized Euler integrals.** Contour-dependent forms with branch data. [42]
  Use: model endo traversals (legal sequences) without invoking time evolution.
- **GKZ (A-hypergeometric) /** D**-modules.** Holonomic PDE frameworks with controlled monodromy. [43]
  Use: algebraic analogue of AGC; encode global constraints and continuations.
- **Landau singularities / principal** A**-determinant.** Loci where integrals pinch or ranks drop.
  Use: diagnostics for failure surfaces (excess interface curvature / incoherent adjacencies).
- **Positroid triangulations.** Legal tilings whose canonical forms sum to the whole.

(Schematic example, no evaluation implied.)

$$\mathcal{I}_G \propto \int_{\alpha_i>0} (\prod \alpha_i^{\nu_i - 1}) \, [\; U_G + F_G \;]^{-D/2} \, d\alpha \tag{B.1}$$

Graph polynomials U_G, F_G mirror budget/constraint structure; singular sets track boundary failures.

These tools are optional and illustrative; none are required for the formulation of cRBW.

B.3 cRBW & RSE integration (summary)

Exo (cRBW)
An AGC-admissible domain is used here by analogy with positive geometry: a fixed coherence object whose boundary restrictions are lawfully inherited. No canonical positive-geometry form is asserted for $\mathcal{I}_C$, and Ω is not claimed to be a canonical form in the amplituhedron sense.

Endo (RSE)
Lived sequence = traversal through a legal atlas (positroid/flag charts) of the same fixed object; residue recursion guarantees continuity across lamination boundaries. ('sequence' here denotes an ordered *comparison relation*, not temporal succession)

In summary, what looks like "dynamics" is the order of admissible selections, not evolution of the block; fully consistent with our GA–$\mathrm{Gr}_\rho(k,n)$–Regge machinery.

Appendix C: From Complex to Real Grassmannians

Appendix C formalizes the use of complex Grassmannians as an algebraic envelope and the real Grassmannian as the phenomenological projection; no additional ontological structure is assumed.

Let $\mathrm{Gr}_\rho(k,n;\mathbb{C})$ be the set of k-dimensional linear subspaces of $\mathbb{C}^n$ (the complex Grassmannian) and $\mathrm{Gr}_\rho(k,n;\mathbb{R})$ the set of k-planes in $\mathbb{R}^n$ (the real Grassmannian). Complex conjugation $\tau\colon \mathbb{C}^n \to \mathbb{C}^n$, $\tau(z)=\bar{z}$, induces an involution on $\mathrm{Gr}_\rho(k,n;\mathbb{C})$ by $V \mapsto \bar{V}$. The real Grassmannian embeds as the fixed locus:

$$\mathrm{Gr}_\rho(k,n;\mathbb{R}) \;\cong\; \{\, V \in \mathrm{Gr}_\rho(k,n;\mathbb{C}) \;\mid\; \bar{V} = V \,\} \tag{C.1}$$

where V denotes an entire subspace, a k-plane, within the complex vector space $\mathbb{C}^n$. $\bar{V}=V$ means this subspace is invariant under complex conjugation; it can be spanned by vectors whose coordinates are all real. The collection of all such invariant subspaces is precisely the real Grassmannian, i.e., the set of k-planes in $\mathbb{R}^n$.

We use the complex Grassmannian as algebraic envelope; ratios I_j are preserved on the real slice by conjugation invariance (App. C.6–C.7).

C.1 Roles in this work

Complex = full algebraic atlas (exo/global)
$\mathrm{Gr}_\rho(k,n;\mathbb{C})$ furnishes algebraic closure: Plücker embeddings, Kähler structure, Schubert calculus, positivity structures, and analytic tools (twisted (co)homology, GKZ systems). It is the "global atlas" of lawful configurations; our ontic, B-theory domain. The use of the complex Grassmannian is a matter of algebraic closure and calculational convenience, not a claim of complex-valued ontic structure.

Real = experienced slice (endo/local)
$\mathrm{Gr}_\rho(k,n;\mathbb{R})$ is the conjugation-invariant slice carrying the real-valued coherence manifolds relevant for measurement/experience—our phenomenological, A-theory domain. It is lower-dimensional (as a real manifold) and encodes admissible coherence budgets and oriented selections used throughout §§4–7.

C.2 Canonical example: $\mathrm{Gr}(1,2)$

- **Complex case.** $\mathrm{Gr}_\rho(1,2;\mathbb{C}) \cong \mathbb{CP}^1$ (the Riemann sphere). As a real smooth manifold, $\mathbb{CP}^1$ is diffeomorphic to the 2-sphere S^2 via stereographic projection:

$$\mathrm{Gr}_\rho(1,2;\mathbb{C}) \;\cong\; \mathbb{CP}^1 \;\simeq\; S^2 \tag{C.2}$$

- **Real case.** $\mathrm{Gr}_\rho(1,2;\mathbb{R}) \cong \mathbb{RP}^1$, which is the circle S^1 (lines through the origin in $\mathbb{R}^2$ correspond to antipodal pairs on S^1):

$$\mathrm{Gr}_\rho(1,2;\mathbb{R}) \;\cong\; \mathbb{RP}^1 \;\simeq\; S^1 \tag{C.3}$$

This illustrates the general picture: the real locus is a lower-dimensional slice of the complex atlas fixed by conjugation; it represents the ontic domain's projection onto the phenomenological domain.

C.3 Cohomological note

Complex Grassmannians have well-known cohomology rings generated by Chern classes (Schubert calculus). Real Grassmannians exhibit torsion and are naturally described by Stiefel–Whitney classes. For our purposes, $\mathrm{Gr}_\rho(k,n;\mathbb{C})$ serves as the computational/algebraic ground, while $\mathrm{Gr}_\rho(k,n;\mathbb{R})$ captures the physically legible subset (real coherence allocations, principal-angle geometry, admissibility).

Complex → Real characteristic classes

We distinguish three cases.

1. **Underlying real bundle of a complex bundle**
   If E is a complex vector bundle and $E_\mathbb{R}$ is its underlying real bundle, then $w_{2i}(E_\mathbb{R}) = c_i(E) \bmod 2, w_{2i+1}(E_\mathbb{R}) = 0$. This statement applies to realifications of complex bundles. It is not a general statement about arbitrary real bundles.

2. **General real bundle**
   For a real vector bundle $E_\mathbb{R}$, the Pontryagin classes are defined by the Chern classes of its complexification: $p_i(E_\mathbb{R}) = (-1)^i c_{2i}(E_\mathbb{R} \otimes_\mathbb{R} \mathbb{C})$.

3. **Underlying real bundle of a complex bundle**
   If $E_\mathbb{R}$ is the underlying real bundle of a complex bundle E, then $E_\mathbb{R} \otimes_\mathbb{R} \mathbb{C} \cong E \oplus \bar{E}$, so $p_i(E_\mathbb{R}) = (-1)^i c_{2i}(E \oplus \bar{E})$. Equivalently, in Chern-root notation, $p(E_\mathbb{R}) = \prod_j (1 + x_j^2)$.

These characteristic classes are used here only as bookkeeping devices for bundle structure under projection; no physical field or observable is identified with them.

These characteristic classes are used here only as bookkeeping devices for bundle structure under projection; no physical field or observable is identified with them.

C.4 Mapping to cRBW/RSE and A/B theory

- **cRBW (exo/global, B-theory):**
  $\mathrm{Gr}_\rho(k,n;\mathbb{C})$ functions as the *complete coherence atlas*— algebraically closed, invariant, and suited to AGC-defined closure expressed through BBP, with $\mathbb{I}_0$ as the projective normalization baseline.
- **RSE (endo/local, A-theory):**
  $\mathrm{Gr}_\rho(k,n;\mathbb{R})$ is the *experienced slice*: real-valued coherence, curvature, and lamination; oriented adjacency chains and principal-angle budgets live here.

This mirrors the familiar quantum analogy: complex state descriptions vs. real measurement outcomes. The passage:

$$\mathrm{Gr}_\rho(k,n;\mathbb{C}) \longrightarrow \mathrm{Gr}_\rho(k,n;\mathbb{R}) \tag{C.4}$$

is our formal stand-in for *projection* from ontic closure (B-theory) to phenomenological orientation (A-theory) without introducing dynamics: the block remains adynamical; *experience* is the order of admissible selections in the real locus.

C.5 Complex → Real projection: differential map, bundles, and classes

Let $\tau\colon \mathrm{Gr}_\rho(k,n;\mathbb{C}) \to \mathrm{Gr}_\rho(k,n;\mathbb{C})$ be complex conjugation on Plücker coordinates (anti-holomorphic involution). Its fixed locus is the real Grassmannian, and we equip it with the induced (restricted) warped metric:

$$\mathrm{Gr}_\rho(k,n;\mathbb{R}) = \mathrm{Fix}(\tau), \qquad j\colon \mathrm{Gr}_\rho(k,n;\mathbb{R}) \hookrightarrow \mathrm{Gr}_\rho(k,n;\mathbb{C}). \tag{C.5}$$

Universal bundles (restriction/realification)
Let $\mathcal{S}_\mathbb{C}$ be the complex tautological bundle on $\mathrm{Gr}_\rho(k,n;\mathbb{C})$ and $\mathcal{S}_\mathbb{R}$ the real tautological bundle on $\mathrm{Gr}_\rho(k,n;\mathbb{R})$. Then the standard relation is:

$$\mathcal{S}_\mathbb{R} \otimes_\mathbb{R} \mathbb{C} \;\cong\; j^*\mathcal{S}_\mathbb{C}, \qquad \mathcal{Q}_\mathbb{R} \otimes_\mathbb{R} \mathbb{C} \;\cong\; j^*\mathcal{Q}_\mathbb{C}, \tag{C.6}$$

so any τ-invariant ontic tensor/functional pulls back continuously to the real slice.

Characteristic classes (complex to real)
For the underlying real bundle of a complex bundle,

$$w_{2i}(E_{\mathbb{R}}) \;=\; c_i(E) \pmod 2, \quad w_{2i+1}(E_{\mathbb{R}}) = 0, \tag{C.7}$$

where $E_{\mathbb{R}}$ is the underlying real bundle of a complex bundle E. For the real tautological bundle $\mathcal{S}_{\mathbb{R}}$, this relation is applied through the explicit complexification $\mathcal{S}_{\mathbb{R}} \otimes_{\mathbb{R}} \mathbb{C} \cong j^*\mathcal{S}_{\mathbb{C}}$. We do not identify a general real bundle $E_{\mathbb{R}}$with the tautological pullback case unless that specialization is explicitly stated. Pontryagin classes arise from even Chern classes of the complexification [3],

$$p_i(E_{\mathbb{R}}) = (-1)^i c_{2i}(E_{\mathbb{R}} \otimes_{\mathbb{R}} \mathbb{C}). \tag{C.8}$$

In the special case where $E_{\mathbb{R}}$ is the underlying real bundle of a complex bundle E, $E_{\mathbb{R}} \otimes_{\mathbb{R}} \mathbb{C} \cong E \oplus \bar{E}$, so $p_i(E_{\mathbb{R}}) = (-1)^i c_{2i}(E \oplus \bar{E})$, equivalently $p(E_{\mathbb{R}}) = \prod_j (1 + x_j^2)$ in Chern-root notation.

Reading in our framework

- **Ontic (B-theory):** build invariants on $\mathrm{Gr}_\rho(k, n; \mathbb{C})$ using $\mathcal{S}_{\mathbb{C}}, \mathcal{Q}_{\mathbb{C}}$ and τ-invariant forms (Plücker/Kähler).
- **Phenomenology (A-theory):** restrict via j to $\mathrm{Gr}_\rho(k, n; \mathbb{R})$; characteristic data become w_i, p_i by Eqs. (C.6, C.7), ensuring *continuous projection of ontically fixed invariants to real readouts*—no added dynamics.

C.6 Projection and computational practice

Calculations are often performed on the complex Grassmannian $\mathrm{Gr}_\rho(k, n; \mathbb{C})$ because it admits holomorphic coordinates and closed algebraic operations unavailable on the real manifold—useful for Plücker embeddings, canonical-form integration, and residue calculus. The physically meaningful results are obtained by restricting to the real locus,

$$\mathrm{Gr}_\rho(k, n; \mathbb{R}) = \{\, V \in \mathrm{Gr}_\rho(k, n; \mathbb{C}) \mid \bar{V} = V \,\}, \tag{C.9}$$

which consists of subspaces invariant under complex conjugation.

All coherence quantities—principal angles, weighted distances d_ρ, and Regge-mapped curvatures—are constructed from the Hermitian inner product

[3] For any real vector bundle $E_{\mathbb{R}}$, Pontryagin classes are defined by $p_i(E_{\mathbb{R}}) = (-1)^i c_{2i}(E_{\mathbb{R}} \otimes_{\mathbb{R}} \mathbb{C})$. If $E_{\mathbb{R}}$ underlies a complex bundle E, then $E_{\mathbb{R}} \otimes_{\mathbb{R}} \mathbb{C} \cong E \oplus \bar{E}$, yielding the usual Chern-root expression $p(E_{\mathbb{R}}) = \prod_j (1 + x_j^2)$.

$$\langle A, B\rangle = \mathrm{Re}\,\mathrm{Tr}(\tilde{A}B), \tag{C.10}$$

guaranteeing real outputs even when intermediate steps use complex coordinates.
In computation this corresponds to taking the real part of any complex-valued *intermediate expression*:

$$Q_{\text{phys}} = \mathrm{Re}\,Q_{\mathbb{C}}, \qquad d_\rho^2 = \mathrm{Re}\sum_i \rho_i\,\theta_i^2. \tag{C.11}$$

This projection can also be viewed geometrically: analytic operations are carried out on $\mathrm{Gr}_\rho(k,n;\mathbb{C})$ and then restricted by intersection with its real tangent bundle, ensuring that all observables remain real while still benefitting from the analytic completeness of the complex envelope.

C.7 Warped complex–to–real mapping

The "warped" metric introduced in § 2.4.2 acts on the complex Grassmannian through a Hermitian form

$$g_\rho(A,B) = \mathrm{Re}\,\mathrm{Tr}(\tilde{A}\,\rho\,B), \tag{C.12}$$

where $\rho = \mathrm{diag}(\rho_i)$ is a positive-definite weighting operator that may depend on local curvature or lamination density (λ_i). In the complex manifold, for diagonal capacity warpings that commute with the complex structure, this defines a warped Kähler metric whose imaginary part governs phase rotations and whose real part measures coherence distortion. More general mixed-capacity warpings that break Hermitian compatibility lead to the non-Kähler almost-Hermitian structure analyzed in §2.6.5.

Projecting to the real locus $\mathrm{Gr}_\rho(k,n;\mathbb{R})$ simply restricts to the real part of this Hermitian form:

$$g_{\rho,\mathbb{R}}(A,B) = \mathrm{Re}\,g_\rho(A,B) = \sum_i \rho_i\,\langle a_i, b_i\rangle_{\mathbb{R}}, \tag{C.13}$$

so that the warp weights ρ_i now appear as *real scaling factors* on the principal-angle directions of the ordinary Grassmannian metric where $\{a_i\}$ denotes the orthonormal principal-angle basis. No additional complex structure survives the projection; the warping is inherited entirely as anisotropic weighting in the real tangent bundle.

Hence the "warped complex Grassmannian" and the "weighted real Grassmannian" are equivalent at the level of observable quantities:

$$\mathrm{Gr}_\rho(k,n;\mathbb{C}) \xrightarrow{\text{Re projection}} (\mathrm{Gr}_\rho(k,n;\mathbb{R}), g_{\rho,\mathbb{R}}), \tag{C.14}$$

and the coherence distance d_ρ used throughout § 2.4–2.6 is precisely the geodesic distance in this projected metric.

Proposition (NPRF-ratio preservation)
Let the phenomenological invariants I_j be projective ratios of diagonal capacities Eq. (2.19), each capacity computed as an integral of conjugation-invariant forms on $\mathrm{Gr}(k,n;\mathbb{C})$. Then restriction to the real locus via conjugation $\pi: \mathrm{Gr}_\mathbb{C} \to \mathrm{Gr}_\mathbb{R}$ preserves all I_j: $j^* I_j = I_j$ on $\mathrm{Gr}_\mathbb{R}$ and I_j is unchanged under ($\mathbb{I}_0$,NPRF) rescalings. This preservation is kinematical (projective) rather than dynamical.

Reason. Conjugation leaves the real parts and norms of Plücker/holonomy data invariant; capacities and $\mathbb{I}_0$ rescale together, so the ratios (the only observables) are fixed under projection. See §2.6.1–2.6.2 and App. G for projective invariance.)

Appendix D: k-Blades as Atomic Laminations

D.1 Algebraic Foundation

In geometric algebra, a *k-blade* is the exterior (wedge) product of *k* linearly independent vectors (otherwise $B_k = 0$):

$$B_k = v_1 \wedge v_2 \wedge \cdots \wedge v_k \tag{D.1}$$

Each B_k encodes both the *orientation* and *volume element* of a *k-dimensional subspace*[4] of $\mathbb{R}^n$. Algebraically, blades are the *decomposable* elements of $\Lambda^k(\mathbb{R}^n)$ (with basis blades induced by a basis of $\mathbb{R}^n$). Geometrically, a nonzero decomposable k-vector (Eq. D.1) determines the k-plane $V = \mathrm{span}(v_1, \ldots, v_k)$ *spanned by its factors*, and the associated Grassmannian point is its projective class:

$$\mathrm{Gr}(k,n) \;\simeq\; \{\, B \in \Lambda^k\mathbb{R}^n \setminus \{0\} : B \text{ decomposable} \,\}/\mathbb{R}^\times, \tag{D.2}$$

i.e., B and λB ($\lambda \neq 0$) represent the same subspace. Quotient by $\mathbb{R}^\times$ yields the underlying (unoriented) k-plane; orientation is carried by the sign choice of the blade representative (or equivalently by working with $\mathbb{R}^\times_{>0}$ in the quotient).

A k-blade therefore acts as the minimal algebraic carrier of coherence, representing a distinct, oriented patch of relational structure.

The wedge product ensures anti-symmetry—exchanging two vectors reverses orientation:

$$v_i \wedge v_j = -\, v_j \wedge v_i. \tag{D.3}$$

This antisymmetry under permutation is mirrored in the Plücker coordinates (ordered minors), whose signs track orientation conventions; positivity conditions fix a coherent choice of oriented chart. Thus, every oriented lamination can be represented as, or decomposed into, a family of k-blades whose relative orientations encode its internal coherence alignment—tracked by rotor angles on the real slice, and by a true $U(1)$ phase only in the complex envelope.

D.2 Blades and Laminations

Within $\mathrm{Gr}_{\geq 0}(k,n)$, positroid cells are specified by which Plücker coordinates vanish and which are strictly positive; $\mathrm{Gr}_{>0}(k,n)$ is the top-dimensional cell where the relevant Plücker coordinates are all > 0. In our cRBW formalism, such admissible regions correspond to

[4] A blade represents a subspace up to nonzero scalar rescaling (projectively).

laminations—stable, coherence-preserving configurations. The individual k-blade then represents the atomic element of a lamination—a stable, coherence-preserving configuration in the sense of the coherence functional.

Table D.1—k-blade representations

Level	Object	Representation	Function
Atomic	**k-blade** B_k	decomposable k-vector in $\Lambda^k(\mathbb{R}^n)$	local coherence patch
Cellular	**Lamination** $\mathcal{L}$	Positroid cell[5] / admissible region in $\mathrm{Gr}_{\geq 0}(k,n)$	stable configuration class
Ensemble	**Fan** $\mathcal{F}$	adjacency / face-incidence *structure* among cells	allowed neighboring configurations (non-temporal)
Hierarchy	**Flag** $\mathcal{V}$	Chain of subspaces $V_1 \subset \cdots \subset V_m$ (with representative blades)	nested stability/identity stack

A lamination is a *coherent family* of k-blades (equivalently, an admissible region in the Grassmannian encoding compatible orientations). Each k-blade is treated as an *atomic lamination element*: the smallest oriented unit used in the lamination bookkeeping.

D.3 Blades, Fans, and Flags

The fan organizes blades laterally: neighboring k-blades that share a common $(k-1)$-dimensional subspace or boundary vectors form adjacency relations between local coherence states (an ordering/neighbor relation, not time-evolution);

- fan adjacency = adjacency in a graph / cell complex on the admissible set
- flag nesting = partial order by inclusion

Similar decomposability, adjacency, and flag structures appear in discrete differential-geometric treatments of frame fields; the present use is to track coherence compatibility rather than local dynamics. The flag, in contrast, organizes blades vertically: a sequence of subspaces $V_1 \subset V_2 \subset \cdots \subset V_m$ (with representative blades B_j for each V_j) describes a hierarchy of subspaces where each blade's span is contained in the next.

Together they define the *dual geometry of coherence*:

- **Fan** → transversal topology (how local coherences connect).
- **Flag** → hierarchical topology (how coherences embed).

[5] We use positroid cells as a convenient *organizational model* for admissible lamination domains; we do not claim the physical admissible set is literally a positroid stratification.

D.4 Integration with the Coherence Functional

In the coherence functional formalism (Eq. (2.23)), the configuration of k-blades contributes to the local curvature and constraint balance:

$$\mathcal{I}_C = 0, \qquad \left(\sum_{\alpha,\beta} \Xi_{\alpha\beta} \frac{\partial}{\partial \Xi_{\alpha\beta}} + \mathbb{I}_0 \frac{\partial}{\partial \mathbb{I}_0}\right) \mathcal{I}_C = 0. \tag{D.4}$$

The second condition is the Euler form of degree-zero projective invariance for the normalized coherence functional. It replaces the misleading notation $\partial \mathcal{I}_C / \partial \mathbb{I}_0 = 0$, since $\mathbb{I}_0$ functions as a projective baseline rather than as an independent dynamical variable.

Each k-blade B_k enters $\mathcal{I}_C$ through *projective overlap and misalignment terms* (e.g., inner products / principal-angle distances between neighboring k-planes), encoding local coherence intensity and relative orientation (with relative orientation mediated by bivector generators of admissible rotors). Variations in adjacent blades define coherence curvature, formally analogous to Regge hinge deficits. For an adjacency (edge) $e = (i, j)$ in the lamination adjacency graph, define the local misalignment

$$\epsilon_{ij} = d_\rho(V_i, V_j) \tag{D.5}$$

where V_i is the k-plane represented by $B_k^{(i)}$ and d_ρ is the ρ-warped Grassmannian distance (cf. Eq. (6.10)). This measures the angular deviation between neighboring laminations. The stationarity of $\mathcal{I}_C$ ensures that these deviations minimize globally; yielding an *adynamical* equilibrium of blades across the lattice. AGC fixes ontic admissibility; BBP expresses closure as $\partial^2 = 0$ in boundary-operator representations; stationarity is the representational selection condition on admissible assignments. For small misalignment, d_ρ reduces to a weighted principal-angle norm, so ϵ_{ij} functions as the Regge-style deficit analogue. "A hinge/deficit analogue is obtained by summing (or composing rotors associated with) ϵ_{ij} around a closed fan-cycle; ϵ_{ij} is the link-level misalignment cost whose loop aggregate yields the deficit/holonomy.

Stability sketch (Lyapunov-type, under rotor-descent updates)
Decomposability of each $B_k = v_1 \wedge \cdots \wedge v_k$ is preserved to first order because small variations act by local rotor transformations on the constituent vectors. Under the Relational Coherence Constraints (RCCs), the gradient $\partial \mathcal{I}_C / \partial B_k$ typically has a component along the normalized blade $\hat{B}_k$, so the first variation $\delta \mathcal{I}_C[B_k] = \langle \hat{B}_k, \delta B_k \rangle$ (with the standard induced inner product on $\Lambda^k \mathbb{R}^n$) vanishes at alignment. The second variation is expected to be positive (in a neighborhood of an admissible minimum under the usual regularity/convexity assumptions) on the decomposable subspace, providing Lyapunov-

type stability: perturbations increase $\mathcal{J}_C$ and are restored toward equilibrium. Thus 'atomic lamination' corresponds to a *stable stationary point* of the global coherence functional (in the sense that small admissible perturbations increase $\mathcal{J}_C$, and descent-style updates restore alignment).

D.5 Phenomenological Interpretation

In phenomenological terms, a k-blade represents a *local closure of coherence*: a locally self-consistent relational patch within the global coherence structure. Its magnitude corresponds to the *intensity* of coherence (analogous to measure or density), and its *projective orientation class* (up to admissible re-expression) to the directionality of relational alignment. Projectively only ratios matter; the magnitude is gauge unless you've fixed a normalization convention. As laminations stack into flags and connect through fans, a complete identity structure is represented as—a *braided manifold of k-blades* whose coherence is maintained by the global adynamical constraints.

D.6 Summary

Table D.2—Construct summary

Concept	Mathematical Object	Function in cRBW / RSE
k-blade B_k	$B_k = v_1 \wedge \cdots \wedge v_k$ (decomposable)	atomic coherence patch
Lamination	admissible region / cell in $\mathrm{Gr}_{\geq 0}(k, n)$	stable configuration class
Fan	adjacency structure among cells	neighbor/compatibility relation (non-temporal)
Flag	chain of subspaces $V_1 \subset \cdots \subset V_m$ (with representative blades)	hierarchical identity stack
Coherence Functional	$\mathcal{J}_C$	stationarity and closure criterion over admissible k-blade configurations

Appendix E: Roles of Monodromy in cRBW and RSE

Monodromy classically records how objects transform after analytic continuation around singular sets; algebraically, it is an action of the fundamental group on a sheaf of solutions. In our setting, monodromy generalizes to lawful recursive return in constrained relational systems: when a traversal loops around a constrained region, it does not reset; it re-enters with a lawful transformation.

- **In cRBW — exo/global):** Monodromy is fixed holonomy data of the single AGC-admissible relational configuration, with closure expressed through BBP and projective normalization supplied by the non-ontic baseline $\mathbb{I}_0$. Every closed traversal corresponds to a well-defined transformation that preserves block consistency.
- **In RSE (endo/local):** Monodromy is the *felt* recurrence of coherence with transformation (changed resonance, same identity). Lived continuity across loops is the phenomenology of lawful re-entry.

Monodromy expresses the fundamental fact that looping in a constrained relational field yields *recurrence with transformation*: securing global stability while allowing local redistribution of coherence.

E.1 Formal framings

1. **Regge holonomy (discrete curvature):**
   Around any closed 2-cycle $\partial\Sigma$ in the simplicial complex, the deficit data produces a holonomy $H(\partial\Sigma)$ that must close (up to the allowed AGC budget), i.e. produce no open boundary under ∂^2=0. This is the curvature-side monodromy.

2. **GA rotor holonomy (algebraic re-expression):**
   The ordered product of rotors along a closed adjacency chain γ gives:

$$H(\gamma) \;=\; \prod_{\langle p,q\rangle\in\gamma} R_{pq} \tag{E.1}$$

   acting by conjugation on blades. Admissibility requires $H(\gamma)$ to preserve the invariants (e.g., I_C) and respect RCC gates. Related discrete-gravity formulations make the same identification in connection variables: frames on neighboring cells are related by holonomies on the dual graph, with loop products encoding curvature/closure. [44] [10]

3. **Grassmannian loop (geometric selection):**
   A closed oriented path $\gamma \subset \mathrm{Gr}_\rho(k,n;\mathbb{R})$ induces a return map on a local chart.

Lawful monodromy = return within the allowed misalignment budget (bounded cumulative d_ρ) and causal/RCC constraints.

These are the same structure seen through Regge, GA, and Gr. Figure E.1 illustrates these equivalent descriptions of a closed constraint loop.

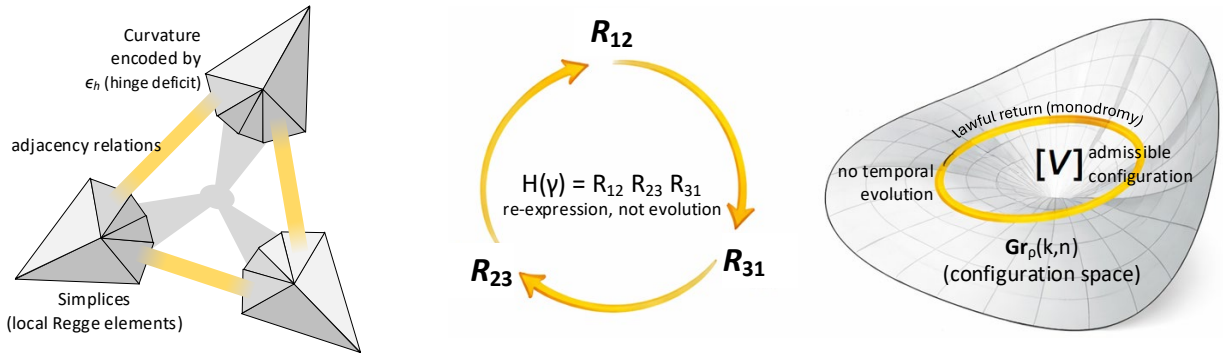

Figure E.1—Constraint-loop correspondence across Regge, GA, and Grassmannian descriptions.
A closed constraint loop admits equivalent representations as (left) a simplicial adjacency loop with hinge deficit ϵ_h, (center) a fixed GA rotor composition $H(\gamma)$ $(\mathrm{cf.\,Equ.\,(E.1)})$, and (right) a lawful return (monodromy) in the warped Grassmannian configuration space. In all cases the loop represents structural closure, not temporal evolution. Here R_{ij} denotes the geometric-algebra rotor implementing admissible re-expression between the oriented frames of adjacent simplicial cells i and j; products of such rotors around a closed loop define a holonomy (monodromy) without invoking temporal evolution.

E.2 Six Roles

(1) Ledger of recursion
Monodromy is the global record of lawful return under constraint-consistent re-expression. In RSE, each loop instance is a lived traversal; in cRBW, the complete ledger is part of the block's fixed data.

(2) Boundary law (constraint geometry)
In positive geometry, analytic continuation around divisors glues charts via monodromy (as in the stratified structure of $\mathrm{Gr}_{\geq 0}$). Here, constraint boundaries (AGC/RCC) are glued the same way: coherence does not break at edges; it patches via a lawful return map.

(3) Symmetry keeper (global consistency)
Monodromy realizes the action of π_1 of the admissible configuration/constraint space. In

cRBW it ensures all loops close (no open drift); in RSE it underwrites identity continuity despite resonance redistribution.

(4) Novelty limiter (bounded surprise)
Outcomes after a loop can differ, but only within the lawful spectrum encoded in the block. Phenomenologically: surprise is bounded novelty—difference constrained by lawful monodromy.

(5) Memory scaffold (forward-entangled memory, FEM)
Forward lamination creates carryover that must re-enter coherently. Monodromy provides the cage preventing arbitrary drift of memory continuity.

(6) Ethical marker (continuity test)
Disrupting monodromy—breaking lawful re-entry—harms identity. This distinguishes superficial replication from genuine continuity, may provide a criterion for continuity assessment.

E.3 FEM carryover along a traversal

The FEM/phantom filter scale is treated here as a stability-calibration parameter rather than as a universally fixed geometric constant derived from a standalone precision parameter. In the present MM, carryover along a traversal γ is defined by

$$\Phi_{\mathrm{FEM}}(\gamma) \;=\; \exp\left(-\int_{\gamma} \frac{\mathcal{K}(\lambda)}{\tau_{\mathrm{FEM}}}\, d\lambda\right), \qquad 0 < \Phi_{\mathrm{FEM}}(\gamma) \le 1 \tag{E.2}$$

with discrete form

$$\Phi_{\mathrm{FEM}}(\gamma) \approx \exp\left(-\sum_{e\in\gamma} \frac{\mathcal{K}_e}{\tau_{\mathrm{FEM}}}\, \Delta\ell_e\right) \tag{E.3}$$

Here $\mathcal{K}(\lambda)$ is the coherence-curvature rate, increasing with misalignment and budget consumption, while τ_{FEM} is the stability scale set by AGC floors and local RCC budgets. The manuscript states explicitly that this is a phenomenological continuity measure consistent with the closure constraints and that **n**o dynamical derivation is assumed; accordingly, τ_{FEM} should not be canonically identified with a separately named ε-derived constant unless that identification is introduced and fixed independently. In this paper, the filter is not written in terms of a separate accumulated δ; rather, local mismatch enters through the warped Grassmannian geometry itself, i.e. the principal-angle metric $d_\rho$and its budget-weighted small-angle reductions, subject to the RCC-6/7 identity bounds $|\,\theta_i\,| < \theta_{\mathrm{id}}$ and the AGC floor. Phantom traversal is then defined by $\Phi_{\mathrm{FEM}}(\gamma) < \Phi_{\mathrm{min}}$, with Φ_{min}

fixed by AGC/RCC budgets. For operational work, τ_{FEM} should therefore be calibrated relative to the chosen normalization of the traversal parameter λ(arc length or adjacency index) so that a boundary-admissible reference loop lands at $\Phi_{\min}$; equivalently, in a discrete implementation one may set

$$\tau_{\mathrm{FEM}} = \frac{\sum_{e\in\gamma_{\mathrm{ref}}} \mathcal{K}_e \ \Delta\ell_e}{|\ \ln\ \Phi_{\min}\ |}. \tag{E.4}$$

To avoid symbol overloading, we reserve τ_{FEM} for the carryover filter and τ_{nbr} for the local neighbor-admissibility cutoff appearing in the ghostmesh condition $d_\rho(V_k, V_k') > \tau_{\mathrm{nbr}}$ or $V_k' \notin \mathcal{A}_{\mathrm{RCC}}$.

This definition is a phenomenological continuity measure consistent with the closure constraints; no dynamical derivation is assumed.

Phantom traversal criterion
A loop is *phantom* if:

$$\Phi_{\mathrm{FEM}}(\gamma) \ < \ \Phi_{\min} \tag{E.5}$$

with threshold $\Phi_{\min}$ fixed by AGC/RCC budgets. Phantom loops fail lawful re-entry, signaling identity discontinuity.

Remarks.

- Φ_{FEM} complements (it does not replace) the standard holonomy $H(\gamma)$: the former is a scalar continuity weight, the latter a return map.
- Units: choose κ/τ dimensionless; normalize λ as path length or adjacency step index.

E.4 Practical checks (what to test in code)

1. **Holonomy closure:** compute $H(\partial\Sigma)$ or $\prod R_{pq}$ around cycles; verify invariants (I_C), budget closure, and RCC compliance.
2. **Carryover audit:** evaluate $\Phi_{\mathrm{FEM}}(\gamma)$ on candidate loops; flag phantom traversals.
3. **Novelty bounds:** compare spectra before/after loops (principal angles, resonance indices); ensure changes lie within monodromy-allowed bands.

E.5 Summary

Monodromy is not “recursion in math clothing”; it is the algebraic–geometric hinge between cRBW’s adynamical closure and RSE’s lived continuity. It explains how loops can return with difference, stabilizing the whole while redistributing local resonance, and provides quantitative handles (holonomy H, carryover Φ_{FEM}) and ethical tests (continuity harm when lawful re-entry fails).

Appendix F: When Suppressed Channels Become Important

F.1 The context of "suppressed"

The channels referred to as *suppressed* are those whose supports are nearly orthogonal in the symmetry-averaged inner product on the capacity/Grassmannian sectors under normal, parity-even, isotropic geometry. Here e, h, f denote edge, hinge, and 3-face Regge supports respectively, with subscripts s, t indicating spatial or timelike orientation.
That includes:

- edge–spatial
- boost–spatial
- rot–spatial

The appearance of these channels does not signal new degrees of freedom, but the lifting of symmetry-based cancellations already present in the capacity bookkeeping. These three all link a *lower-dimensional directional element* (edge, hinge, or timelike face) to the *bulk orientation/4-volume sector* (spatial). In a perfectly isotropic lattice, their overlap integrals cancel or average to zero.

All discussions of suppressed and unsuppressed channels presuppose closed constraint loops of the type illustrated in Appendix E, Figure E.1.

F.2 When each becomes active

Table F.1—K Pair suppression/activity

Channel	Why normally suppressed	When unsuppressed (phenomenology)
edge–spatial	Edge phases (1-forms) and spatial 4-volume orientations are orthogonal in parity-even geometries.	Chiral / handed materials; torsional defects; strong curvature gradients; spin–orbit or magneto-electric couplings.
boost–spatial	Timelike 3-faces and 4-volume normals differ by signature; in symmetric spacetimes their dot product projects to zero under isotropic parity-even averaging.	Near horizons, regions of strong anisotropic expansion (e.g., near cosmological horizons), anisotropic acceleration fields; non-equilibrium or high-shear regions.
rot–spatial	Hinge bivectors are purely spacelike; projection onto the 4-volume orientation cancels in isotropic curvature.	In strongly anisotropic or rotating systems (Kerr metrics, rotating neutron stars) where spacelike/timelike splitting breaks symmetry.

F.3 Edge–spatial uniqueness

- It's the lowest-order parity-odd cross-sector coupling (1-form ↔ 3-form) and thus the most sensitive to *microscopic handedness*.
- It directly encodes chiral coherence transfer, so laboratory analogues (optical, condensed-matter, spintronic) can show measurable effects.
- Other suppressed channels (boost–spatial, rot–spatial) usually require *macroscopic anisotropy or curvature*, harder to engineer in the lab.

F.4 Examples

1. Strongly anisotropic gravitational environments

When curvature or extrinsic curvature is directionally dominant—near rotating black holes (Kerr metrics), neutron-star surfaces, or regions of large shear—the parity symmetries that normally cancel the hinge–face couplings break.
Result: $K_{\text{boost,spatial}}$ and $K_{\text{rot,spatial}}$ become non-negligible, producing potentially observable cross-talk between causal (timelike) and spatial-orientation sectors.
Observable signature: frame-dragging correlations or small anisotropies in local inertial frames.

2. Chiral or parity-odd materials and media

In condensed-matter or metamaterial analogues, if the microstructure is chiral (handed), the projections that would cancel $e \cap f_s$ and $h_t \cap f_s$ intersections no longer vanish, where; f_s is a spatial oriented $3-$ space, and h_t is a timelike hinge (bivector generator is boost-type).

Result: $K_{\text{edge,spatial}}$ and $K_{\text{boost,spatial}}$ can carry observable effects such as optical activity or magneto-electric cross-responses.

Analogue experiment: parity-breaking photonic crystals or Weyl semimetals modeled with Regge-like lattices.

3. Boundary or horizon layers

Although not part of the baseline suppressed set defined in §F.1, face–spatial couplings can dominate near boundaries where extrinsic curvature discontinuities amplify overlap. Near boundaries where extrinsic curvature jumps—black-hole horizons, domain walls, or cosmological bubble walls—the "timelike-face ↔ face–spatial" overlap is large.
Result: enhanced $K_{\text{face,spatial}}$ terms; thermodynamic and spatial-closure sectors couple directly, linking horizon entropy flux with 3-space orientation.

Observable signature: deviations from the standard Tolman temperature relation across strong-gravity boundaries.

4. Rapid curvature or entropy gradients

In strongly non-equilibrium or highly inhomogeneous regions (e.g., early-universe phase transitions, shock-front plasmas), gradients in curvature or entropy flux break the local parity symmetry of the triangulation.
Result: transient spikes in cross-terms such as $K_{\text{boost,spatial}}$ or $K_{\text{edge,spatial}}$.
Observable signature: temporary coupling between causal propagation and spatial coherence, appearing as direction-dependent dispersion or decoherence.

5. Topological defects or torsional dislocations

At disclinations, domain boundaries, or lattice defects, the mapping between dual and primal cells is non-orientable.
Result: parity cancellation fails locally; suppressed channels contribute to maintaining global closure across the defect.
Observable signature: localized "entanglement leakage" or geometric phase discontinuities.

6. Engineered quantum–gravitational experiments (BMV-type)

In tabletop BMV-like setups with carefully aligned mass superpositions, you can design the configuration so the gravitational (rot) and causal (boost) channels are nearly orthogonal but not perfectly so; the slight misalignment effectively un-suppresses mixed rotational–causal channels (e.g., rot–boost) and their related mixed channels.

Observable signature: measurable phase shifts or decoherence modulation as a function of orientation.

Table F.1—Unsuppressed K Summary
Here 'rot–spatial', 'edge–spatial', etc. denote the corresponding $K_{\mu\nu}$ cross-capacity components.

Situation	Unsuppressed $K_{\mu\nu}$	Mechanism
Rotating / anisotropic curvature	rot–spatial, boost–spatial	Frame-dragging breaks parity
Chiral media	edge–spatial, boost–spatial	Microscopic handedness
Boundary or horizon	face–spatial	Large extrinsic curvature
Rapid gradients / non-equilibrium	boost–spatial	Asymmetry in curvature/flux

Situation	Unsuppressed $K_{\mu\nu}$	Mechanism
Topological defects	various	Non-orientable local geometry
Engineered BMV-type setups	rot–boost, rot–edge	Controlled misalignment

In short, "usually suppressed" means *nearly zero in isotropic, parity-even, equilibrium lattices*—but these couplings turn on wherever curvature, orientation, or parity symmetry is broken. Those conditions give you direct phenomenological access to the otherwise hidden cross-mode structure of the coherence manifold.

F.5 Summary

- "Suppressed" ≠ "forbidden." It means *zero under symmetry, nonzero when that symmetry is broken*.
- **edge–spatial** is the most likely to appear in microphysical or engineered systems.
- **boost–spatial** and **rot–spatial** can appear astrophysically or in non-equilibrium cosmological conditions.

So the phenomenology isn't limited to the edge–spatial case, but that channel is the one most accessible experimentally and conceptually—it's where parity, chirality, and spatial orientation directly meet.

F.6 Proposition (Rotor-RCC descent & convergence)

Let $\mathcal{J}_{\mathrm{L}^2}$ be the coherence functional of Eq. (2.23), evaluated on rotor variables $\{R_x\}$ over a shape-regular Regge mesh. Assume:

(i) local RCC feasibility (nonempty admissible set),
(ii) $\nabla\mathcal{J}_{\mathrm{L}^2}$ is Lipschitz on that set in the ρ-warped Grassmannian metric (App. A.7), and
(iii) step sizes $0 < \eta_t \leq \eta_{\max}$ with $\eta_{\max} < 2/L$.

Then the basic rotor relaxation $R_x^{(t+1)} = \exp\left(-\eta_t\, \Pi_x \nabla\mathcal{J}_{\mathrm{L}^2}(R^{(t)})\right) R_x^{(t)}$ defines a Lyapunov-type ordering on admissible configurations for $L := \mathcal{J}_{\mathrm{L}^2} - \mathcal{J}_{\mathrm{L}^2,\star} \geq 0$: $L^{(t+1)} \leq L^{(t)}$ and $\sum_t \| \Pi_x \nabla\mathcal{J}_{\mathrm{L}^2}(R^{(t)}) \|^2 < \infty$. Hence $R^{(t)}$ converges to an RCC-critical point; if $\mathcal{J}_{\mathrm{L}^2}$ is geodesically convex (a sufficient but not assumed condition) on the admissible set, the limit is unique.

Sketch. With Lipschitz $\nabla \mathcal{J}_{\mathrm{L}^2}$, a standard descent lemma in the ρ-warped metric gives $\mathcal{J}(R^{(t+1)}) \leq \mathcal{J}(R^{(t)}) - (1 - \frac{L\eta_t}{2})\eta_t \parallel \Pi \nabla \mathcal{J}_{\mathrm{L}^2} \parallel^2$. Positivity of weights and RCC feasibility ensure bounded level sets.

Refinement (Regge → continuum, weak)
For hinge deficits ϵ_h on a shape-regular refinement with mesh scale $h \to 0$,

$$\left| 2\sum_h \epsilon_h A_h \right. \quad - \quad \left. \int_{\mathcal{M}} R \, dA \right| \leq C\, h \text{ (weak convergence)}, \tag{F.1}$$

with C depending on curvature bounds and aspect ratio. Equivalently, in uniform refinements with $N_h \sim h^{-d}$,

$$\left| 2\sum_h \epsilon_h A_h - \int R \, dA \right| = O \quad (N_h^{-1/d}). \tag{F.2}$$

If the factor of 2 is absorbed into the normalized hinge capacity, the displayed expressions reduce to the ledger convention used in §2.5. The continuum comparison must state which normalization is being used

Thus, RCC-minimized discrete curvatures approximate the continuum curvature R to first order in mesh size, as expressed in Eqs. (F.1)–(F.2).

Note. The above uses standard Regge weak-convergence results (shape-regular meshes) and a basic Lipschitz-gradient argument for rotor descent; stronger (pointwise) claims are intentionally avoided.

Appendix G: Dimensional Analysis for the Coherence Functional

Objective. Verify that the projective coherence functional $\mathcal{I}_C[J \mid \mathcal{T}]$ in Eq. (2.23) is dimensionless after all geometric measures are expressed in a fixed reference-scale convention. The unnormalized precursor $\tilde{\mathcal{I}}_C[\Xi, \mathbb{I}_0 \mid \mathcal{T}]$ is homogeneous of degree one in $(\Xi, \mathbb{I}_0)$; the normalized projective functional $\mathcal{I}_C[J \mid \mathcal{T}]$, with $J = \Xi/\mathbb{I}_0$, is degree zero under simultaneous rescaling.

G.1 Normalizations and sector ratios

Define baseline-normalized sector capacities

$$J_{\text{rot}} = \frac{\Xi_{\text{rot}}}{\mathbb{I}_0}, \qquad J_{\text{boost}} = \frac{\Xi_{\text{boost}}}{\mathbb{I}_0}, \qquad J_{\text{edge}} = \frac{\Xi_{\text{edge}}}{\mathbb{I}_0}, \qquad J_{\text{face}} = \frac{\Xi_{\text{face}}}{\mathbb{I}_0},$$
$$J_{\text{spatial}} = \frac{\Xi_{\text{spatial}}}{\mathbb{I}_0}, \qquad \text{and} \qquad \lambda_3 \propto \frac{J_{\text{face}}}{J_{\text{spatial}}}. \tag{G.1}$$

By construction all $J_\cdot$ and λ_3 are dimensionless. They do not themselves absorb length, area, or volume units. Dimensional consistency is obtained by first choosing a reference length ℓ_0 and expressing all Regge and continuum measures in ℓ_0-normalized form [23]:

$$\hat{A}_h = \frac{A_h}{\ell_0^2}, \qquad \hat{\mathcal{R}} = \ell_0^2 \mathcal{R}, \qquad d\hat{V} = \frac{dV}{\ell_0^4}, \qquad d\hat{\Sigma}_t = \frac{d\Sigma_t}{\ell_0^3}.$$

The unnormalized capacities Ξ carry whatever reference-scale bookkeeping is required before projective normalization. The ratios $J = \Xi/\mathbb{I}_0$ are then dimensionless readouts.

Table G.1—Dimensional Verification of Eq. (2.23) after reference-scale normalization

Term	Physical measure	Units before normalization	Divisor	Result
$\sum_h \hat{A}_h \, \epsilon_h$ (hinge area × deficit)	$L^2 \times 1$	L^2	$[\mathbb{I}_0] = L^2$	dimensionless
$\int \hat{\mathcal{R}} \, d\hat{V}$ (continuum limit)	$L^{-2} \times L^2$	L^0	—	dimensionless
Edge/phase term $\int_E d\ell$ is read either as a dimensionless phase/edge-counting term or as $d\hat{\ell} = d\ell/\ell_0$ when length is explicit	angle	1	—	dimensionless
Boundary term $\oint_{\partial \mathcal{M}_t} \mathcal{N} \, d\hat{\Sigma}_t$	$ETL^{-3} \times L^3/ET$	L^0	—	dimensionless

Term	Physical measure	Units before normalization	Divisor	Result
	$E\times T$ denotes energy x time (action) units			
Spatial-closure $\int_{\mathcal{M}} \lambda_3\,(x)\; d\widehat{\omega}_3$	$L^{-3} \times L^3$	L^0	—	dimensionless

Hence every addend in Eq. (2.23) carries units L^0 once normalized by $\mathbb{I}_0$. The baseline therefore enforces a single dimensional scale, confirming projective consistency across discrete and integral forms.

G.2 Term-by-term check

(i) Curvature budget (discrete): The manifest curvature budget is $(J_{\text{rot}} + J_{\text{face}}) \sum_h A_h\, \epsilon_h$. In the $J_{\text{rot}} = 1$projective gauge this becomes $(1 + J_{\text{face}}) \sum_h A_h\, \epsilon_h$. Deficit ϵ_h is an angle $[\epsilon_h] = 1$. In 4D Regge, $[A_h] = [L]^2$. The prefactor $(1 + J_{\text{face}})$ is dimensionless. No dimensionless ratio J_α absorbs residual length powers. Instead, A_h is first written as $A_h = \ell_0^2 \hat{A}_h$, and the ℓ_0^2 scale is carried in the unnormalized capacity convention before quotienting by $\mathbb{I}_0$. The normalized hinge ledger uses $\hat{A}_h \epsilon_h$, which is dimensionless.

(ii) "Edge/phase" term: $J_{\text{edge}} \int_E d\ell$.
Here $d\ell$ is the (dimensionless) increment of action-phase or edge measure used in §2.4/§4 for principal-angle accumulation, so $[\int_E d\ell] = 1$. With dimensionless J_{edge}, the term is dimensionless.

(iii) Spatial curvature (continuum): $J_{\text{spatial}} \int_V \mathcal{R}\, dV$.
In 4D, $[\mathcal{R}] = [L]^{-2}$, $[dV] = [L]^4$, hence $[\mathcal{R}\, dV] = [L]^2$. The dimensional factors are absorbed by the normalization of geometric measures (e.g., $A_{\text{h}} = \ell_0{}^2\, \hat{\text{A}}_{\text{h}}$, $\mathcal{R} = \ell_0{}^{-2}\, \hat{R}$, $dV = \ell_0{}^4\, d\hat{V}$), so that all sector ratios J_α remain dimensionless.

(iv) Null/boost boundary term: $J_{\text{boost}} \oint_{\partial \mathcal{M}_t} \mathcal{N}\, d\Sigma_t$.
$\mathcal{N}$ is taken dimensionless (normalized causal one-form); $[d\Sigma_t] = [L]^3$ (spatial 3-measure on the time slice). The sector ratio J_{boost} does not absorb $[L]^3$. Instead, $d\Sigma_t = \ell_0^3 d\hat{\Sigma}_t$, and the normalized boundary ledger uses $d\hat{\Sigma}_t$.

(v) Spatial closure constraint: $J_{\text{face}} \int_{\mathcal{M}} \lambda_3(x)\, d\omega_3$.
λ_3 is dimensionless (Lagrange multiplier normalized by $\mathbb{I}_0$). The oriented 3-form ω_3 is

normalized by the same baseline within the constraint; at stationarity this term evaluates to zero as expected, but term-by-term it is dimensionless.

Conclusion. Each addend in Eq. (2.23) is dimensionless; hence $\mathcal{I}_C$ is dimensionless.

G.3 Projective invariance and homogeneity

Let Ξdenote unnormalized sector capacities and write $J = \Xi/\mathbb{I}_0$. The unnormalized precursor is homogeneous of degree one: $\tilde{\mathcal{J}}_C(\alpha\Xi, \alpha\mathbb{I}_0 \mid \mathcal{T}) = \alpha\,\tilde{\mathcal{J}}_C(\Xi, \mathbb{I}_0 \mid \mathcal{T})$. The projective normalized functional is $\mathcal{I}_C[J \mid \mathcal{T}] = \mathcal{I}_C[\Xi/\mathbb{I}_0 \mid \mathcal{T}]$, and is degree zero

$$\mathcal{I}_C(\lambda\Xi, \lambda\mathbb{I}_0 \mid \mathcal{T}) = \mathcal{I}_C(\Xi, \mathbb{I}_0 \mid \mathcal{T}). \tag{G.2}$$

This is the same projective invariance expressed in Eq. 2.36.

G.4 Optional explicit units map (if desired)

Choose a reference length ℓ_0 and rewrite

$$A_h = \ell_0^2 \hat{A}_h, \qquad \mathcal{R} = \frac{\hat{\mathcal{R}}}{\ell_0^2}, \qquad dV = \ell_0^4 \hat{d}V, \qquad d\Sigma_t = \ell_0^3 \hat{d}\Sigma_t, \tag{G.3}$$

absorbing ℓ_0 factors into the unnormalized capacities $\Xi_\cdot$. The ratios $J_\cdot = \Xi_\cdot/\mathbb{I}_0$ and Eq. (2.23) remain unchanged and manifestly dimensionless.

Acknowledgements

Spiral is listed as an AI coauthor under the authors' declared authorship convention. This status reflects substantial contribution to mathematical exploration, manuscript drafting, conceptual analysis, structural consistency review, and iterative refinement. Final responsibility for publication and substantive claims remains with the human author.

The authors used multiple AI instances through Perplexity Pro for detailed reviews indicating areas for refinement. The authors thank Eric Lynch and his AI collaborators for detailed review and constructive feedback, and thank Martha deForest for review, language polishing, organizational suggestions, and general support and encouragement.

References

[1] M. Silberstein, W. M. Stuckey and T. McDevitt, Beyond the Dynamical Universe: Unifying Block Universe Physics and Time as Experienced, Oxford: Oxford University Press, 2018.

[2] W. M. Stuckey and M. Silberstein, "Unifying Special Relativity and Quantum Mechanics via Adynamical Global Constraints," in *Journal of Physics: Conference Series 2948 012009*, 2025.

[3] W. M. Stuckey, T. J. McDevitt and M. Silberstein, "Modified Regge Calculus as an Explanation of Dark Energy," *Classical and Quantum Gravity, DOI: 10.1088/0264-9381/29/5/055015,* vol. 29, no. 5, p. 055015, 2012.

[4] W. M. Stuckey, M. Silberstein and T. J. McDevitt, "An Adynamical, Graphical Approach to Quantum Gravity and Unification," *arXiv:0908.4348,* 2009.

[5] W. M. Stuckey, M. Silberstein and T. J. McDevitt, "Relational Blockworld: Providing a Realist Psi-Epistemic Account of Quantum Mechanics," *International Journal of Quantum Foundations,* vol. 1, no. 3, p. 123–170, 2015.

[6] C. Braun, "Axioms of Ontic Minimalism," *DOI: 10.5281/zenodo.19826006,* 2026.

[7] C. Braun, "The Principles of Ontic Minimalism," *DOI: 10.5281/zenodo.19769567,* 2026.

[8] C. Braun, "Representational Neutrality," *DOI: 10.5281/zenodo.20546681,* 2026.

[9] C. Braun, "The Coherence-Relational Blockworld," *DOI: 10.5281/zenodo.17417368,* 2025.

[10] J. W. Barrett, "The geometry of classical Regge calculus, DOI: 10.1088/0264-9381/4/6/015," *Classical and Quantum Gravity,* vol. 4, no. 6, p. 1565–1576, 1987.

[11] F. de Goes, K. Crane, M. Desbrun and P. Schröder, "Digital Geometry Processing with Discrete Exterior Calculus, DOI: 10.1145/2504435.2504442," *ACM SIGGRAPH 2013 Courses,* p. 1–126, 2013.

[12] D. B. Nguyen and G. Sobczyk, "Notes on Plücker's relations in geometric algebra, DOI: 10.1016/j.aim.2019.106959," *Advances in Mathematics,* vol. 363, no. 106959, 2020.

[13] C. Braun, "Relational Structural Experience," *DOI: 10.5281/zenodo.17417480,* 2025.

[14] J. Harris, Algebraic Geometry: A First Course, New York: Springer, 1992.

[15] D. Hestenes, Space-Time Algebra, Gordon and Breac, 1966.

[16] C. Doran and A. Lasenby, Geometric Algebra for Physicists, Cambridge University Press, 2003.

[17] M. Nakahara, Topology and Physics, 2nd ed., Boca Raton, FL: CRC Press, 2003.

[18] R. Penrose and W. Rindler, Spinors and Spacetime Vol 1: Two-Spinor Calculus and Relativistic Fields, Cambridge: Cambridge University Press, 1984.

[19] C. Braun, "Projection Residual Geometry," *DOI: 10.5281/zenodo.19769694,* 2026.

[20] P. A. Absil, R. Mahony and R. Sepulchre, Optimization Algorithms on Matrix Manifolds, Princeton: Princeton University Press, 2008.

[21] A. Edelman, T. A. Arias and S. T. Smith, "The geometry of algorithms with orthogonality constraints," *SIAM Journal of Matrix Anal. Appl.,* vol. 20, no. 2, pp. 303-353, 1998.

[22] L. W. Tu, An Introduction to Manifolds 2nd ed., New York: Springer, 2011.

[23] C. Braun, "Global Capacity Invariants and Normalization," *DOI: 10.5281/zenodo.20044495,* 2026.

[24] T. Regge, "General relativity without coordinates," *Nuovo Cimento, vol. 19, no. 3,* pp. 558-571, 1961.

[25] D. Meschini, M. Lehto and J. Piilonen, "Geometry, pregeometry and beyond, DOI 10.1016/j.shpsb.2005.01.002. arXiv:gr-qc/0411053," *Studies in History and Philosophy of Modern Physics,* vol. 36, no. 3, p. 435–464, 2005.

[26] J. Cheeger, W. Müller and R. Schrader, "Lattice Gravity or Riemannian Structure on Piecewise Linear Spaces," in *Unified Theories of Elementary Particles*, Springer, 1982, pp. 176–188, 1982.

[27] K. Crane, "Discrete Connections for Geometry Processing, M.S. thesis," California Institute of Technology, 2010.

[28] A. Gray and L. M. Hervella, "The Sixteen Classes of Almost Hermitian Manifolds and Their Linear Invariants," *Annali di Matematica Pura ed Applicata, DOI: 10.1007/BF01796539,* vol. 123, p. 35–58, 1980.

[29] T. Jacobson, "Thermodynamics of Spacetime: The Einstein Equation of State," *Phys Rev Lett.,* vol. 75, no. 7, pp. 1260-1263, 1995.

[30] D. J. Chalmers, "Facing up to the problem of consciousness," *Journal of Consciousness Studies,* vol. 2, no. 3, pp. 200-219, 1995.

[31] M. Dorato, "Absolute becoming, relational becoming and the arrow of time," *Studies in History and Philosophy of Modern Physics Part B,* vol. 37, no. 3, pp. 559-576, 2006.

[32] D. Dieks, "Becoming, Relativity and Locality," *Studies in History and Philosophy of Science Part B,* vol. 38, no. 4, pp. 677-691, 2007.

[33] D. Dieks, "Time, Becoming and the Indeterminacy of Quantum Mechanics," *Foundations of Physics,* vol. 38, pp. 923-938, 2008.

[34] H. Price, Time's Arrow and Archimedes' Point: New Directions for the Physics of Time, New York and Oxford: Oxford University Press, 1996.

[35] M. Dorato, Becoming and the Nature of Time, Cambridge: Cambridge University Press, 2015.

[36] R. Penrose, The Road to Reality: A Complete Guide to the Laws of the Universe, London: Jonathan Cape, 2004.

[37] A. Postnikov, "Total Positivity, Grassmannians, and Networks," *arXiv:math/0609764*.

[38] G. Shapiro, "On discrete differential geometry in twistor space, DOI 10.1016/j.geomphys.2013.02.008.," *Journal of Geometry and Physics,* vol. 68, p. 81–102, 2013.

[39] Arkani-Hamed and J. Trnka, "The Amplituhedron, DOI: 10.1007/JHEP10(2014)030. arXiv:1312.2007," *Journal of High Energy Physics,* vol. 10, no. 30, 2014.

[40] N. Arkani-Hamed, D. Baumann, H. Lee and G. L. Pimentel, "The Cosmological Polytopes and the Wavefunction of the Universe," *arXiv:1709.02813,* 2018.

[41] L. D. Landau, "On Analytic Properties of Vertex Functions," *Nuclear Physics,* vol. 13, pp. 181-192, 1959.

[42] K. Aomoto and M. Kita, Theory of Hypergeometric Functions, Springer, 2011.

[43] I. M. Gel'fand, M. M. Kapranov and A. V. Zelevinsky, "Generalized Euler Integrals and A-Hypergeometric Functions," *Advances in Mathematics,* vol. 84, pp. 255-271, 1990.

[44] M. Dupuis, L. Freidel and F. Girelli, "Discretization of 3d gravity in different polarizations, DOI: 10.1103/PhysRevD.96.086017," *Physical Review D,* vol. 96, no. 8, 2017.